ADDIS ABABA UNIVERSITY

SCHOOL OF GRAGUATE STUDIES

SCHOOL OF EARTH SCIENCE

PETROGENESIS OF NECH SAR VOLCANICS AT SOUTHERN PART OF ARBA MINCH AREA IN GAMO GOFA ZONE FROM SOUTH MAIN ETHIOPIAN RIFT

BY

WORKINESH MAMO MELAKU

A Thesis Submitted to the School of Graduate Studies of Addis Ababa University in Partial Fulfillment of the Requirements for the Degree of Master of science in Geological Science (Geochemistry)

Jun, 2018

Addis Ababa, Ethiopia

ADDIS ABABA UNIVERSAITY

SCHOOL OF GRAGUATE STUDIES

SCHOOL OF EARTH SCIENCE

PETROGENESIS OF NECH SAR VOLCANICS AT SOUTHERN PART OF ARBAMINCH AREA IN GAMO GOFA ZONE FROM SOUTH MAIN ETHIOPIAN RIFT

BY

WORKINESH MAMO MELAKU

ADVISOR: DEREJE AYALEW (Prof.)

A Thesis Submitted to the School of Graduate Studies of Addis Ababa University in Partial Fulfillments of for the Degree of Master of Science in Geological Science (Geochemistry)

Jun, 2018

Addis Ababa, Ethiopia

ADDIS ABABA UNIVERSITY

SCHOOL OF GRADUATE STUDIES

SCHOOL OF EARTH SCIENCE

PETROGENESIS OF NECH SAR VOLCANICS AT SOUTHERN PART OF ARBAMINCH AREA IN GAMO GOFA ZONE FROM SOUTH MAIN ETHIOPIAN RIFT

BY

WORKINESH MAMO MELAKU

Approved by the Examining Committee

Dr. Balemual Atnafu	_____	_____
Head, school of Earth Science	signature	date
Prof. Dereje Ayalew	_____	_____
Advisor	signature	date
Prof.Gezahign Yirgu	_____	_____
Examiner	signature	date
Dr.Mulugeta Alene	_____	_____
Examiner	signature	date

Declaration of Originality

I hereby declare the thesis is my original master's degree work under the supervision of Proffessor Dereje Ayalew, School of Earth Science, and Addis Ababa University during the year 2018. I further declare that this work has not been presented or submitted to any other University or Institution for the award of any Degree or Diploma. All sources and materials used for the thesis have been duly acknowledged.

Workinesh Mamo Melaku _____ _____

Signature date

This is to certify that the above declaration made by the candidate is correct to the best of my knowledge.

Prof. Dereje Ayalew (Advisor) _____ _____

Signature date

Abstract

The Nech Sar volcanics, are locate on the southern Ethiopia within the floor of south Main Ethiopian Rift. The study area is found locate about 521 km south of Addis Ababa. The main objective of this thesis is to understand the petrogenesis of volcanic rocks that are exposed on south of Arba Minch town. Field investigations, petrographic and whole rocks geochemical analysis methods have been applied in order to meet the main and specific objectives of this work. The studied volcanics are all of Quaternary age and include basaltic lava flow and scoria, rhyolite lava, unweldded tuff and intermediates rocks. The basaltic rocks range from aphyric to porphyritic and mildly porphyritic basalt. The acidic rocks are characterized as alkali feldspar and quartz rich rocks on the basis of field and petrographi descriptions. The geochemical data indicate that the Nech Sar volcanic products vary from basalts through basaltic tarchyandisite, trachyandesite, trachydacite and rhyolite. The mafic rocks comprise a suite of transitional to weakly sub alkaline basalt and are characterized by enrichment of highly incompatible trace elements e.g. high La/Yb ratio (11-27). The Nech Sar volcanic rocks are genetically inter related by the process of fractional crystallization starting from mantle derived basaltic magma with limited involvement of crustal contamination. - This is shown by major oxide (MgO, CaO, Fe_2O_3, TiO_2 Na_2O and K_2O) and selected trace element (Ni, Co, Cr, V, Sc, and Rb, Zr, Y, Nb) versus SiO_2 Harker diagrams which exhibit either decreasing or increasing correlation that define continuous and regular trends. Similarly plots of selected (HFSE) incompatible trace elements (e.g. Nb versus Zr, Rb versus Th, Ta versus Th and Nb versus La) form moderately_ positive_ linear relations. The plots of (Tb/Yb)N (0.92-1.7) versus $(La/Sm)_N$ and La/Sm ratio versus Sm/Yb (2-2.5), suggest that the Nech Sar basaltic rocks are derived from garnet_ free_mantle source, i.e is spinel peridotite mantle.

Key words**: Petro genesis, Fractional crystallization, mantle source and Nech Sar volcanic rocks.**

Acknowledgements

This thesis work was accomplished with help of, support and inspiration of different institutions and persons. First I would like give my gratitude to Addis Ababa University School of Earth Sciences and Dilla University for providing an opportunity to study my for my Master‘s degree and funding the research project.

Second, I would most like to express my deepest gratitude, appreciation and honor to my advisor Prof. Dereje Ayalew for his guidance, constructive comment, supervision, encouragement and inspiration. His guidance helped me in all the time of research and writing of this thesis. - I am also indebted to Prof. Gezahign Yirgu for his interest in my work and his encouragement and willingness to discuss my various ideas and questions.

I would like to thank Tesfaye Guja and Tsegaye Wolde who wholeheartedly supported me during my field work. My gratitude goes to all Arba Minch Nech Sar Park and Zuria woreda peoples for their friendly and cooperation

Last, but not least, I would like to acknowledge my family who unreservedly supported me throughout my study and thesis work. I am very much indebted for the amount of work put into this task.

Table of Contents

List of Figures

List of Tables

List of Acronyms

EARS	East African Rift System
MER	Main Ethiopian Rift
NMER	North Main Ethiopian Rift
CMER	Central Main Ethiopian Rift
SMER	South Main Ethiopian Rift
NSV	Nech Sar Volcanoes
ICP-AES	Inductive Coupled Plasma –Atomic Emission Spectrum
ICP-MS	Inductive Coupled Plasma-Mass Spectrum
WFB	Wonji Fault Belt
TAS	Total Alkaline versus Silica
CIPW	Cross, Iddings, Pirsson and Washington
HY	Hypersthene
XPL	Cross Polarized Light
PPL	Plain Polarized light
LOI	Loss of Ignition
ANBGS	Arba Minch Nech sar Basalt from Ganta Scarpment
ANPAS	Arba Minch Nech sar Basalt from Sech area
ANVBK	Arba Minch Nech Sar Basalt from Kulfo river area
ANSBA	Arba Minch Nech Sar Sample from small Bonke
ANTB	Arba Minch Nech Sar Sample from large Bonke area
ANISC	Arba Minch Nech Sar Sample from Scoria Cone
ANRGW	Arba Minch Nech Sar Rhyolite from Ganta

CHAPTER ONE

1. INTRODUCTION

1.1. Back ground

Investigation of the petrogenesis of volcanic rocks is important to understand the source of magma, its evolution and tectonic setting and genesis of the rock because petrogenesis means the process of origin and formation of igneous rock. Volcanic rocks exposed on the Earth's surface are as a result of partial melting of rocks within the mantle or crust. Basalt is a common volcanic rock and by the forms of lava flows, lava sheets and lava plateaus and it can be consider as direct representative of mantle of the Earth's interior.

This research conducted Southern Main Ethiopian Rift located in Arba Minch area, about 9 km far from Secha town. The main purpose of doing this research work is to investigate the petrogenesis of the volcanic rocks constituting of the Tosa Shucha site. The geochemical and petrographical data obtained - on both felsic and mafic rocks will help to constrain the source of the magma.

The Ethiopian rift system is characterized by long history of magmatism associated with different degree of lithospheric extension, formation of different volcanic rocks and make an opening across the Ethiopian plateau, the present day topography of which is cause of dynamic support from sub lithospheric depth, by considered to be due to presence of the mantle plum and the MER is links region between the Kenya rift and Afar triple junction where extensional deformation started to develop in late Oligocene-early Miocene to recent times (Ebinger et al., 1989; Ebinger et al., 1993; Ebinger et al., 2000; Bellahsen et al., 2003). Large igneous provinces_ are related to the composite effect of the continental break up and rising of hot mantle plume head as well as belong to late Eocene to middle Miocene plus quaternary basalt (George et al., 1998). Fissural flood basalt volcanic rocks are transitional to theolitic composition (Mohr, 1983) in the northern Ethiopian and Somalia plateaus whereas the shield volcanoes are alkaline (Eberz et al., 1988; Tadiwos Chernet et al., 1998). These shield volcanoes are found on top of the plateau volcanic and erupted with in the 30Ma-10Ma time range Kieffer et al. (2004).

The Main Ethiopian Rift (MER) is the key sector of East African Rift System (EARS) Connected with Red Sea Rift and Gulf of Aden Rift in the north and Kenyan Rift in the south (Corti, 2009). It is classified in to Northern (NMER), Central (CMER) and Southern

(SMER) based on structural feature of the rift segments Fig 1.1 (Giday Wolde Gabriel et al., 1990; Bonini et al., 2005; Kurz et al., 2007; Keranen and Klemperer, 2008; Corti, 2009). Initially the magmatic activities was started at (45–35 Ma) which is ~500-m-thick Amaro and Gamo tholeiitic basalts and are succeeded by the ~500-m-thick Getra-Kele alkali basalts, dated as 19–11 Ma by K-Ar methods are occurred dominantly in SMER and shows north ward propagation up to Goba Bonga transverse lineament whereas the northern sector of the rift start to develop by 11 Ma and propagates south ward until the Boru Tura structural high (George et al., 1998; Mohr, 1983; Wolde Gabriel et al., 1990; Bonini et al., 2005; Tsegaye Abebe et al., 2010). In case of the CMER it was initiated at 9.7-8.3 Ma ago with significant rifting at 5-3 Ma ago and with the eruption of voluminous silicic eruptions (Bonini et al., 2005).

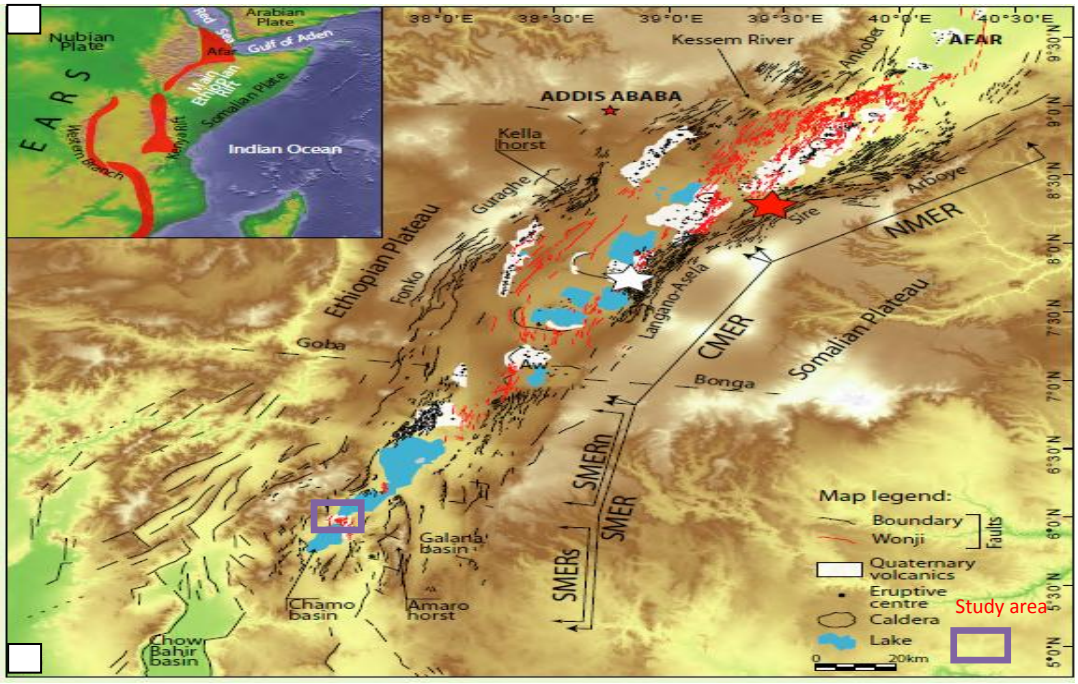

Figure 1. 1: *Tectonic sketch map of the Main Ethiopian Rift (from Corti, 2009).*

The Main Ethiopian Rift (MER) connects the Afar depression to the Kenya Rift and on the basis of varying rift trend, lithospheric characteristics and fault patterns, is usually divided in three main segments: Northern MER (NMER), Central MER (CMER) and Southern MER (SMER). The SMER was further divided in a northern (SMERn) and a Southern sector (SMERs). The MER is characterized by a fault pattern Composed of a Mio-Pliocene NE-SW border fault system and a Quaternary N-S to N20°E-trending system (Wonji Fault Belt), composed of en-echelon right stepping faults obliquely affecting the rift floor.

1.2. General description of study area

1.2.1. Location of study area

The study area is located in South Nation Nationalities and Peoples Regional State of Gamo Gofa Zone, southern part of Arba Minch area about 521 km away to wards south from the

capital city of Ethiopia, Addis Ababa. Geographically, the study area is bounded between (334000 to 344000) E and (656000 to 663252) N from (UTM). The total area covers 70 km^2 with average elevation 1366m amsl.

1.2.2. Accessibility

The study area is accessed by asphalt road which run from Addis Ababa through Butajira, Halaba, Hosanna, Wolaita and Arba Minch town. The specific area accessed by weather gravel, and by foot.

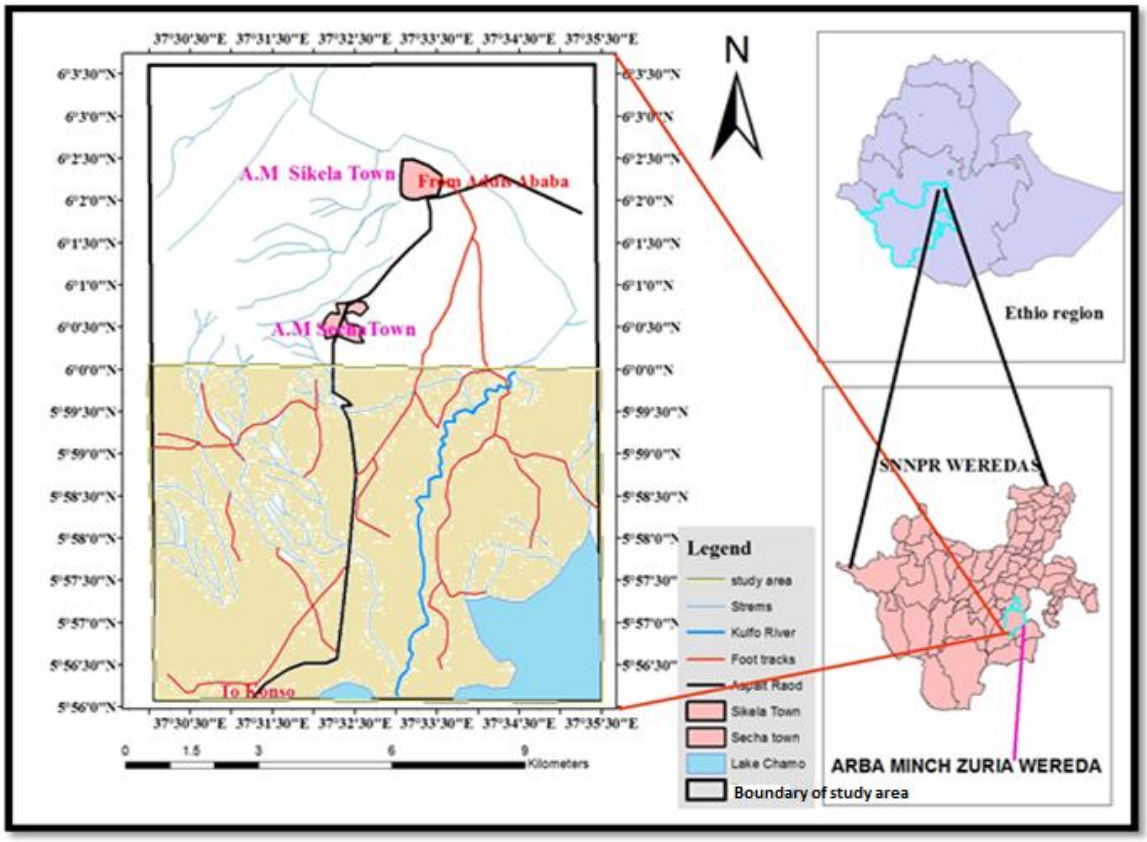

Figure 1. 2: *Location and accessibility map of study area.*

1.3. Physiographic and Drainage character

1.3.1. Physiography

The study area is characterized by different topographic features are observed, these include, ridges, flat land, high land with maintain peak and general rugged terrain and low land toward rift floor. The ridges are found in the north eastern and north western from Lake Chamo, the north western ridge start from northern Arba Minch and extend to Ganta ochole, Gerese and north eastern ridge from large and small Bonke with maintain peak. In another

hand the flat land of Nech Sar national park, Merkeb Tabia and kumba quarry site are low land of study area. In the southern part of Arba Minch area Kulfo river and its tributaries are flow in fracture and faulted formation of the rock and external processes including weathering and erosion by the surface run off are the result of volcanic and denudation.

1.3.2. Drainage

The major rivers in the study area are kulfo and other small streams flow to the Chamo Lake. Lake Chamo is one of the lakes in Ethiopia which is formed with in the rift system. The lake aligned to the rift orientation and it covers a large area. All rivers Sile and Kulfo and tributaries are draining to this lake. The density and distribution of both streams and rivers are varies from area to the other. Kulfo is the largest widest river, other than in this area; there are many tributaries that join the lake Chamo; generally the study area is characterized by dendritic drainage pattern.

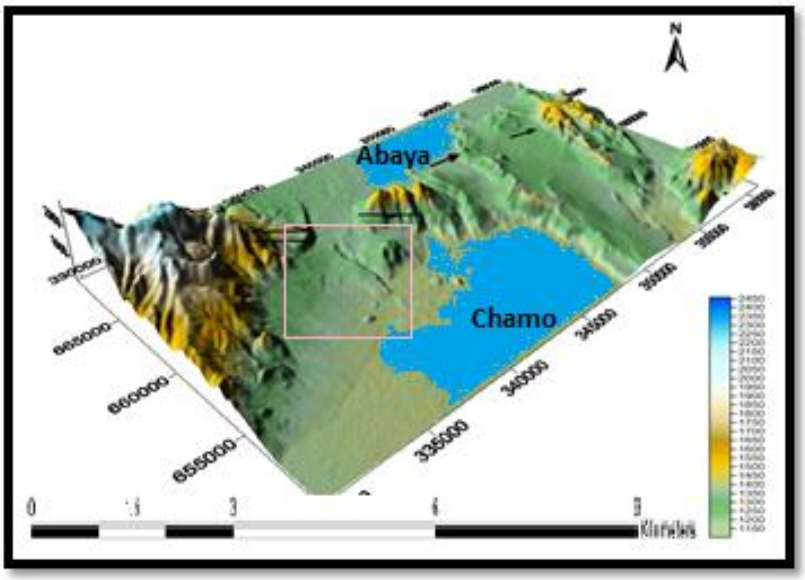

Figure 1. 3: *Physiography and drainage map of study area.*

1.3.3. Climate and Vegetation

1.3.3.1. Climate

According to National meteorological Agency of Gamo Gofa Zone (2010) the area characterized by semi- arid climate condition and bi-modal distribution, with two rainy and two drier seasons occurring intermittently. The first rainy seasons fall mainly from February to July and second from September to October and received mean annual rain fall 887.5mm.The mean minimum and mean maximum temperature amount are about 17˚c and

32˚c respectively. However, the north western highland of the study area Ganta is characterized by relatively cold climate.

1.3.3.2. Vegetation

The density and distribution of vegetation in the study area varies from place to place depending on the altitude, soil type and humidity and /or precipitation. Accordingly, there is area of forest, woodland and bush land. The forest cover (e.g. Maytenus arbutifolia, Gerwia bicolor, Maytenus senegalensis and Dombeya torrid*)* mostly occurs along the middle Kulfo River vally and its tributers as well as round forty springs. The woodland (e.g. cactus trees and acacia) is common in the middle slope of Ganta Mountain. The bush land (e.g. brevispica, mellifera, nilotica, seyal, sengal) occure alonge the Nech Sar National park and in both Large and small Bonke middle slope. The bush land type of vegetation is more dominant especially in north eastern part of Lake Chamo however; the central and southern low lands of the study are characterized by scarce bush trees.

Figure 1. 4: *Photograph from study area that showing vegetation cover and low land around kumba quarry site as well as, high lands of Ganta escarpment, and large Bonke region.*

1.3.4. Population and Settlement

The study area is mostly inhabited by five largest ethnic groups reported in Arba Minch Zuria woreda, the Gamo (69.53%), the Amhara (7.94%), the Wolaita (6.75%), the Zayse (6.02%), and the Oromo (3.64%); all other ethnic groups made up 2.28% of the population. Gamo is spoken as a first language by 65.77%, 16.97% Amharic, 5.93% Zergula, 5.13% Woliata, and 2.46% spoke Oromiffa; the remaining 3.74% spoke all other primary languages. The majority of the inhabitants were Protestants, 53.91% of the population reporting that belief, 29.31% practiced Ethiopian Orthodox Christianity, 12.6% Muslims and practiced traditional beliefs (As reported national census Arba Minch Zuria woreda, 2007). There is different ethnic group live in the town. However, the rural people of the area live in the highlands and on the low land suitable for farming and domestic animal breeding. Their livelihood depends on agricultural practice cultivating different kinds of crop such as maize, wheat, teff, peat and bean. In addition to this mango and banana is the most dominant fruit in study area. As reported 2016 national census the total population for this zone of 180,529 of whom 92,198 were men and 92,330 Women 36.31% its population were urban dweller and remain 63.69% are rural dweller.

1.4. Statement of the problem

The south section of Ethiopian rift which is one segments of main Ethiopian rift that studied a lot by different researchers. Some previous researchers has been focused on regional works on southern main Ethiopia rift regarding, geology, structural, petro graphic, geochemistry and both volcanology and geothermal studies have done regional level (Ebinger et al., 1993; Georg, 1998; Georg and Roger, 1999; George and Rogers, 2002; Rooney et al., 2012). However, there are different parts of Igneous terrain in south main Ethiopian rift that require study of specific area concerning lithologic unite identification, determine the detail local geology of the area, identify the link between mafic and felsic rock from constrain source of magma and geochemical characters of the rock by studying geochemical composition and classification. Therefore, southern Arba Minch area is part of south main Ethiopian Rift that required more specific investigation. In this work an attempt has been designed to map the particular area, with relatively detailed scale (1:25000) to describe lithological units, geological formation of the area and classification of the rock. So, such studies particular area can give chance to support scientific idea

.

1.4.1 Significance of the study

❖ To understand the geochemical and petrographical characteristics of the rock and process evolved in differentiation magmatic genesis.

❖ Used to know source of the magma and systematic classification of the rocks based on both petrographic and geochemical investigation

❖ To contributes some dataset on-going studygeochemistry of volcanic rock of the south main Ethiopian rift.

1.5. Objectives

1.5.1. General objective of the research

The basic objective of the thesis is investigation of the petrogenesis of Nech Sar volcanic rocks at southern part of Arba Minch from Southern Main Ethiopian Rift by using major and trace element geochemistry, petrography and detail field mapping.

1.5.2. Specific objectives of this research

✓ To study geochemical characters of the rocks.

✓ To understand the process involved in the modification of magma genesis.

✓ To constrain magma source based on trace element geochemistry.

✓ To produce geological map of the study area at the scale of 1:25,000.

1.6. Methodology

In order to perform the general and specific objectives by successfully, the following methods were used. The research methodology focuses on collection of primary data as well as secondary data, sample analysis, data synthesis and interpretation. The research was conducted in three stages: Pre-field, Field and Post field activity

1.6.1. Review of Literature

The revision of previous work from different books, journal by revising and compiling of published and unpublished reports related to study title and study area.

1.6.2. Field work

Major activity conducted during field work was traversing and detailed description of exposed units. The 24 appropriate samples of rock collected from the field for further laboratory analysis (petrography and geochemical analysis), recording of GPS reading at each sampling station and taking photos of different lithological units and measuring major geologic structures.

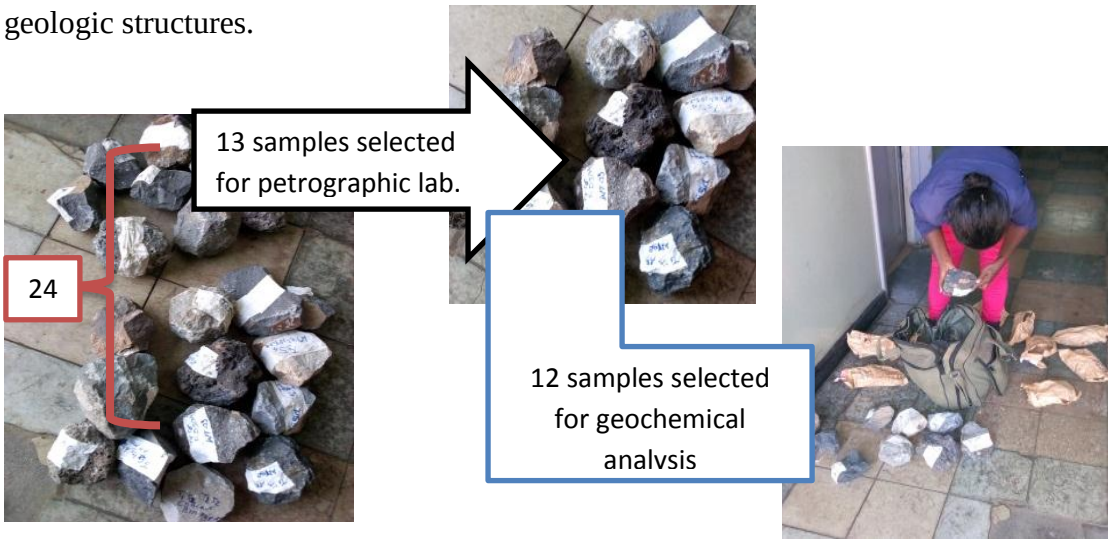

Generally 13 samples selected from 24 samples for laboratory analysis.

1.6.3. Petrography analysis

The fresh and representative 13- rocks samples have been selected for petrographic analysis. The thin section preparation such as cutting to appropriate size rock slabed, grinded, mounted, and again grinded and covered was procedure have done at the geological survey of Ethiopia. The sample selection for descriptions of mineral assemblage was based on difference of lithology, alteration and their importance to construct geological map of the study area through identification of lithology unite .Therefor, 8 thin section selected from 13 samples for description and their mineral assemblage modal proportion has been examined under petrographic microscopy in petrography laboratory of Earth science by researcher.

1.6.4. Geo-chemical analysis

Sample preparation for geochemical analysis includes removal of the weathered part; break the sample into desirable sizes and Crush the broken fresh sample in a jaw crusher and finally the crushed sample will be milled down to micron size particles in an agate ball automatic milling machine. To minimize cross contamination of samples, after crushing and milling every single rock sample, the Jaw crusher and the ball mills are blown by an air compressor

and washed out to remove any possible contaminant, then dried to continue with the second sample. The samples of acidic and intermediate are prepared first then after finishing all acidic rocks the mafic rocks are prepared. The sample preparation is done in Addis Ababa ALS milling room and 12 powdered sample were sent to Australian laboratory science ALS for geochemical (trace and major element) analysis in Ireland. Major element analyzed by ICP-AES using multi element inductively coupled plasma whereas trace element are analyzed by both ICP-MS using multi element mass spectrometry technique

1.7. Review of previous work

The MER which occupies at the southern part of the country is referred to as the Southern Mian Ethiopian Rift (SMER). It is the area of interaction between main Ethiopian rift (MER) and Kenya rift in which the magmatism started in late Eocene and continue to the recent geological time (Melody et al., 2013; George et al., 1998). Some geological work have been done regionally on south main Ethiopian rift regarding geology, structural, geochemistry, tectonic evolution, volcanology and geothermal.

Southern Ethiopian flood basalts erupted in two episodes: the pre-rift Amaro and Gamo transitional tholeiites (45–35 million years) followed by the syn-extensional Getra-Kele alkali basalts (19–11 million years).These two volcanic episodes are distinct in both trace element and isotope ratios (Zr/Nb ratios in Amaro/Gamo lavas fall between 7 and 14, and 3–4.7 in the Getra-Kele lavas whereas 206Pb/204Pb ratios fall between 18–19 and 18.9–20, respectively (Rogers and George, 2002) suggest that these transition tholeiitic basalt (45-35 Ma) found in southern Ethiopia genetic related with Kenya plume based on various line of evidence that supported view of African plate moved slowly north-east ward during Tertiary. The timing of this movement is not well explained, may be 30-20 Ma (Silver et al., 1998; O'Connor et al., 1999; Collet et al., 2000,;Roger et al., 2002). As stated by George et al. (1998) the southern Ethiopia flood basalt would have been situated above the mantle thermal anomaly now beneath Kenya rather than the one now presently beneath Ethiopia at 45 Ma. The Eocene Amaro and Gamo basalts of southern Ethiopia are the product of decompression melting of a mantle plume in response to limited crustal extension, probably associated with the development of the Kaisut– Lokichar rift system of north-western Kenya based on the compositional difference between the source regions of northern and southern Ethiopian basalts which is consistent with that interpretation and moreover, the Nd and Sr isotopic systematic of Neocene to Recent basalts from Kenya (Roger et al., 2002; George et al., 1998)

and the Nd isotopic composition of the East African mantle plume are similar to those of the Amaro and Gamo basalts (Rogers et al., 2000; Georg et al., 1998; Georg and Roger, 1999). However, Miocene (19-11Ma) Getra-Kele alkaline basalts which erupted subsequently in southern Ethiopia rift and characterized by isotope and trace element geochemistry, e.g. Sr and Pb isotope ratio are distinct from Kenyan mantle plum as well as their Nd^{143}/Nd^{144} different from that of Afar mantle plum. Therefore, they were derived from a lithospheric mantle source region that had been by trace enriched element and by migrating carbonate-rich melts with high Zr/Hf ratios that may have occurred during the Pan-African orogeny around 300–500 Ma. Melting was coincident with development of the main Ethiopian Rift, but was initiated by conductive heating of the lithosphere as a result of the emplacement of the Afar mantle plume beneath Ethiopia (Roger et al., 2002). The two magmatic episodes are consistent with northward migration of the African plate as originally stated by George et al. (1998) and recently defined from hot-spot trails in the south-central Atlantic (O'Connor et al., 1999, as cited in Rogers., 2002).

In case of Quaternary basalts of the south Main Ethiopian Rift (MER) were predominantly formed by melts derived from the 'tail' of the Afar plume (Ebinger et al., 1993; Furman et al., 2006) influence of the plume signature appears to decrease along the MER away from the Afar to southern Ethiopia (Rooney et al., 2012). Therefore, the southern Ethiopia, a progression of melts derived from a mantle plume source to enriched continental lithosphere mantle through time (George and Rogers, 2002). As stated George et al.(1999) those recent volcanic activity is confined to the area of active extensional tectonics in SMER and constitutes a group of volcanic cone with youthful morphology and the mafic rock types range from basalt through hawaiite to mugearite that over lines panafrican basement rocks. According to Ebinger et al. (1993) the geochronologic time of this young mafic product is between 0.68-1.34 Ma has been confirmed by K-Ar dating.

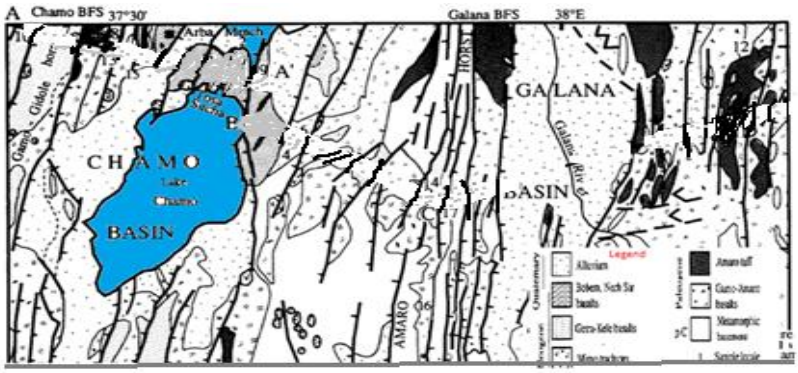

Figure 1. 5: *The geological map of Gamo-Gidole across Amaro-Horest of Amaro region in south main Ethiopian rift (Ebinger et al., 1993).*

CHAPTER TWO

2. GEOLOGIC AND TECTONIC SETTING

2.1. Geological setting

At the northern end of the East African Rift system extends southwards through Ethiopia, Kenya and Tanzania into Mozambique (Macdonald, 2002 and Corti, 2009), the active Main Ethiopian Rift (MER) and the Afar Depression represent two distinct stages in the transition from a continental rift to a rift system that shares many characteristics with a slow-spreading oceanic ridge (Ebinger, 2005).

2.1.1. Ethiopian flood basalt volcanism

The EAR flood basalts plateau magmatism locates along the NNE-SSW running Ethiopia-Kenya. It is widely accepted that the distribution and the timing of flood basalt magmatism resulting from up welling complex and heterogeneous of African mantle plum (Kieffer et al., 2004; Meshesha and Shinjo, 2004). For north western plateau basalts many outers have been stated that, there is three mantle source for Ethiopian continental flood basalt as a potential source, this are old continental Lithosphere, the HIMU type Afar mantle plum and depleted mantle (Vidal et al., 19991; Deneil et al., 1994; Steward and Rogers, 1996 and Meshesha, 2004).

According to Meshesha and Shinjo, (20004) the extensive flood basalts are found in Ethiopia, Saudi Arabia and in Yemen. In this region the continental flood basalt magmatism is subdivided in to two groups: first is pre-rift volcanism contained transitional – sub alkaline flood basalt and second syn-post rift volcanism which consists mainly alkaline volcanics. In addition, this flood volcanism is predominantly composed of basaltic lavas together with rhyolitic ignimbrites and pyroclastic-fall deposits, and less common basaltic pyroclastic rocks and rhyolitic lavas. It cover an area of at least 6×106 km^2 and have a total volume of about ~3.5×105 km^3 (Dereje Ayalew et al., 2002; Kieffer et al., 2004; Ukstins-Peate et al., 2005, 2008; Mohr, 1983; Mohr and Zanettin, 1988; Dereje Ayalew et al., 2009). Most of the flood basalts and rhyolites were erupted in a short time period (~1 Myr) at 31–29 Ma, (Wolfenden et al., 2005). In southern and south-western Ethiopia, small amounts of tholeiitic (40–45 Ma) and alkali (~35 Ma) basalts, together with associated evolved magmas, occur due to Afar mantle plume impact (Georg, 1998). However,_ according to_ Rogers et al. (2000 and 2002)

this magmatism is attributed to the effect of the Kenyan mantle plume resulting in the bimodal volcanism covering large area (basaltic flows and associated rhyolites).

The Ethiopian Oligocene flood volcanism is overlain by low-angle shield volcanoes that spatially are magmatism similar to the underlying flood basalts, i.e. tholeiitic shields overlie tholeiitic flood basalts and alkaline shields overlie alkaline flood basalts in north Ethiopian (Kieffer et al., 2004) suggest the Ethiopian plateau is made of flood basalts and shield volcanoes. These flood basalts are characterized compositionally tholeiitic to alkaline lava flows and mostly occurred through fissures (Kieffer et al., 2004; Mohr and Zenatin et al., 1988) and have been divided on the basis of their whole-rock geochemistry into Low-Ti tholeiitic and High-Ti alkali basalts based on trace element and titanium concentration (Pik et al.,1998). The High-Ti alkali basalts, ankaramites and picrites have been further subdivided in to an enriched HT_2 and intermediate HT_1 group (Pik et al., 1998). The nature of mantle plume responsible for the formation of Ethiopian plateau volcanic and its interaction with the continental lithosphere has been investigated by Baker et al. (1996), Hofmann et al. (1997) and Pik et al. (1998, 1999).

The impinging Afar plume is assumed to have triggered flood basalt volcanism in the homonymous region ~ 30 Ma ago (Hofmann et al., 1997). There is no consensus on the number(s) of mantle plumes; some authors assume that there are two compositionally distinct mantle plumes that are found beneath East African rift system one beneath the present Ethio-Afar dome and the other beneath the Kenya Plateau (Rogers et al., 2002), while others argue that there is existence of a single channeled plume (Ebinger and Sleep, 1998).

The magmatism in southern Ethiopia is related to a Kenya mantle plume (Rogers et al., 2006) suggst in agreement with plate motion reconstructions. However, rifting in East Africa has been typically associated to the upwelling of starting thermal plumes, in which a heat source at a boundary layer (the core-mantle boundary) forms a thermally buoyant spherical head connected to a tail or conduit that feeds source material to the head (as in the classical model by (Griffiths and Campbell, 1990) and Corti et al., 2009). From the channeled plume model, the two-plume model states , the occurrence of the oldest basalts in southern Ethiopia and their distinct geochemical signatures with respect to flood basalts of the Ethiopian plateau argue for the activity of two separate mantle plumes (Afar and East African or Kenyan plumes). According to Rogers, 2006 and 2002 the old basalts of Southern Ethiopia represent the first manifestation of the East African plume and, as the African plate migrated north,

subsequent magmatic activity is represented by progressively younger episodes further south through Turkana, Kenya and into northern Tanzania.

2.2. Main Ethiopian Rift Magmatism

The Main Ethiopian Rift formed as a result of the divergence of the Nubian, Somalian, and Arabian plates above an anomalously hot (Rooney et al., 2012; Ferguson et al., 2013), slow-seismic-wave speed mantle (Montelli et al., 2004; Benoit et al., 2006; Bastow et al., 2005, 2008; Corti et al., 2015). The idea is supported by Corti, (2009). The MER is a ~500 km long zone of active continental rifting between the Nubian and Somalian plates and is considered a typical example of an active continental rift (Ebinger et al., 2005).

The volcanism started during the Eocene-late Oligocene with the eruption of flood basalts that have generally been related to either one or two mantle plumes impinging, that the base of the lithosphere under Afar or Afar-Northern Kenya (Ebinger and Sleep, 1998; George et al., 1998; Rogers et al., 2000). As suggested by Davidson and Rex, (1980); Ebinger et al. (1993); George et al.(1998) the oldest flood basalts crop out in the broadly rifted zone of southern Ethiopia and that are Eocene in age 45 Ma. According to Hofmann et al. (1997); Pik et al. (1998) and Ukstins et al.(2002), the flood basalts forming the Ethiopian Plateau is apparently erupted in a short time interval (<5 Ma) with the greatest eruption rates occurring from 31 to 28 Ma. Starting from these early episodes of volcanism, magmatic activity in the MER was episodic rather than continuous (Girdler, 1983; Giday Wolde Gabriel et al., 1990). In contrast the second episode of flood basalt volcanism has been described in the southern Ethiopia at 19–11 Ma (Ebinger et al., 1993) and in the MER-Afar transition zone at about 10–11 Ma (Tadiwos Chernet et al., 1998; Wolfenden et al., 2004). Time-correlative basaltic units are widespread both in the western (Wollega, Fursa and Lake Tana basalts, 11–9 Ma) and in the eastern (Upper Trap and Anchar basalts, 10.5–9 Ma) plateaus (Mohr and Zanettin, 1988 and references therein). The 11–10 Ma-old basalts have also been documented in the Omo Canyon rift (Giday WoldeGabriel and Aronson, 1987; Giday Wolde Gabriel et al., 1990).

In the Central MER, early eruption of flood basalts was locally followed by under saturated intermediate and acidic rocks at ~17–12 Ma (Kazmin et al., 1980; Giday WoldeGabriel and Aronson, 1987; Giday WoldeGabriel et al., 1990) and by eruption of late Miocene (11–8 Ma) basalts and subordinate silicic flows (Morton et al., 1979; Kazmin et al., 1980; GidayWoldeGabriel et al., 1990; Abebe et al., 1998; Tadiwos Chernet et al., 1998; Mazzarini et al., 1999).

After these episodes of pre-rift activity (with widespread flood basalts and subordinate felsic products), rifting in the various MER sectors was characterized by volcanism with fundamentally bimodal character. Widespread late Miocene-Pliocene rhyolitic ignimbrites (~7–3 Ma) with intercalated minor mafic lavas occur throughout the Northern and Central MER (Meyer et al., 1975; Morbidelli et al., 1975; Morton et al., 1979; Kazmin et al., 1980; Giday WoldeGabriel et al., 1990; Tadiwos Chernet et al., 1998; Mazzarini et al., 1999). Mainly basaltic central volcanoes grew mostly on the Somalian plateau during Pliocene times, giving rise to an important phase of off-axis volcanism.
In the Quaternary (<1.6–1.8 Ma), bimodal volcanic rocks (lava, pyroclastic and volcano clastic strata) were generally closely associated with Wonji Fault Belt affecting the rift floor (Giday WoldeGabriel et al., 1990).

The volcanic rocks are exposed both on plateau and escarpment of main Ethiopia in north Ethiopia tertiary volcanic rift, either plateau or escarpment volcanic consist mafic lava and felsic pyroclastic rocks or it comprise bimodal volcanic which is mafic lava (scoria cone series and ignimbrite), Whereas the Quaternary volcanic rocks dominate in rift-floor and consist of three units, the Dofan mafic volcanic rocks, the Fantale felsic rocks, and the Sabure scoria cones are the main example (Tadiwos Cherenet et al., 1998; Zanettin et al., 1980; Feyisa et al., 2017, According to Feyisa et al. (2017) the MER the mafic lava strongly suggests there is at least three sources component (Afar plum, depleted Asthenosphere mantle and enriched pan African lithospheric mantle) based on variation in trace element and isotope composition. According to Mulugeta Alene et al. (2017) and Rooney et al. (2012) the isotopic variations observed on modern basalts that erupted along the Afar (WORMIL basalts) and MER as the result of mixing from three dominant mantle reservoirs; the Afar plume, the asthenosphere upper mantle (depleted mantel) and enriched lithospheric mantle respectively. However, the modern Main Ethiopian rift basalts were derived from melting of amphibole-bearing spinel peridotite of lithospheric mantle at pressures 1.01 and 1.24 GPa for MER basalts, with associated depths of melting of and 30–37 km. The basalts were derived through melting of veined lithospheric sources in response to mantle upwelling, progressive rifting and associated lithospheric thinning (Dereje Ayalew et al., 2016). This is apparent from the compositional data for the axial basalts that indicate contrasting trace element contents of the host lithospheric mantle and enclosed enriched veins and crustal assimilation appears to be negligible throughout the rift.

In case of SMER a new laser 40Ar/39Ar age for the volcanic succession in southern Ethiopia confirms the presence of two distinct magmatic phase at 45–35 Ma and 19–12 Ma. The Earliest phase predates both extension and magmatism in northern Ethiopia by 15 Ma and cannot be related to any simple model of melting in response to extension over a single mantle Plume (Georg and Rogers., 1998) they proposed and a model in which the Ethiopian province was initially related to the thermal influence of the Kenyan, and subsequently, the Afar mantle plume during northward movement of the African plate in the Tertiary. Therefore, Southern Ethiopian flood basalts erupted in two episodes: the pre-rift Amaro and Gamo transitional tholeiites (45–35 million years) followed by the syn-extensional Getra-Kele alkali basalts (19–11 million years) (George and Rogers, 2002) These two volcanic episodes (Amaro and Gamo transitional tholeiites and Getra-Kele alkali basalts) are distinct in both trace element and isotope ratios (Zr/Nb ratios in Amaro/ Gamo lavas fall between 7 and 14, and 3–4.7 in the Getra-Kele lavas whereas 206Pb/204Pb ratios fall between 18–19 and 18.9–20, respectively). And based on these distinctive chemistries of the two episodes record the tapping of two distinct source regions: a mantle plume source for the Amaro/Gamo phase and an enriched continental mantle lithosphere source for the Getra-Kele phase. After this the volcanic activity was resumed in the early Pleistocene with eruption of ignimbrites and basalts (Zanettin et al., 1978; Ebinger et al., 1993) and earlier successions are followed by the Arba Minch olivine basalt 1.34-0.77 Ma (Ebinger et al., 1993), 0.66 Ma old trachyte basalt of the Bobem volcano and pumiceous tuff as well as scoria cone and basalts in the Bridge of God area (Ebinger et al., 1993; Bonini et al., 2005). This mafic lava was caused by heating of lithosphere by the underlying of Afar mantle plume (Ebengire et al., 1993; George and Rogers, 1999). It is composition varies from basalt through to hawiite and mugearite and they are derived from melt of incompatible element enriched lithospheric mantle source. This enrichment was affected by migrating carbonate rich melts during pan-African orogeny that is 500-800 Ma (George and Rogers, 1999).

When one talks about geology of southern Ethiopia, the Late Proterozoic metamorphic basement rocks of southern Ethiopia consists of highly deformed gneisses, amphibolites, and granulites interlayered with plutonic rocks of Archean to Proterozoic age (Davidson, 1983; Mengesha Tefera et al., 1996). The basement is unconformable overlain by sandstones a 6-m-thick Late Cretaceous/Early Tertiary lateritic horizon interpreted as the product of the erosion of the basement rocks during Paleocene (Mengist Teklay et al., 1996; Ebinger et al., 1993; Balestrieri et al., 2016) and by transitional to tholeiitic flood basalts-with intercalated felsic

units. These Tertiary basaltic succession reaches a maximum thickness of 1 km and composed transitional tholeiitic and pyroclastic rocks that are mainly exposed in Amaro, Gamo, Gidole 500 m thick and around the Chew Bahir areas or Amaro- Gamo basalts (45-30 Ma) and the Miocene volcanism (19–11 Ma) 500m thick formed a large volume of alkali basalts and trachytes (Ebinger et al., 1993). The Getera- Kele alkali basalt that are similar to the syn-rift volcanics of the MER (Alemayu et al., 2016c) whereas, Plio-Pleistocene volcanism was mostly limited to the axial zones of the rift (Yemane et al. 1999) and consist mafic lava composition alkaline basalt to intermediate rock and some pyroclastic deposition associated with alluvial from Figure 2.1 (George et al., 1999).

2.3. Tectonic setting of MER

The Main Ethiopian Rift (MERS) is a roughly NE trending sector of the East African Rift system that includes a series of rift segments extending from the Afar Triple Junction at the Red Sea-Gulf of Aden intersection to the Kenya Rift. This rift system shows different stages of development from initiation through break up to oceanic spreading in the north (Ebinger et al., 1996), because the system opened by faulting and magmatism, with a long-rift variations in style of extension interpreted as the expression of different stages in an evolutionary rift sequence (Cort et al., 2015; Keir et al., 2013). It is characterized by active extensional tectonics accommodating the 6–7 mm/yr relative movement between the Ethiopian and Somalian plates (Chuand Gordon, 1999; Fernandes et al., 2004; Bonini et al., 2005). Though Ethiopian rift system is classified in to Afar and MER (Corti, 2009) it is consisting of three rift segments (NMER, CMER and SMER) reflecting different orientation of the fault boundaries (Giday Wolde Gabriel et al., 1990; Bonini et al., 2005; Kurz et al., 2007; Keranen and Klemperer, 2008; Corti, 2009).

The topographic expression of the northern MER is defined by ~NE striking border faults that become more N–S in the central and southern MER (Corti, 2009 and references therein) and have accommodated extensional strain during Miocene times (Wolfenden et al., 2004). However, since ~2 Ma, the locus of extension has shifted in-rift to a ~20-km-wide zone of ~NNE striking Quaternary–Recent faults, fissures and chains of aligned volcanic cones (Ebinger and Casey, 2001). This Quaternary–Recent volcano-tectonic lineament was first described by Mohr (1962; 1967b) as the Wonji Fault Belt (WFB), and has been referred to in more recent literature as axial Quaternary magmatism segments (Ebinger and Casey, 2001; Keir et al., 2006a as cited in Rooney et al., 2011).

The different MER segments are bounded by major Miocene border faults, which form the main escarpments separating the ~100 km wide rift valley from the surrounding plateaus (Boccaletti et al., 1998). This plateau basalt exposed along northwest ward of Ethiopia support to mantle lithospheric thinning/melt by plum process during Oligocene time but the extension, basin subsidence and rift-flank uplift began during or after the second flood-basalt phase 11-8 Ma (Ebinger et al., 1993**).** However**,** the MER propagated into the Afar depression after 11 Ma (Wolde Gabriel et al., 1990; Wolfenden et al., 2004). In addition to this the total amount of extension of the MER increase northwards, being largest in the Afar triple junction and the MER itself gets wider and deeper northwards (Hayward and Ebinger, 1996; Lahitte et al., 2003; Abebe et al., 2007). According to Corti (2009) MER extends along NE-SW direction at the Red Sea - Gulf of Aden triple junction in the Afar depression and N-S in the south at the Turkana depression. The NMER is oriented N40°E where it is bounded by the Arboye and Sire boundary faults in the southeastern and by the Ankobor and Boru-Tura structural high in the Northwest side (Wolfenden et al., 2004).

In case of Central MER, the rift valley oriented and characterized by major rift escarpments on both western and eastern margins; boundary faults show an average trend around N30°E .The western margin is well expressed by the N25°E–N35°E-trending and ESE-dipping Guraghe and Fonko faults, whereas the eastern margin is well represented by the N30°E-trending and WNW-dipping Asela–Langano fault system (Corti et al., 2009). The transition from the central to the northern sector is marked primarily by a change in trend of the rift margins from NNE-SSW (central) to NE-SW (northern**) (**Rooney et al., 2012; Ferguson et al., 2013).

In case of SMER, the area is located in the overlap region between the southward propagating rifting of the Main Ethiopian Rift and the northward propagation of the of the N–S striking Kenya Rift system (WoldeGabriel and Aronson,1987; Ebinger et al., 2000 ; Bonini et al.,2005). These overlap region lies between Lake Turkana and Lake Chamo, and has been referred to as a 'broadly rifted zone' defined by volcanism and numerous horsts and grabens over the 300 km rift width (Davidson, 1983; Wolde Gabriel et al., 2000; Wolde Gabriel and Aronson, 1987; Ebinger et al., 2000) and modern tectonic activity is currently dominated by the southwestward migration of the Main Ethiopian Rift (Bonini et al., 2005) though rift propagation is irregular (Keranen and Klemperer, 2008). In SMER the boundary fault are oriented N0°E to N20°E due to rotation of the rift valley from N20°-35° to N 5°-20° (Corti, 2009). It is characterized by the Chencha major fault in the west, which is curvilinear in

shape oriented N-S and N40°E and the Agereselam linear shaped NNE-SSW trend boundary fault in the east (Corti, 2009). This MER is bifurcated in to two basins, Galana (Abaya) in eastern and Ganjuli (Chamo) basin in western, separated by N-S trending of Amaro horest. The rift is delimitated by few, widely spaced, and large normal faults that strike ~N0°–25° in eastern Galana basin (Balestrieri et al., 2019; Ebengir et al., 1993). In Gofa Province there is series of sub-parallel roughly NE–SW trending basins settled to the west of the Southern MER and most of these basins are half-grabens (Ebinger et al., 2000; Balestrieri et al., 2016), showing triangular shape with widening of the basins toward the south. Their western margin is marked by large ~N40°E-striking and southeast-dipping normal faults. Some of these faults are highly segmented by ~N150°E-striking transverse faults that locally delimit the basins to the south (Philippon et al., 2014) and the Chow Bahir basin is the youngest expression of the now-inactive eastward migrating N–S orientated rift basins. This area is so called broadly rifted zone (BRZ) and the complex region of interaction with the Kenyan rift (Ebinger et al., 2000). Although the SMER has been affected by an early Miocene deformation phase related to the northern propagation of the Kenyan rift, a significant slip on border faults occurred only during the Pliocene (Bonini et al., 2005). Generally this MER sector by a rotation of the rift valley from N20-35° to N5-20°E; accordingly, the orientation of the boundary faults is N0°E to ~N20°E (Cort e, 2009).

The MER started to develop during Miocene time (Davidson and Rex, 1980; Wolde Gabriel et al., 1990; Tadiwos Chernet et al., 1998) and progressively deepened during the Pliocene and Quaternary, evolving through a sequence of interacting half-graben segments, marking the boundary between the Nubia and Somalia plates (Hayward and Ebinger, 1996). The overall mean direction of the MER remains NE–SW (N40-E).

The youngest part of the MER is the axial zone, which coincides with the so-called Wonji Fault Belt, mainly formed during the Quaternary (Mohr, 1987; Boccaletti et al., 1998, 1999). As stated by Acocella and Korme, (2002) the separate distributions of the opening directions for the extension fractures in the northern and southern branches of the MER. The northern branch of the MER, characterized by a mean trend of $N47^0$ E is associated with a mean extension direction of $N51^0$W. The southern branch, characterized by a mean trend of $N32^0$ E is associated with a mean extension direction of $N54^0$W. The opening directions of the Holocene extension fractures measured along the axial part of the MER are consistent with an overall NW–SE trend, with a mean value of $N52^0$ W ± 20 is perpendicular to the mean MER trend $N40^0$E. The extension fractures in the axial part of the MER point out overall NW–SE

extension direction, with a normal distribution and a mean value N52^{0}w this associated with mean trend N23^{0}E in SMER and N470 E trend with associated mean extensional direction N51^0 E with over all NE-SW MER trend and NNE-SSW of Wonji fault belt (Acocella and Korme, 2002).

In case of the CMER it was initiated at 9.7-8.3 Ma ago with significant rifting at 5-3 Ma ago and with the eruption of voluminous silicic eruptions Bonini et al. (2005).

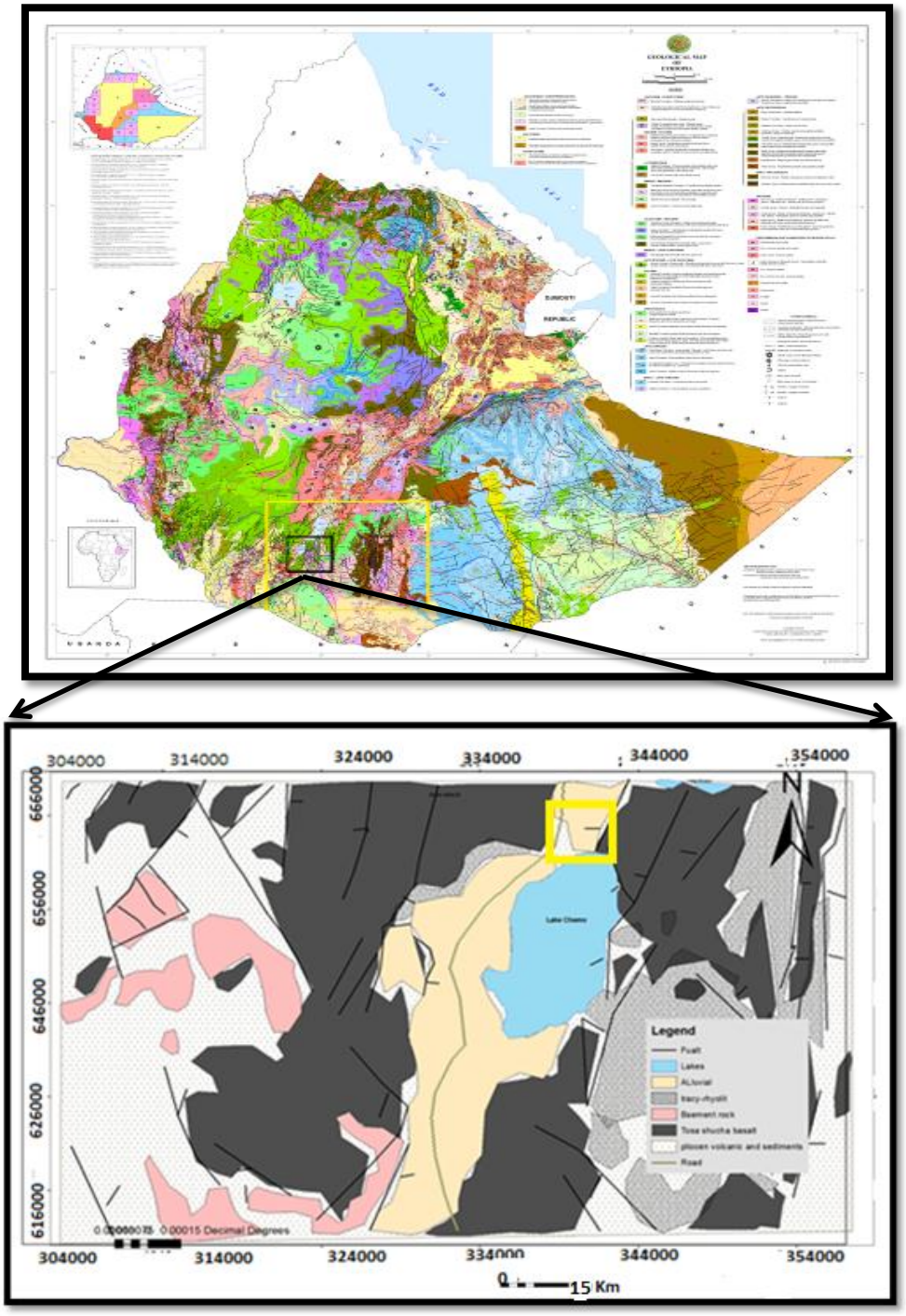

Figure 2. 1: Simplified Geological map of Arba Minch area taken from Geological survey of Ethiopia and re-edited at 2015 map, the square line indicate the study area.

CHAPTER THREE

3. GEOLOGY AND PETROGRAPHY OF STUDY AREA

3.1. Introduction

The area was investigated along selected traverse mostly by following foot track and gravel road (Fig .3.1). The various rock types exposed along different outcrops of study area specially; road cut, hill side, quarry Site, mountain top and mountain side. They were identified and classified based on field absorption, petrographic and geochemical point of view.

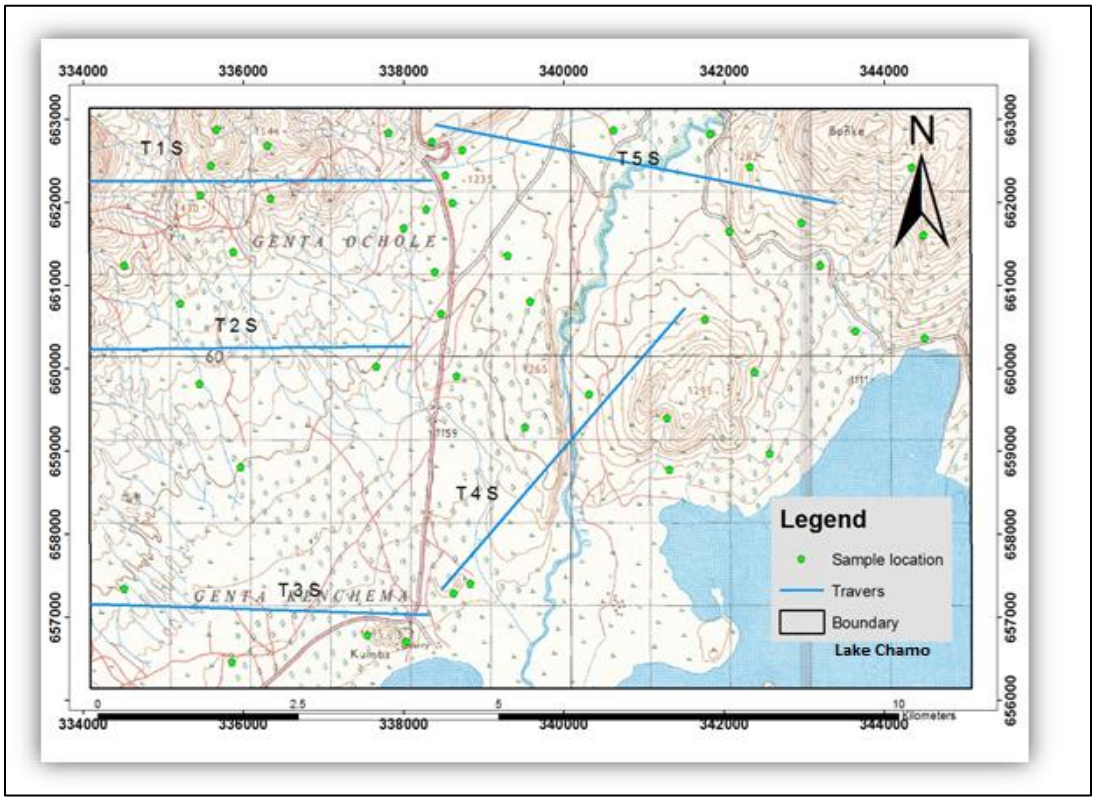

Figure 3. 1: *Sample location in the study area along selected traverse at the scale of 1:25,000: The data point mostly from road cut, quarry site, mountain top, hill side and mountain side.*

3.2. Lithology of study area

The rocks description and production of cross sectional map is based on the contact relation from only field information based on lithology variety for recent volcanism and geological map that prepared in this work. However, the stratigraphic section of the study area not discussed because the absence of data about recent age of the rock in detail and the area is not well studied especially quaternary rock stratigraphy secession previously. The study area is located in the southern part of Arba Minch particularly in center of rift floor of south Main

Ethiopian Rift. The area consist variety of lithology units; Such as basalts, intermediate rocks, scoria, unweldded tuff and Rhyolites. The basalt is most dominant rock unit according to field expedition and classified as aphyric basalt, porphyritic basalt, mildly porphyritic basalt and scoria based on their texture from petrographic investigation. The lithologies are shown blew.

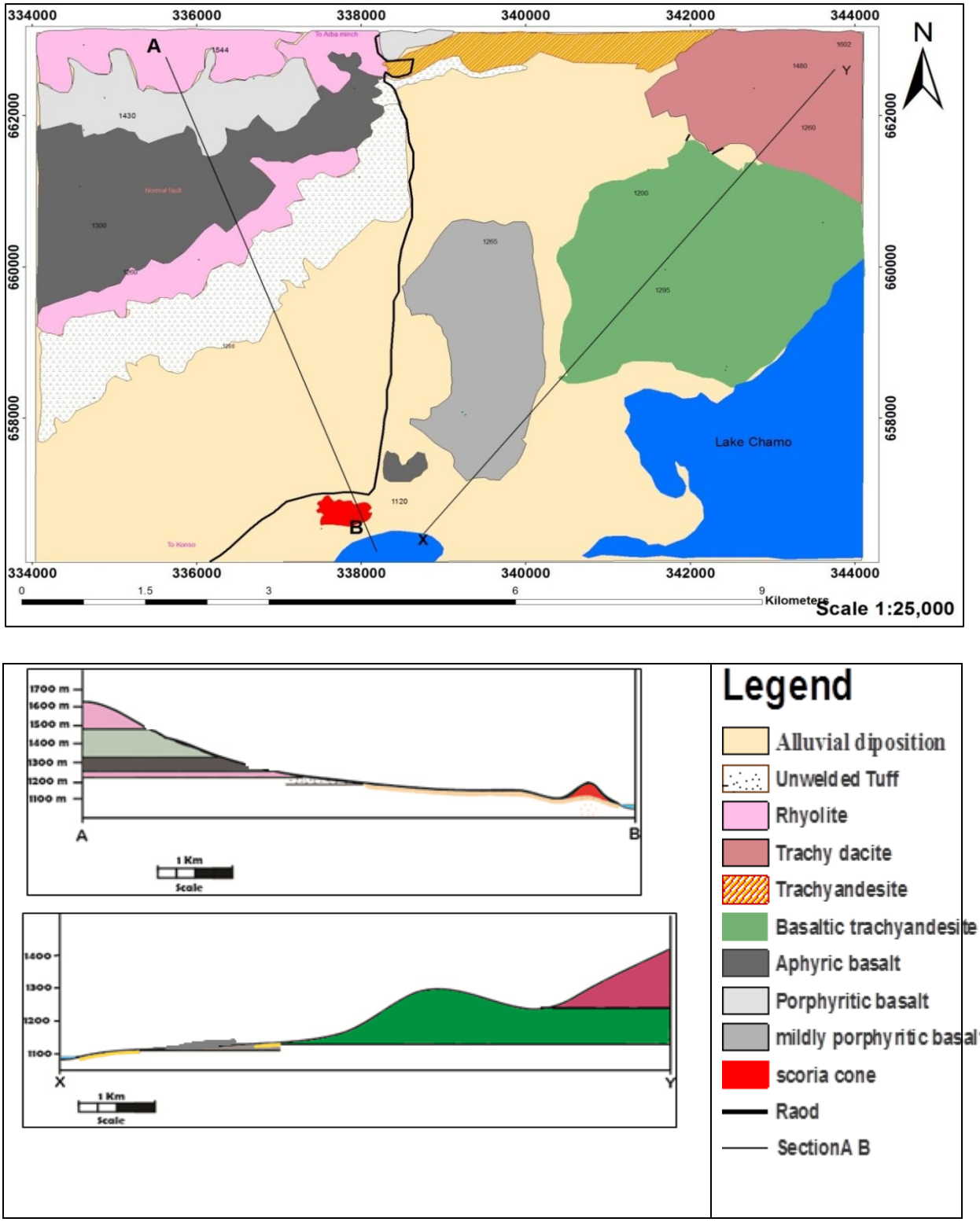

Figure 3. 2: Geological map of study area and geological cross-section map of study area.

3.2.1. Rhyolite

From eight major lithological units the rhyolite is Main one and locate especially north western of Lake Chamo in study area. The rhyolite rock observed in study area is lava flow form with flow bend exposed along contact with aphyric and porphyritic basalt on its bottom and top respectively at Ganta escarpment. The rock is characterized by light gray colored and having fine to medium grain k-feldspar phenocryst visible on hand specimen. At the western part of study area the rhyolite lava flow exposed along fault scarp (e.g. 0335952 E-0660942N locations) that run NE-SW direction around Ganta area. Generally, this unit has a maximum vertical thickness of 95 m, grey color and porphyritic in texture. In the other area rhyolite unit makes a massive block that is slightly jointed and having fine to moderate grain size.

Figure 3. 3: *Field photo and out crop of rhyolite exposed along Gant scarp that contains rhyolite lava flow (a) along fault scarp and (b) along road cut round Ganta scarp that locate in western part of study area.*

The sample (WGR) prepared for petrographic examination. The characterized by variety of porphyritic texture which has clusters of phenocryst, specially quartz and k-feldspars set in glassy ground mass or volcanic glassy. The dominant phenocrysts are alkali feldspar. Due to overgrowth of alkali feldspar phenocrys on quartz the rock shows radiate texture in photo (A&B). The intersertal texture formed by Fe-Ti oxide embedded on alkali feldspar and quartz whereas cryptocrystalline texture formed fragment of quartz and elongated medium grain of Fe-Ti oxide mineral on this sample. Maximum grain size of the phenocryst along there is 0.16 m Fe-Ti oxides, 0.87 mm alkali feldspar and 0.8 mm quartz. The average grain shape of all the phenocrysts is subdural.

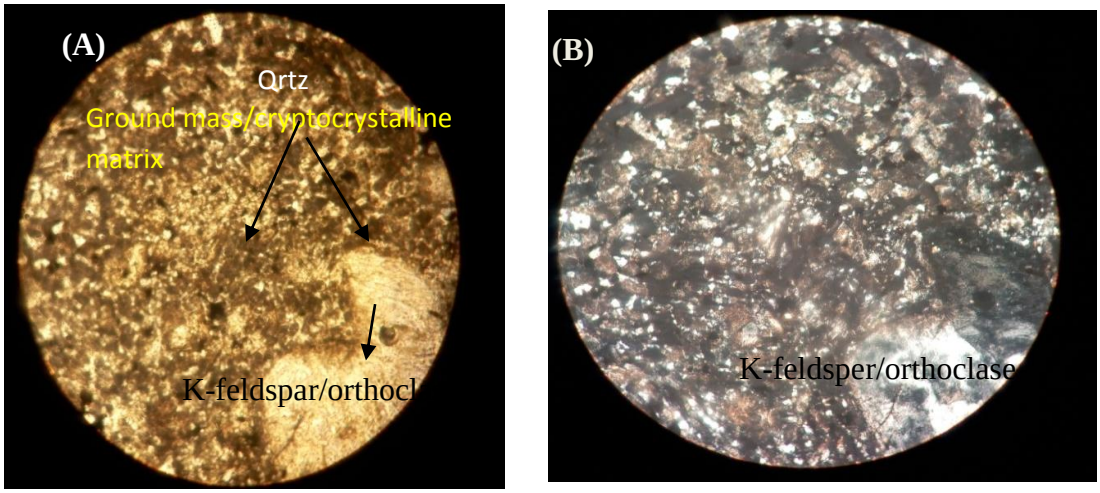

Figure 3. 4: *Microphoto picture of rhyolite sample WGR1 A&B. under optical microscope XPL (B) and PPL (A). The photo is taken 10 x magnifications in the view of 0.2mm.*

3.2.2. Unweldded tuff and volcanic ash flow.

Pyroclastic ash and unwldded tuff are other lithology units that exposed on study area especially along rift floor. Ash flow is the main lithological unit associated with alluvial diposition that enormously covers the study area in plain view. Relative to the other geological units, ash has a large proportion in area coverage and form a gentle slope. Depending on characteristic seen on the field; the ash flow unit is composed of pumice fragment and formed by pyroclastic flow which characterized by light grayish to white reddish in color and show intercalation of ash flow with lithic fragment layer. It found at different exposure part of study area, especially at bottom of scoria cone and unweldded tuff unit, in another area this unit associated with the alluvial deposition and reworked soil which is the alteration weathering product of surrounding rocks such as basalt, rhyolite, trachyandesite and scoria.

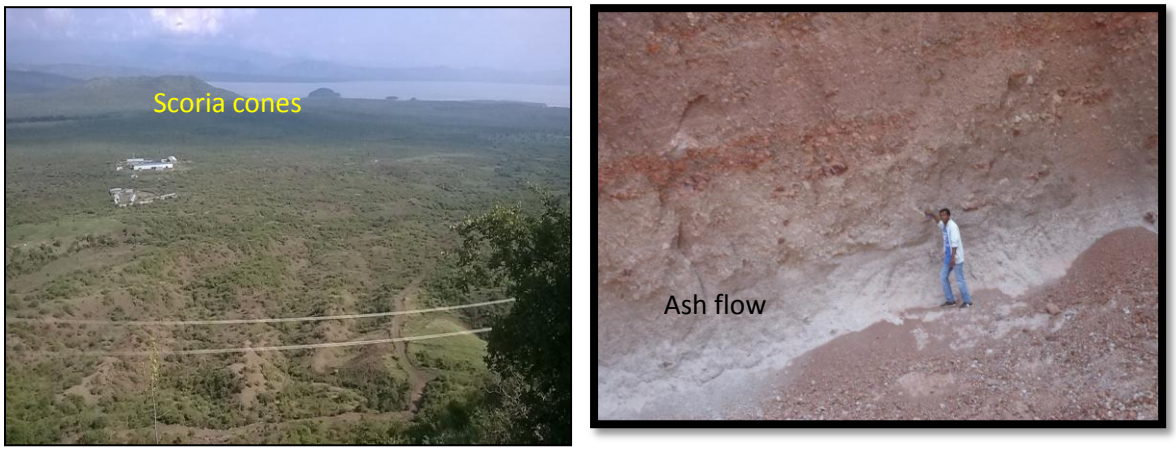

Figure 3. 5: *Exposure of volcanic ash and reworked soil bottom of scoria con and at the rift floor in central part of study area and alluvial deposit along north western part of Lake Chamo.*

The unweldded tuff exposed at bottom of aphyric and trachyandesite along road cut and on the different exposures the deposit show poor sorting, variation in vertical thickness cliff of 1-2m thick, white to brownish and poorly sorted pumice fragments and random distributed small sized angular rhyolite block are set on this rock, the fragments are hold together dominantly by ash sized material (matrix). This type of lithology unit found on southward from Arba Minch town and covers a small area relative to the ash flow and alluvial deposit, The unit is overlain by different rock units namely; aphyric basalt rhyolitic lava flow and trachandesite.

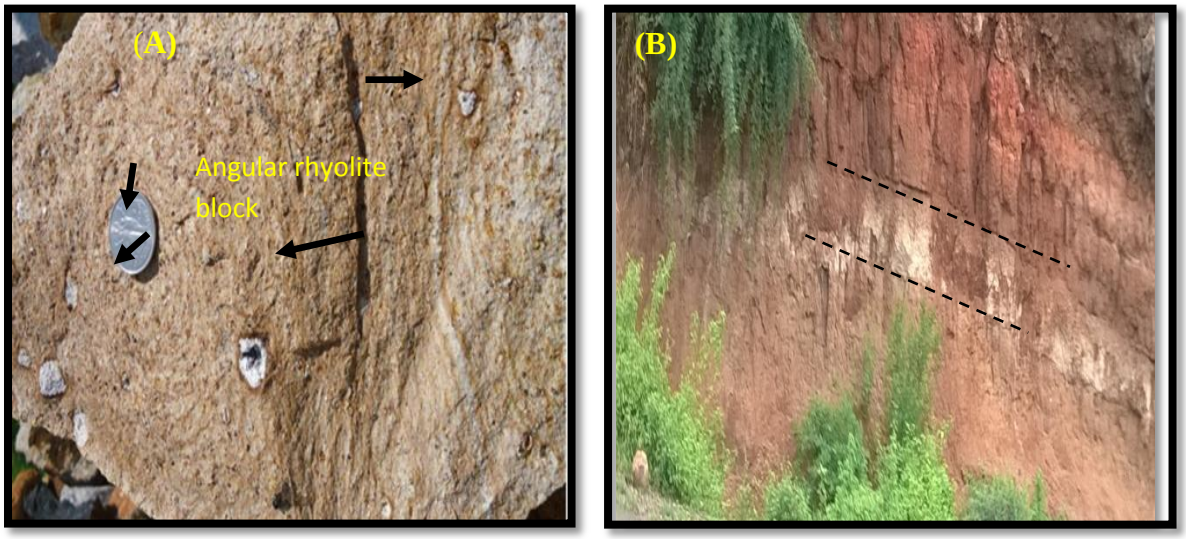

Figure 3. 6: *Unweldded tuff units in out crop of study area (A) are the selected sample and (B) is the field out crop of this rock.*

3.2.3 Intermediate rocks

The intermediate lava found on the study area by forming gentle slope and steep cliff and exposed along northern and northeastern of study area. They characterized by half mafic and half felsic behavior or they are being intermediate between felsic and mafic composition. Two samples (WT02 and WTLB) selected for petrographic analysis and description. Depending on field investigation from different exposure, the unit show dome like structure especially round Bonke region along NNE-SSW trending major fault which locate eastern from Kulfo River. Based on geochemical data result intermediate rocks are classified into basaltic trachyandesite, trachyandesite and trachydacite.

3.2.3.1 Trachydacite

This rock is one of intermediate rock type in study area. It is located round Nech Sar Natinal

Park in local name Tiliku Bonke region which is near to the Tosa Shucha area that is recent volcanic activity confides to active tectonic. The sample characterized by light gray to dark gray in color and consist large phenocryst probably plagioclase and Alkali feldspar minerals on ground mass. The rock is porphyritic with texture and exposed along mountain side and road cut in study area.

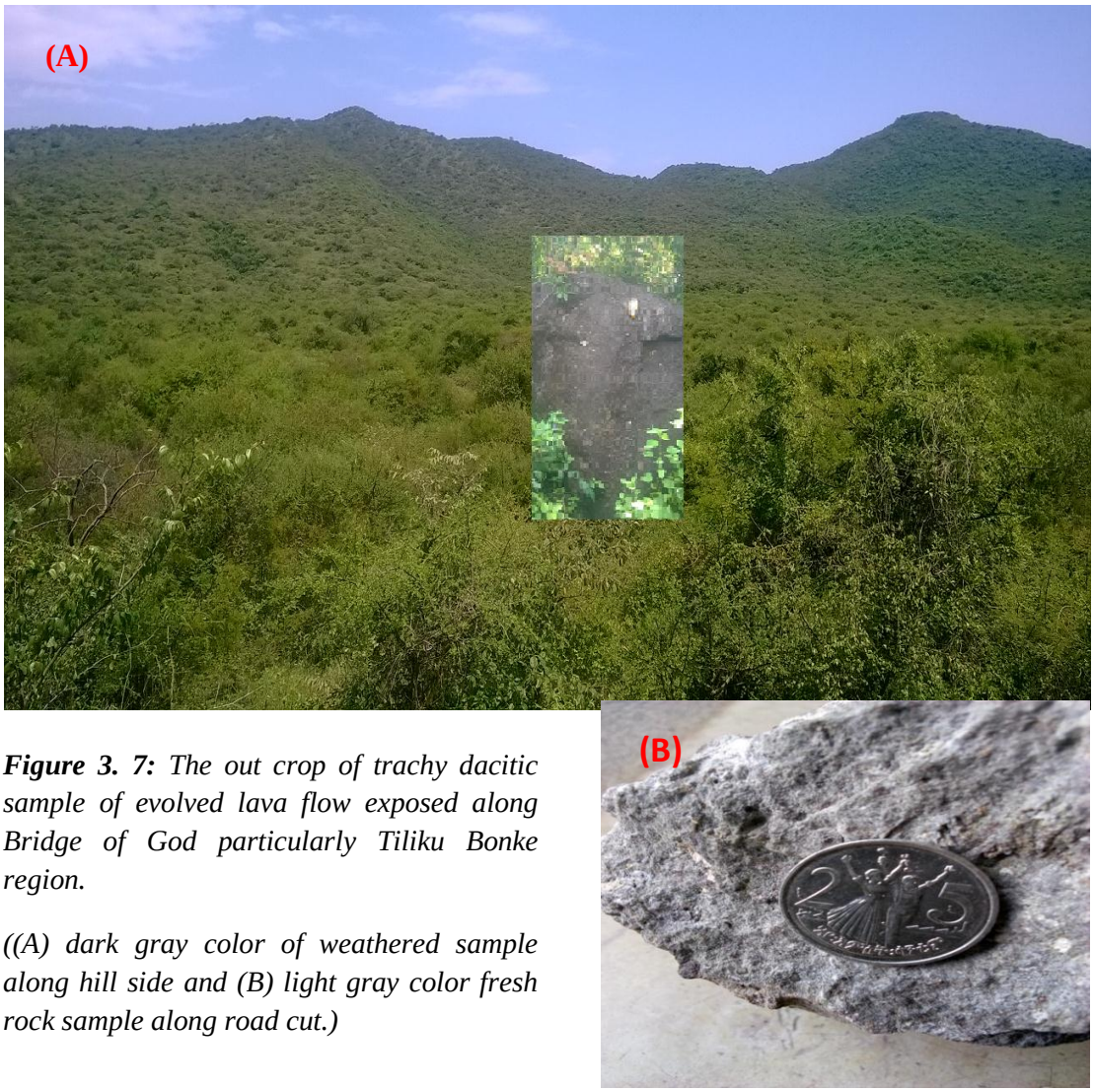

Figure 3. 7: *The out crop of trachy dacitic sample of evolved lava flow exposed along Bridge of God particularly Tiliku Bonke region.*

((A) dark gray color of weathered sample along hill side and (B) light gray color fresh rock sample along road cut.)

The sample (WTLB) selected for petrography analysis. The sample show seriate texture (Figure 3.8 WTLB) which is grain size has large variation under petrographic examination. The visible grain are mineralogical composition characterized by euhedral crystal shaped phenocryst of sanadine surrounded the microcrystalline groundmass of plagioclase, quartz and Fe-Ti oxide minerals with average grain size. The plagioclase is fine to medium grain of anhedral crystal shape with modal proportion 20%, alkaline feldspars with modal proportion 30% and quartz 21% set in glassy ground mass.

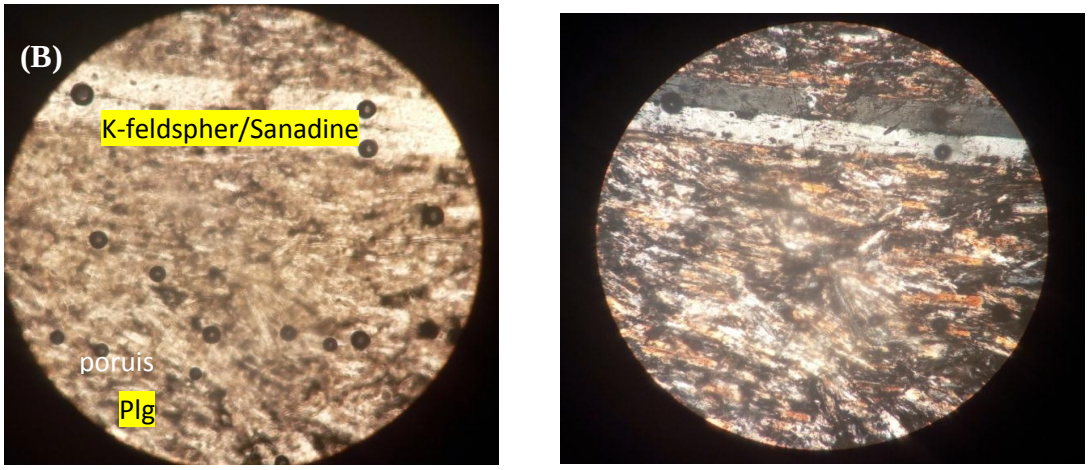

Figure 3. 8: *Microphoto picture of trachy dacite sample (WTLB) (A) & (B) Under optical microscope XPL and PPL. The photo is taken 10 x magnifications in the view of 0.2mm.*

3.2.3.2 Trachyandesite

This unit is another lithology from intermediate rock which covers small portion of study area especially exposed along northern part of study area specifically round Secha town. The rock has light to light gray fresh in color and characterized by medium grain phenocryst of plagioclase feldspar visible on hand specimen .Depend on field investigation from different exposure show that exfoliated structure on weathered rock sample (Figure 3.9 B). The hand spacemen characterized by medium grain plagioclase phenocryst with ground mass.

Figure 3.9: *Trachy andesitic rock out crop exposed along steep cliff of study area .The light reddish weathered and light gray fresh colored sample along road cut (A) and light gray colored with exfoliated structure on weathered surface of rock (B).*

The sample (WT02) selected for petrographic description. The sample show trachytic texture that show the plagioclase feldspar mineral aligned with single universal alignment direction and parallel orientation. The sample characterized by maximum amount of ground mass

composed of plagioclase; very fine grained pyroxene and opaque minerals (Fe-Ti oxide) show again show parallel orientation. The visible mineral grain is composition fine to medium grain phenocrysts of plagioclase set in are seen in pyroxene and opaque minerals (Fe-Ti oxide) ground mass.

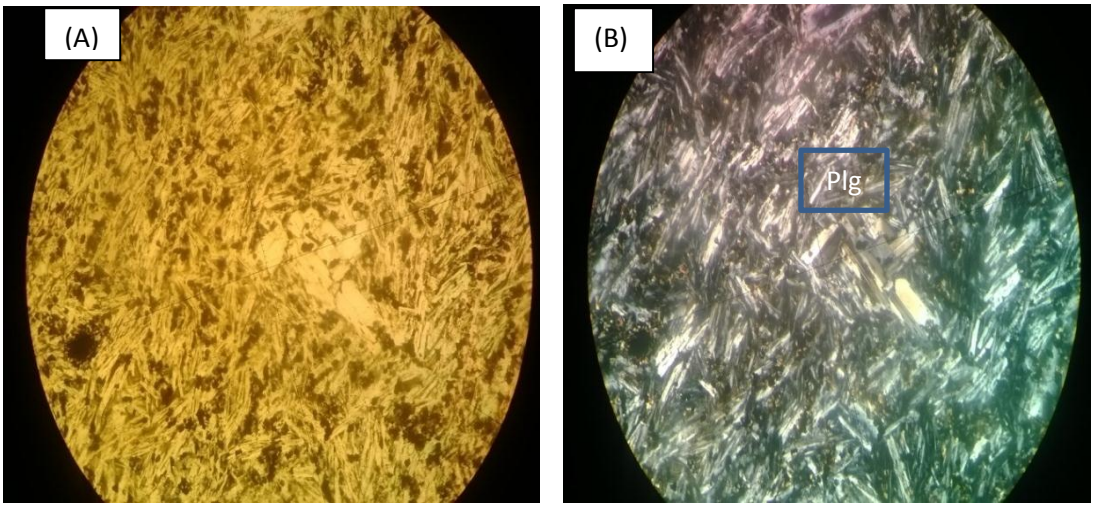

Figure 3.10: *Microphoto picture of trachyandesite sample (WT02) (A) under optical microscope PPL and XPL (B).The photo is taken10x magnification in the view of 0.2m.*

3.2.4 Basalt and scoria units

These lithology units are covering large portion of study area by forming steep cliff, fault exposure and gentle slope. These two varieties units are easily identifiable on a topographic map; form a cone like structure with a gentler slope on one side of the cone. The cone is made of scoria while gentle slope is formed by the associated basaltic lava flow (scoricias basalt). This basalt lava flow exposed dominantly along central part of study area and characterized by dense, has very small thin and interior vesicles without any secondary mineral filling (see Fig 3.19 A). It covers very small area and show similar character with that of aphyric basalt by both field absorption and petrographic description. The basalt lava flow found adjacent on round Ganta escarpment in western part of study area. Round this area the basalt unit forms a clear sharp contact with the rhyolite that covers the high land of the study area. Generally the basalt lava exposed on study area is show the following characters; Aphyric to porphyritic and mildly porphyritic texture and having dark, black and light gray to dark gray in color.

The scoria is another variety of lithology unit which exposed in study area and out cropped mainly kumba quarry site around Chamo Lake. The cone show large elliptical geometry and characterized by pyroclastic in texture with large fragmented. Quarry type of exposures is observed due to excavation activities for the purpose as a raw material of aggregates for

gravel and Asphalt roads on nearby localities. A typical example for quarry type exposure is on the Kumba scoria cone (Fig.3.17) that exposed 72 m vertically thick scoria deposit. The rock has dark to reddish in color. There is also ash flow which is light colored and fine grained fragment dust material found bottom of the cone which is one of volcanic formation in study area.

Based on their texture characteristics the basaltic units are classified in to Aphyric basalt, porphyritic and middle porphyritic basalt.

3.2.4.1 Aphyric basalt

This lithology unit is major one of basalt lava that exposed along northwestern part in study area, mainly outcropped on quarry side and stream cut. The aphyric basalt has black fresh and light to gray weathered in color (Figure 3.11 (b)) and characterized fine grained, massive groundmass which formed due to high rate of crystallization lattice that means it formed magmatic eruption by fast cooling rate. There is no any visible mineral on surface of hand specimen except, some calcite inclusion on ground mass.

Figure 3. 11: *The outcrop of aphyric basalt lava flow of aphyric textural basalt (a)). The rock exposed hill side along Ganta scarp and (b) is exposed along stream cut with highly fractured.*

The petrographic investigation of this sample show microcrystalline texture (Fig 3.12) which is the mineral grain probably visible under microscopy rather than hand specimen. The ground mass of pyroxene, plagioclase and opaque minerals (Fe-Ti oxide) showed sub parallel orientation. The average crystalline shape of anhedral phenocryst of plagioclase, orthopyroxene, interstitial glasses and few rounded bright interference colored cryptocrystalline olivine set in ground mass. However, plagioclase is dominant phenocryst

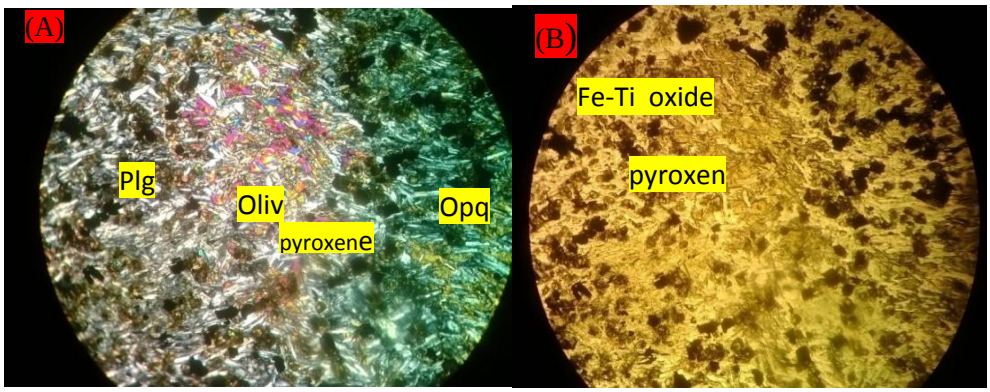

Figure 3. 12: *Microphoto picture of Aphyric basalt sample (WTG01) A&B Under optical microscope XPL and PPL respectively. The photo is taken10X magnification in the view of 0.2mm.*

3.2.4.2 Porphyritic basalt

This lithology is another textural variety of basalt unit. The lithology is located on northwestern and central part of study area, specifically round Ganta scarp and Arba Minch Secha town. Porphyritic basalt is characterized by the porphyry texture and it has black to dark gray in color and the rock has ground mass with phenocryst. The phenocryts are mainly composed of plagioclase feldspar, olivine and pyroxene (Fig. 3.13 (a)) formed by the magma rise to surface with large crystalized phenocryst and the rock have ground mass around mineral crystals. These porphyritic basalt lava show high amount of plagioclase phenocryst, fresh olivine and small amount of pyroxene with dark gray in color (Fig .3.13 (b)) which formed by quickly rate of cooling matrix and mineral formed prior to the extrusion that brought the magma to the surface.

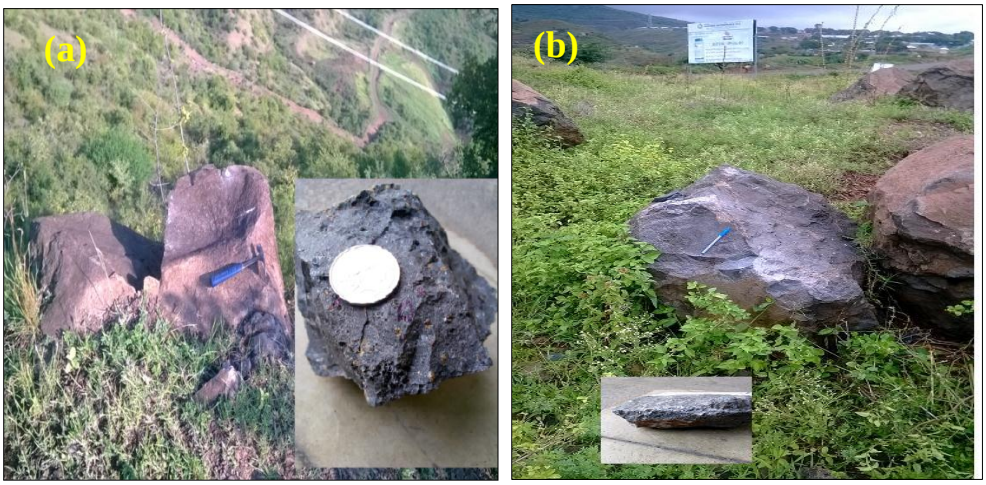

Figure 3.13: *(a) The out crop of porhyritic basalt exposed along hill side of Ganta scarp, and (b) exposed along road cut around Sech town near to rift floor.*

The sample (WT01) selected for petrographic examination. The microscopic interpretation of porphyritic basalt sample show seriate texture (crystal size show large variation) from (Fig

3.14c). This type of texture is porphyritic texture in which phenocryst show wide range of grain. The most dominant phenocryst is plagioclase feldspar with modal proportion 40% which characterized by growth zoning (Fig 3.14 (a)) and there are also elongated plagioclase without zoning 14% of euhedral shaped phenocryst of pyroxene (cpx) and 9% of fresh medium to coarse grain olivine minerals are there. Grain shapes of the phenocryst show that subdural (olivine and plagioclase, euhedral orthopyroxene and anhedral (Fe-Ti oxides)). The plagioclase feldspar shows a clear growth zoning.

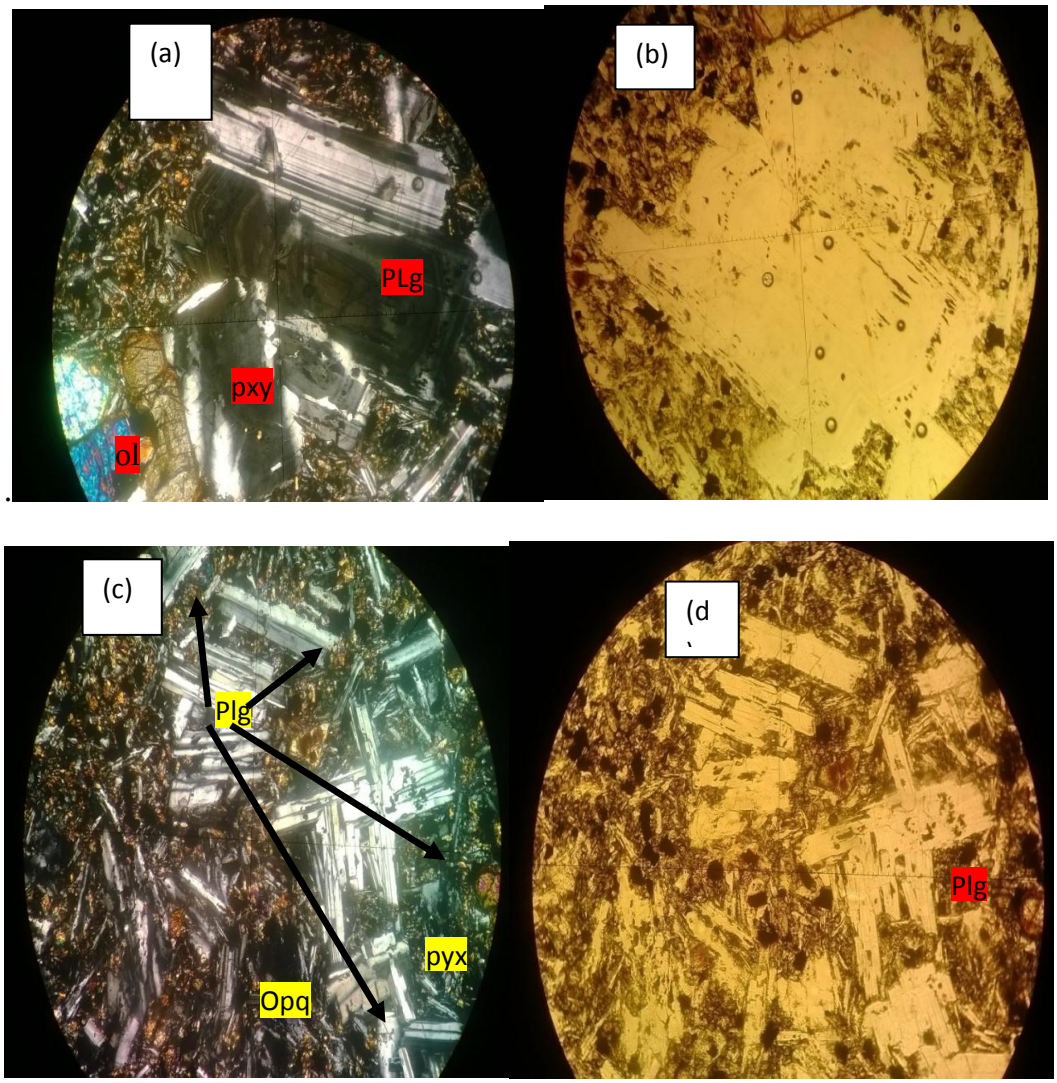

Figure 3. 14: *Microphoto picture of porphyratic basalt sample (WT01) a&d under optical microscope XPL and b& c under PPL. The photo is taken10x magnification in the view of 0.2mm.*

3.2.4.3 Mildly porphyritic basalt

The porphyritic basalt is another lithology of basalt unit in study area. The rock is mainly locate round of the scoria cone and cover large portion, especially north eastern and central

part of study area at specific location of 0338700-0342338E and 0659672-0661075N with average altitude of 1188-1290m. This rock distributed in rift floor and exposed along road cut. The hand specimen has black and light to dark in color and characterized by vesicular appearance (with irregular structure vesicle) (see Fig 3.15 A). This rock unit is formed by preserve gas bubbling and in open space by filling secondary materials during crystallization. When the magma finally reaches the surface as lava and cools, the gases expand and often are able to escape to the atmosphere as the lava cools and solidifies to form a volcanic rock. Since vesicles are open cavities, they sometimes become filled in with secondary alteration minerals such as calcite and quartz.

Figure 3. 15: *The out crop of middle porphyritic basalt exposed along NNE- SSW trended fault scarp distribute on rift floor.*

The sample (WT03) selected for petrographic description. The microscopic interpretation of mildly porphyritic basalt shows intersertal texture. The photograph below indicate that the ground mass (pyroxene and volcanic glass) is dominant proportion than the visible phenocryst which show the different sized crystal grain of mineral e.g. plagioclase, pyroxene (cpx) and olivine crystals set in glassy ground mass. In addition to that, there is large opened sub spherical gas cavity are randomly distributed on groundmass. The phenocryst of plagioclase characterized by lamellar twinning with modal proportion 23%, pyroxene 14%, olivine 4% and Fe-Ti oxide 15%. However, the dominant modal proportion is 40% of groundmass in this sample.

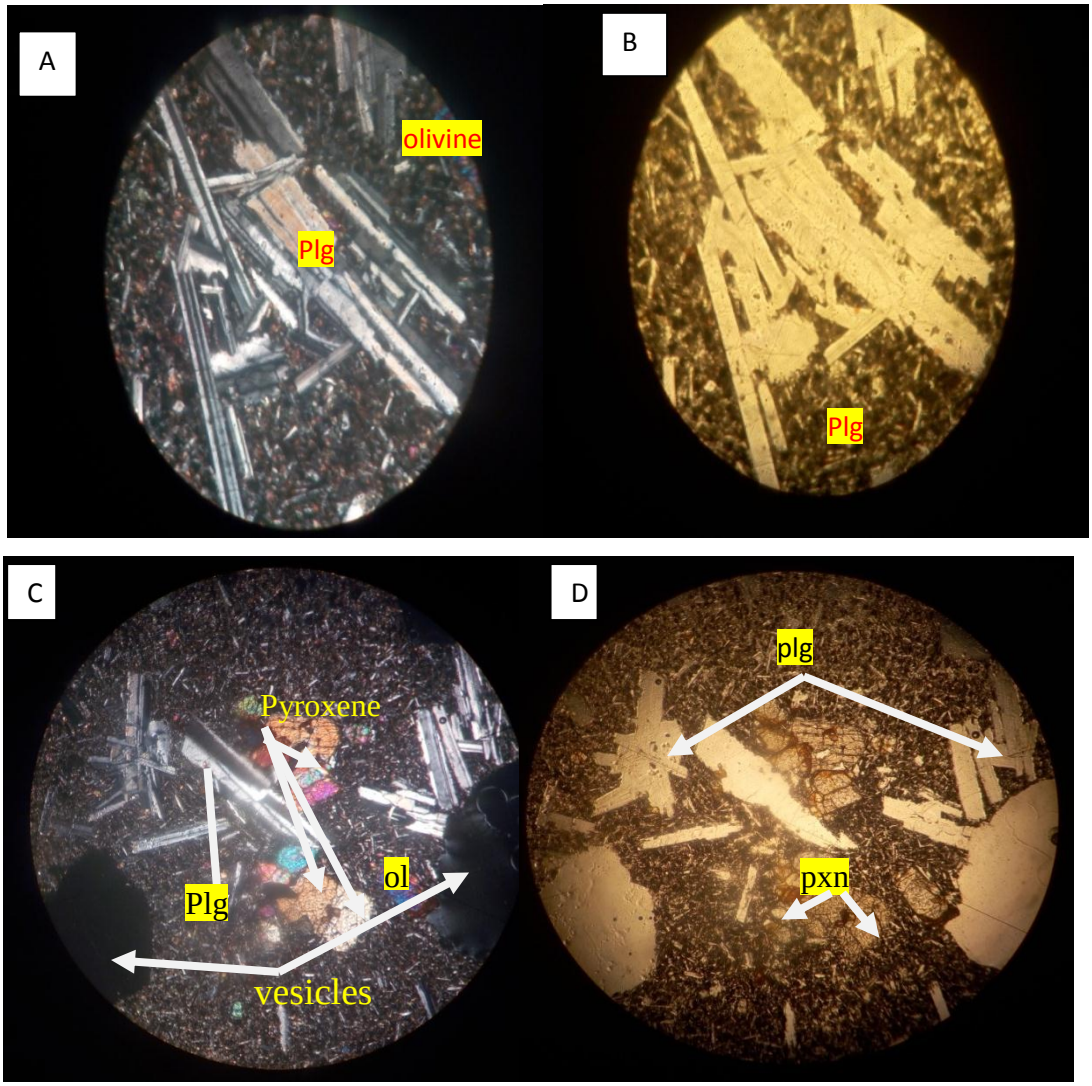

Figure 3. 16: *Microphoto picture of middle porphyritic basalt sample (WT03) A&C Under optical microscope XPL and B & D PPL. The photo is taken10x magnification in the view of 0.2m.*

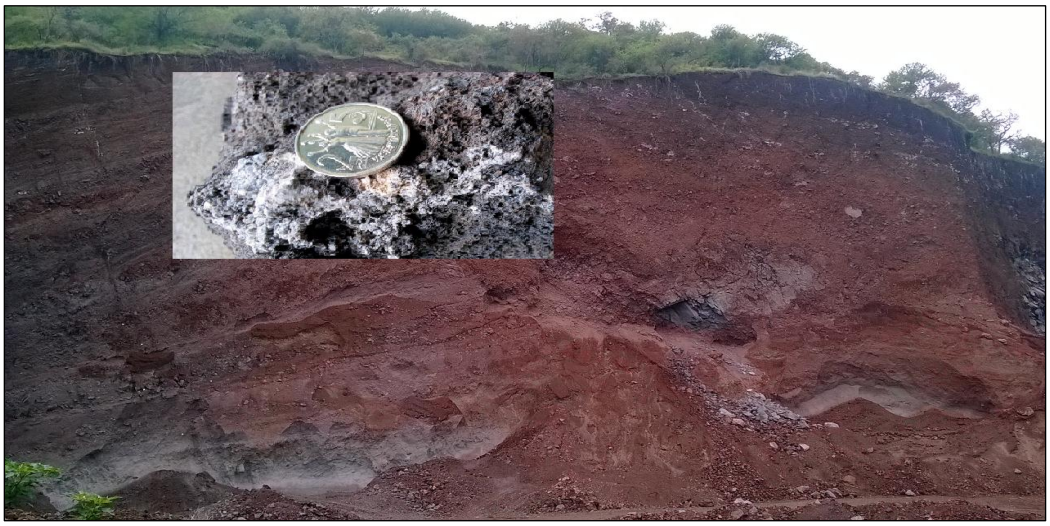

Figure 3. 17: *Out crop of scoria rock selected from Kumba quarry site of scoria cone which thick 74 m in study area.*

The sample (WT001) selected for petrographic description. The microscopic investigations of scoria unit show that the phenocrysts of plagioclase with lamellar twining surrounded by small amount of opaque (Fe-Ti oxide) minerals set in glassy ground mass. In the ground mass there is also highly porous space.

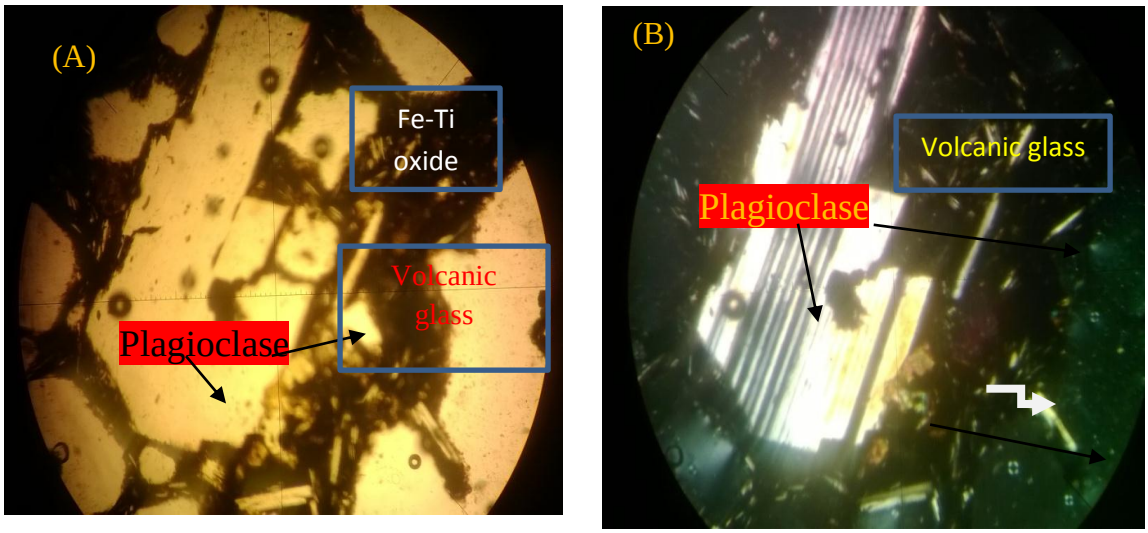

Figure 3. 18: *Microphoto picture of scoria cone sample WT001 of A, and B, is scoria unite which characterized by abundant vesicles that make up of 50% of rocks and has density greater than 1.*

Figure 3. 19: *Out crop of socricias basalt dark gray weathered and reddish to light gray fresh in color.*

3.3 Geological structure of study area

Since the Nech Sar volcano found in center of south main Ethiopian rift According to Bonini et al. (2005); Cort et al. (2009); Ebengir et al. (1993), there is narrowing accompanied by physiographical complexity with major boundary fault $N0^0$ E to $N20^0$ E and corresponding E-W trend transverse lineament . The study area is largely affected by rift tectonics**.** This rift tectonics affected of some of rocks of the area by discontinuity which makes the rocks less strength than the original rock unit. In general the geological structure observed in area is

grouped in to primary and secondary form. The primary geological structures are formed during rock formation process. These geological structures are discussed with lithologic unit description section e.g. flow bending of rhyolite and ash depositional layering however the secondary geological structures are structures which formed by a process that transpired on the rock after the rock formation process. The secondary geological structures that exposed in study area are joints and faults.

3.3.1 Joints

Joint is a fracture and have insignificant relative displacement between the blocks found on two sides of fractures. These structures are widely distributed in most of rock units, such as aphyric, porphyritic, mildly porphyritic basalt and rhyolite unit. Joint that observed in basaltic lava flow has orientation of NE-SW strike and (some NW-SE present) locate at 338000E-338407 and 662709- 662900N with elevation 1345m (Fig. 3.20 (a) and (b)) respectively. The orientation measurements of both joints and faults are presents in **Appendix II.**

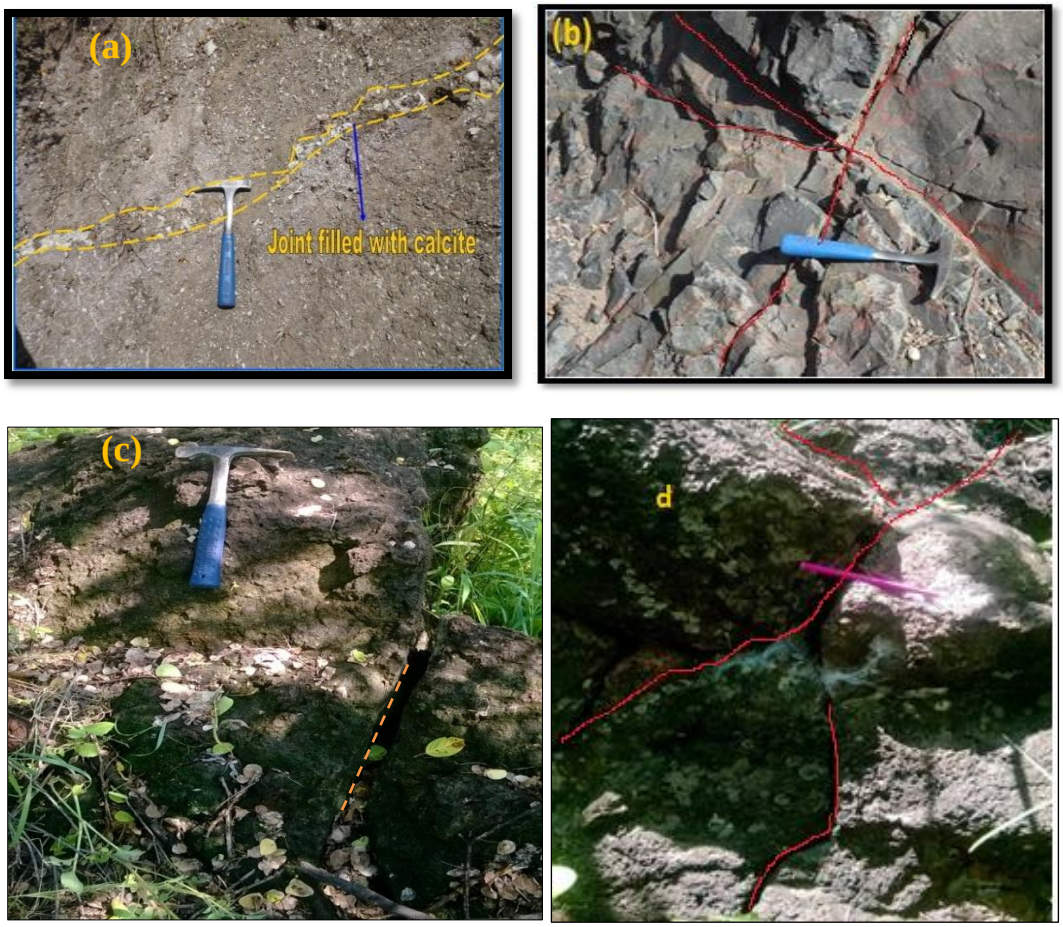

Figure 3. 20: *Joint exposed along aphyric and middle porphyritic basalt general orientation strike NE-SW and NW-SE respectively but there is some complex orientation along Tosa Shucha area from photo (d)).*

3.3.2 Fault

As stated by Mohr (1962; 1967b) Wonji Fault Belt is Quaternary–Recent volcano-tectonic lineament was first described and has been referred to in more recent literature as axial Quaternary magmatic segments (Ebinger and Casey, 2001; Keir et al., 2006a). The study area is mainly associated with active fault region. The normal fault is the dominant tectonic structure found in area. These geological structures more take place on the basaltic lava flow and rhyolite. The study area is obviously known that south Arba Minch town which is located at the floor of the south Main Ethiopian Rift system. The study area is characterized by a different sequence of normal fault systems. The western boundary/normal fault along basaltic lava flow was oriented with NE-SW tend (Fig 3.21 (a)) whereas fault along rhyolite lava flow oriented with strike NE-SW (Fig 3.21 (b)) is located at 337672-338423E and 062870-62762N with elevation1440 m. In generally their direction is parallel to the MER (NE-SW). However, the eastern boundary/ normal fault in study area characterized by trending in NNE-SSW directions parallel to the Wonji Fault Belt. The Detail their orientation measurement present in **Appendixes II**.

Figure 3. 7: *Photo picture major normal fault cuts aphyric basalt and rhyolitic lava flow with orientation NE-SW (a) and (b) and eastern part normal fault with orientation NNE-SSW on trachydacitic out crop (c)*

CHAPTER FOUR
4. GEOCHEMISTRY

4.1 Introduction

Many petrogenetic studies in the rift involve the use of geochemical data to discriminate the petrogenetic processes and origin of the rock (Dereje Ayalew et al., 2016; 2000; 2011; 2002; 2006; Georg and Rogers, 1999). Major elements, trace elements and isotopic character in magma have been used for petrogenetic study (Trua et al., 1999 and Dereje Ayalew et al., 2006). In this study only major and trace element data have been used to investigate petrogenesis of volcanic rocks. Major and trace element analysis of the samples are plotted in the variation diagram, and as chondrite and primordial mantle normalized patterns.

4.2 Methodology

A total 12 samples selected for geochemical analysis (5 basalts unite, 2 scoria unite, 3 intermediate rocks and 2 acidic rocks) were selected for whole rock geochemical analysis based on their freshness and representatives of the study area. These samples are represent the lithological distribution in the study area and encountered for both geochemical and thin-section analysis. For geochemical analysis the sample preparation has been conducted in ALS Addis Ababa crushing and milling room and gets whole rock geochemical analyzed in the Australian laboratory Science (ALS) in Ireland. Major elements were analyzed by analytical method of ICP-AES using Multi-Element Inductively Coupled Plasma whereas trace elements were analyzed by analytical method of ICP-MS using Multi-Element Mass Spectrometry techniques. The detection capacity of the method ranges between 0.1 and 100% for major elements and generally 0.01 to 10,000 ppm for trace elements except for Cr (10-10,000 ppm), V (5-10,000 ppm), Ni (1-10,000) and Pb (2-10,000). Here only Cr in the rhyolites and scoria cone is reported less than the detection limit (<10ppm) whereas the others are above the sensitivities of the instruments.

4.3. Results

From total twelve samples one sample shows slightly high value LIO. Whereas the two samples show moderately low value LOI. The sample that shows LOI > 1.90 is collected from evolved lava. In contrast the samples show LOI < 0 are collected from scoria cone. The results are presented in Table 4.1

Table 4. 1 The geochemical result of NSV samples. The NSV samples are presented on the table the notation stands for LD- Detection Limit. The major element (including LOI) and trace element value of concentration is expressed by wt. % and ppm respectively. The geochemical data is normalized in volatile free base.)

Sample	ANBGS	ANPBGS	ANSC2	ANPBAS	ANVBKR	ANSB	ANIAS	ANSDP	ANTB	ANISC	ANRCAP	ANRGW
SiO2	47.2609	46.7778	48.3151	48.6416	49.7463	52.5048	55.2023	55.5056	60.6904	61.0846	67.8697	71.788
TiO2	1.74815	1.92732	1.82704	2.06752	1.96	1.76689	1.63488	1.31776	0.55641	0.72507	0.22055	0.14378
Al2O3	15.9061	15.8101	15.0223	16.7299	17.262	16.8658	18.3671	17.9195	18.0319	17.1832	17.4937	14.3268
Fe2O3	13.6701	11.3933	11.419	11.0867	11.0934	10.1395	8.18448	9.44395	6.33694	7.07191	2.38596	3.30697
MnO	0.20327	0.16061	0.1827	0.1698	0.16914	0.16063	0.16147	0.21963	0.17517	0.18872	0.02005	0.08216
MgO	8.34434	9.26521	8.38408	5.96284	5.20346	3.9755	2.4725	1.89678	0.86553	0.92372	0.23058	0.16432
CaO	9.21842	11.1423	11.013	10.4874	9.47169	8.23211	5.36886	4.92163	3.10149	3.06913	0.4411	0.53405
Na2O	2.73402	2.29874	2.33455	2.96644	3.13402	3.73456	4.72298	5.38085	6.14116	5.86015	5.86466	4.8783
K2O	0.51835	0.91347	1.02517	1.39832	1.50234	2.14838	3.27985	2.81521	3.8846	3.63528	5.44361	4.74479
P2O5	0.39638	0.31118	0.47706	0.48941	0.45767	0.47184	0.60551	0.57902	0.21638	0.25824	0.03008	0.03081
Total	**100**	**100**	**100**	**100**	**100**	**100**	**100**	**100**	**100**	**100**	**100**	**100**

Mg#	54.97154	61.92553	59.48866	51.82292	48.40352	43.95117	37.66334	28.65762	21.45594	20.71269	16.19718	9.039548
LOI	1.68	1.15	1.42	0.84	0.42	-0.04	1.95	0.47	0.82	-0.19	1.77	1.73
Li	10	10	10	10	10	10	10	10	10	10	10	10
K	4222	7535.03	8363.06	11592	12586	17719.7	26910.8	23350.3	31216.6	30305	44961.8	38255
Sc	29	28	29	24	25	20	7	6	5	4	3	0.8
Ti	10320	11520	10800	12420	11820	10560	9720	7920	3000	4380	1320	840
V	284	305	248	283	273	220	86	30	21	8	4	4
Cr	250	410	540	90	80	30	<L.D	<L.D	10	10	9	8
Ni	131	196	217	67	52	28	1	3	7	2	2	0.5
Ga	19.1	16.1	15.6	16.6	18.2	18.4	20	20.6	19.6	20.9	30.9	47.3
P	1702.8	1353.52	2052.11	2139.4	2008.45	2052.11	2619.71	2532.39	873.239	1135.21	130.98	130.98
Rb	7.2	32.7	26.3	33.3	33.6	48.9	90.6	70.5	97.1	111	113.5	365
Sr	278	601	516	670	541	486	709	633	372	426	25.3	14.1
Y	27.8	19.4	21	24.2	24.9	26	29.4	31	27	29.4	66.1	129.5
Zr	149	94	102	131	143	192	249	246	277	309	976	1560
Nb	18.8	46.7	52.2	58.9	47.2	57.3	109.5	117	121.5	122	190.5	784
Cs	0.02	0.39	0.13	0.21	0.18	0.05	0.58	0.6	0.61	0.48	0.49	1.76
Ba	190	374	449	510	536	546	949	1105	1270	1160	272	18
Hf	3	2.4	2.5	2.9	3.4	4.8	5.6	5.3	5.9	6.4	21.1	40.6
Ta	0.4	1.7	2	2.4	2.3	2.8	5.7	6.1	5.9	6.7	10.8	43.3

La	18.1	32.2	38.8	39.9	34.2	43.2	72.4	80.4	75.1	78.9	141.5	150.5
Ce	36.2	57.7	66.5	71	60.2	73.6	124	136	121.5	133	242	286
Pr	4.78	6.45	7.25	8.08	7.01	8.33	13.55	14.1	11.95	13.4	30.3	31
Nd	21.2	25	27.7	32.4	28.1	31.6	47.9	48.9	41	44.7	108.5	104.5
Sm	4.61	4.5	4.94	5.58	5.39	5.56	7.47	7.23	5.88	6.94	18.05	20.8
Eu	1.54	1.46	1.68	1.8	1.85	1.69	2.29	2.33	1.77	1.96	2.66	0.45
Gd	5.26	4.34	4.49	5.26	5.06	5.29	6.5	6.52	4.68	5.73	14.1	17.45
Tb	0.74	0.6	0.65	0.77	0.75	0.78	0.93	0.87	0.72	0.92	2.1	3.32
Dy	5.04	3.58	3.99	4.5	4.39	4.58	5.44	5.58	4.28	5.44	12.25	20.5
Ho	1.01	0.75	0.86	0.85	0.94	0.96	1.14	1.11	0.94	1.06	2.55	4.37
Er	2.63	1.93	2.17	2.28	2.69	2.7	3.12	3.31	2.78	3.2	7.18	12.25
Tm	0.41	0.25	0.28	0.35	0.35	0.41	0.47	0.47	0.36	0.51	1.14	2.16
Yb	2.77	1.65	2.04	2.25	2.37	2.47	3	3.13	2.73	3.24	7.78	13.2
Lu	0.37	0.25	0.23	0.32	0.32	0.36	0.42	0.45	0.43	0.49	1.07	1.87
Pb	<L.D.	5	7	2	4	3	7	9	11	5	19	32
Th	1.54	5.06	5.58	5.74	5.68	9.55	15	14.45	14.3	18.55	20.7	75.5
U	0.38	0.79	0.97	0.89	0.98	0.76	2.31	2.67	2.1	2.38	4.78	13.1

Table 4. 2 CIPW normative minerals calculations (in wt. %) CIPW normative minerals calculations (in wt%) were performed using the norm-calculating program based on (after Thompson, 1984).

CIP Norm mine	ANBGS	ANPBGS	ANSC2	ANPBAS	ANVBKR	ANSB	ANIAS	ANSCP	ANTB	ANISC	ANRCAP	ANRGW
Quartz	1.25	0.00	1.28	0.49	2.37	3.53	2.46	2.59	3.62	6.65	21.3	28.97
Plagioclase	52.72	49.59	47.20	53.31	55.10	54.50	59.19	61.94	62.13	59.41	51.57	13.73
Orthoclase	3.07	5.38	6.09	8.27	8.86	12.71	19.38	16.67	22.93	21.51	32.15	38.01
Diopside	6.38	13.25	14.27	10.99	7.16	7.23	0.00	0.36	1.96	1.49	3.00	4.00
Hypersthene	17.82	10.58	14.26	9.75	9.63	6.56	6.15	4.56	1.26	1.60	0.57	0.40
Olivine	0.00	4.46	0.00	0.00	0.00	0.00	0.00	0.00	0.00	0.00	0.00	0.00
Rutile	0.00	0.00	0.00	0.00	0.00	0.00	0.47	0.00	0.00	0.00	0.20	0.05
Ilmenite	0.43	0.34	0.39	0.36	0.36	0.34	0.34	0.47	0.39	0.41	0.04	0.17
Hematite	13.67	11.39	11.42	11.09	11.09	10.14	8.18	9.44	6.34	7.07	2.39	3.31
Apatite	0.93	0.72	1.11	1.14	1.07	1.09	1.41	1.34	0.51	0.60	0.07	0.07
Sphene	3.74	4.29	3.99	4.61	4.34	3.90	2.40	2.63	0.88	1.27	0.00	0.00

4.3.1 Major element geochemistry

The major elements comprise most of the rock, found in high concentration, and form their own minerals with crystal lattice, expressed as weight present. In most case the elements are listed as Si, Ti, Al, Fe, Mn, Mg, Ca, Na, K and P and whose oxides are normally found at levels greater than 0.1% by mass, such as SiO_2, TiO_2, Al_2O_3, FeO, Fe_2O_3, MnO, MgO, CaO, Na_2O, K_2O and P_2O_5. The main goal of using major element geochemistry is to classify the rocks and the fractionation order of mineral crystallization.

The major element analytical data of the twelve samples collected from the study area is used in oxide form. The raw analytical data readjusted to volatile free bases to use for the interpretation and to draw the graphs by normalizing the major element concentration value to 100% by subtracting the volatile concentration (that is presented as LOI). Major element data can be used in reconstruction of variation diagrams, which reveal interrelationship between elements in the data set. The variation diagram have been constructed for major element oxide wt. %. The SiO_2 is chosen as X-axis differentiation index because it shows greater variability than any other oxides and it is the major constituent of the rocks of study area because it serves as index of advancing fractionation from basalt to rhyolite.

As shown in Fig 4.1 the total alkali silica (TAS after Le Bas et al., 1986) classification diagram of Nech sar volcanic rocks indicate that the analyzed samples are mainly classified as basalts, basaltic trachyandesite, trachyandesites, trachyte/trachydacites and rhyolite. All basalts are suite transitional to weakly sub alkaline on TAS diagram and from Hy-norm basalt from CIPW norm mineral calculation. The result present in Table 4.2 and Analytical data of major and trace element reported in Table 4.1

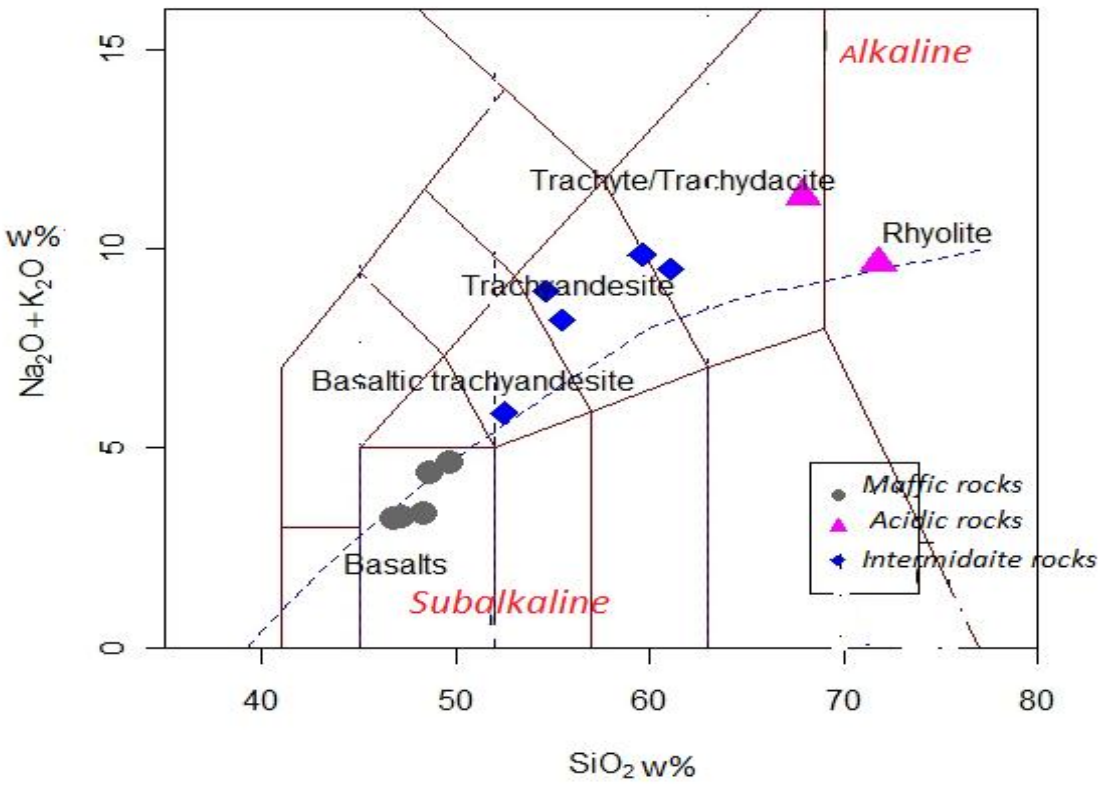

Figure 4. 1: *TAS diagram (after Le Bas et al., 1986) and overlay of alkaline-sub alkaline basalt classification diagram) for samples collected from southern Arba Minch (NSV*

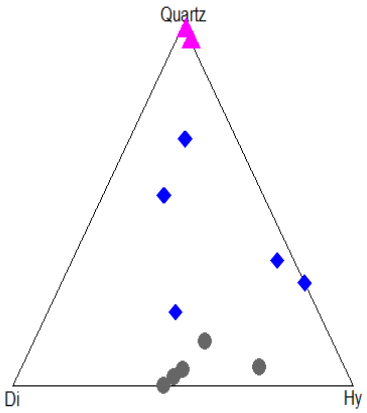

Figure 4. 2: *The classification of basalt and related rocks according CIPW normative composition expressed as Di-Hy-Q (after Thompson, 1984). The basalts are hypersthene norm However; the felsic rock classification is expressed by An- Di which shows all felsic rocks are silica saturated.*

The variations of major elements as function of silica for analyzed rocks are plotted for selected major elements on each sample to get the variation that is shown on the general major element variation diagram of types of rocks. Different symbols are used to represent different rock types. The major element content of Nech Sar volcanic rocks define continues

trend, which represent changing the composition of the magma during fractional crystallization. All basaltic samples are characterized by low Ni (<250 ppm) and Mg# (<65) contents. These values are very low compared to a primary magma. According to Rebino Gill, 2010 from books of igneous rock and process 2nd edition, the Mg number value for primary melt greater than 65 and Ni>250 ppm. The Mg# number calculated from MgO by the formula of ((MgO/40)/ (MgO/40 + Fe_2O_3/80))*100.

The general major element variation diagram of mafic, intermediate and acidic rocks is plotted and presented in the next section. The major element variation diagram on the different plots shows linear slope and curvilinear trend. For instant MgO, CaO, Fe2O3 and TiO_2 against SiO_2 show negative trend which indicate sharply decrease with silica increase, whereas Al_2O_3 and P_2O_5 show inflected trend with SiO_2 indication of accommodation of Al and P bearing mineral for mafic and some intermediate rocks but slightly decrease for acidic rocks correlate with SiO2 increase. However, K_2O and Na_2O correlates positive with SiO_2 increasing up to 67 % wt. SiO_2 and then decrease slightly for rhyolite rock with silica increase. In case of MnO plot become constant variation for all rocks.

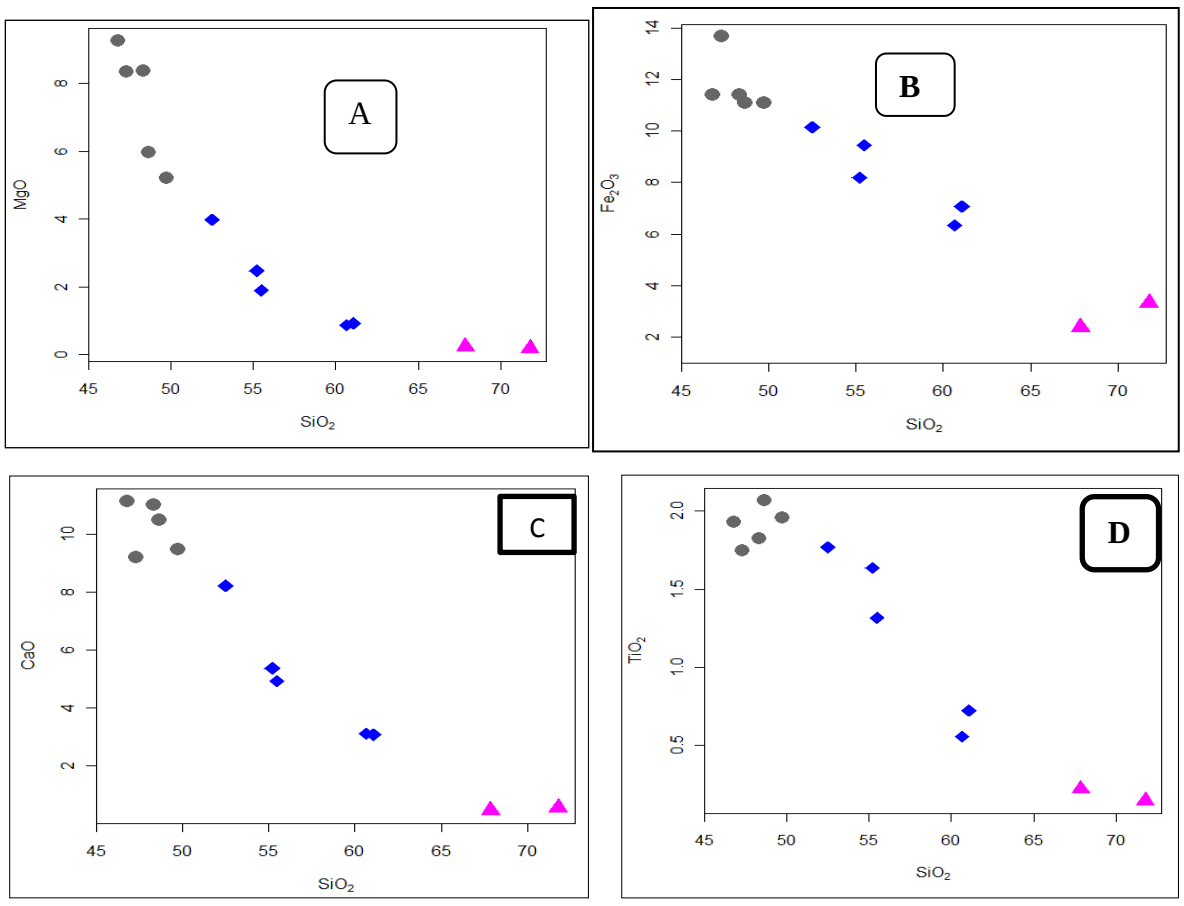

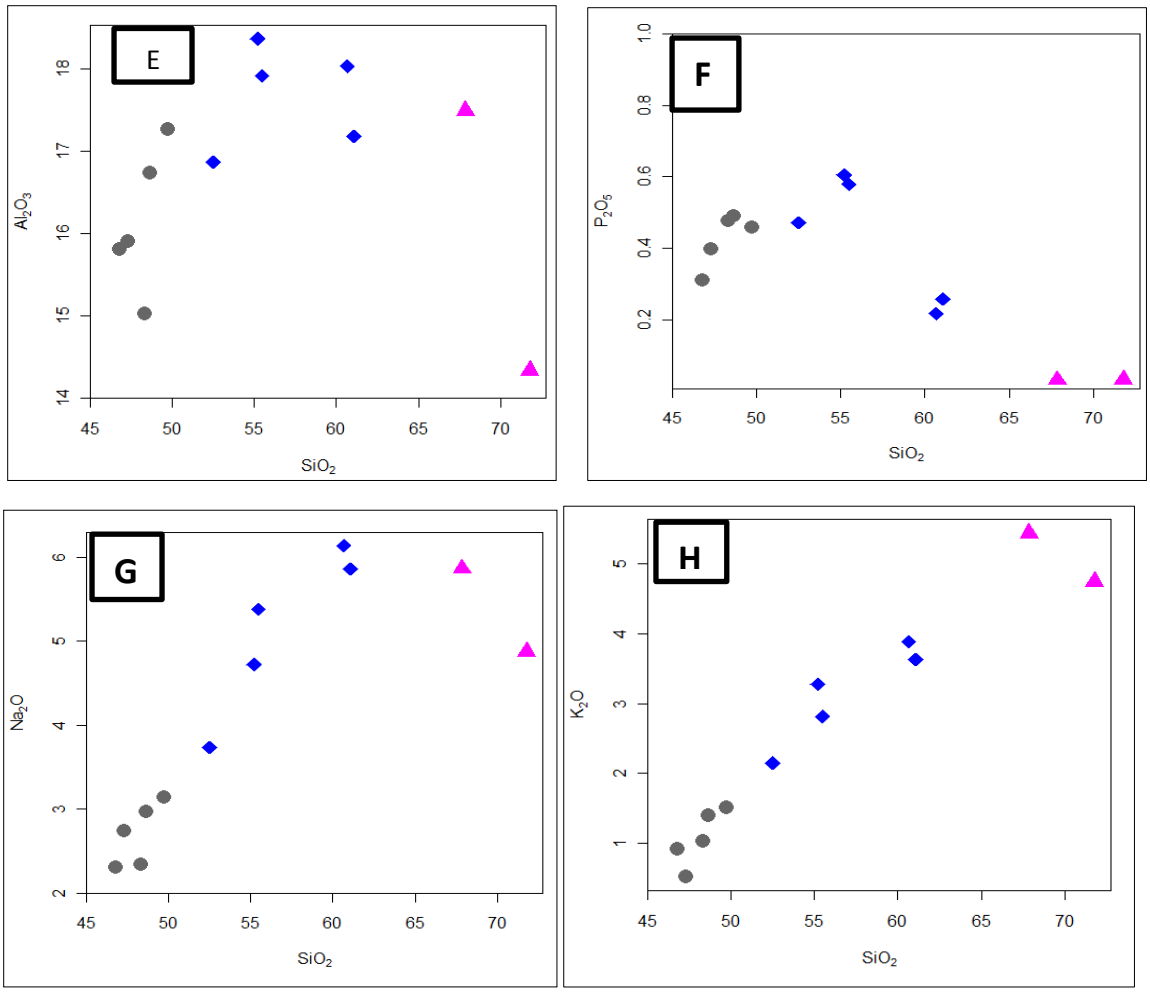

Figure 4. 3: *Variation diagram of whole rock composition for all representative rock samples that collected from Nech sar volcanic rocks.*

The chemical changes that explain the magma differentiation can be investigated by plotting analyses of the erupted rocks in variation diagrams. Initially the MgO, CaO, TiO_2 and Fe_2O_3 content fall steeply for the mafic samples and after which it decline more gently both for intermediate and felsic rocks in the diagram for against SiO_2 suggest that the olivine fractionation from system in initial level then followed by clinopyroxene, Fe-Ti oxide, plagioclase and apatite. The variation diagram of Al_2O_3 and P_2O_5 with SiO_2 shows the removal of Al and P bearing minerals such as plagioclase and apatite respectively from system for some evolved and felsic rocks whereas both are show positive trend with SiO2 increase for mafic rocks and moderately accommodation of their bearing minerals. However, the variation diagram of K_2O and Na_2O versus SiO_2 is continues increasing with SiO2 and doesn't show clear removal of K and Na bearing minerals , this means it show moderately accommodation for all mafic and intermediate rocks but removal of K bearing mineral such as alkaline feldspars for rhyolite. The distribution of sample and slope of trend in the

diagrams express the crystallization order controlled by that early crystallized of olivine followed clinopyroxene, Fe-Ti oxide (ilmenite and hematite), plagioclase and apatite. The general trend from the major element variation diagram show a characteristic of igneous melt broadly flow the principle of fractional crystallization.

4.3.2 Trace element variation

Trace elements, that is, those with a concentration commonly less than 0.1% and expressed in parts per million (ppm) or more rarely by parts per billion (ppb) (Rollinson, 1993). Though trace elements, by definition, constitute only a small fraction of a system of interest, they provide geochemical and geological information out of proportion to their abundance. In igneous geochemistry, trace elements are useful in understanding condition at which the rocks are formed and magmatic processes such as partial melting and fractional crystallization will affect trace element abundances and in evaluating the composition of magma sources White, (2013). Based on mantle melt the trace elements are classified into compatible and incompatible. Compatible elements are preferentially incorporated into one or more crystallizing minerals relative to the melt; for example; Cr, Co, V, Sc, nickel is preferentially taken up by olivine; whereas, incompatible elements are performed in melt or do not easily fit in to crystal structure of mantle mineral during partial melting of magma. For example; K, Cs, Rb, Sr, Ba, REE, Ta, Hf, U, Pb, Th, Nb, and Zr… etc

The trace element data presentation and interpretation given in the section of this chapter is with the same grouping and symbols of main volcanic products, mafic, intermediate and acidic rocks, used on the major elements data presentation. The diagram in Fig 4.4 shows variation of trace element versus SiO_2. All compatible trace elements made negative correlation with SiO_2 that implies the fractionation of Mg, Fe, Ca and Ti bearing minerals like olivine, clino Pyroxene plagioclase and Fe-Ti oxide for compatible trace element specially Ni, Cr, Sr and V. The incompatible trace elements (Rb, Ba, Zr, Nb and Y) against SiO_2 plot show clear positive trend line; the acidic and some intermediate rocks have high value. The negative and positive trends of the compatible and incompatible elements show the differentiation and fractionation of magma. The Mg and Fe and Mg are the major substitution elements for the compatible trace elements specially Ni and Cr. The trend of Sr and Ba indicates the differentiation process and removal of feldspar.

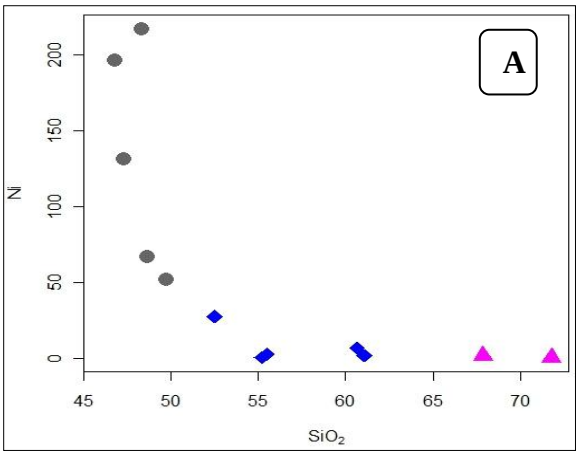
A
Ni
0
50
100
150
200
45
50
55
60
65
70
SiO2

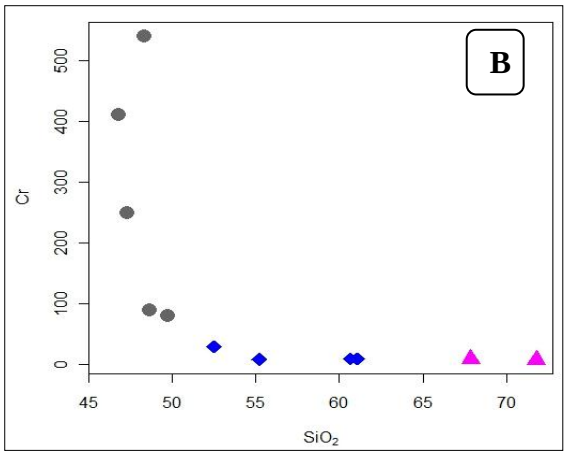
B
Cr
0
100
200
300
400
500
45
50
55
60
65
70
SiO2

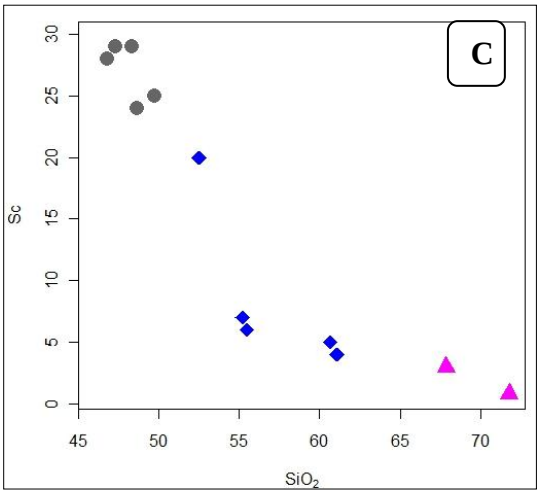
C
Sc
0
5
10
15
20
25
30
45
50
55
60
65
70
SiO2

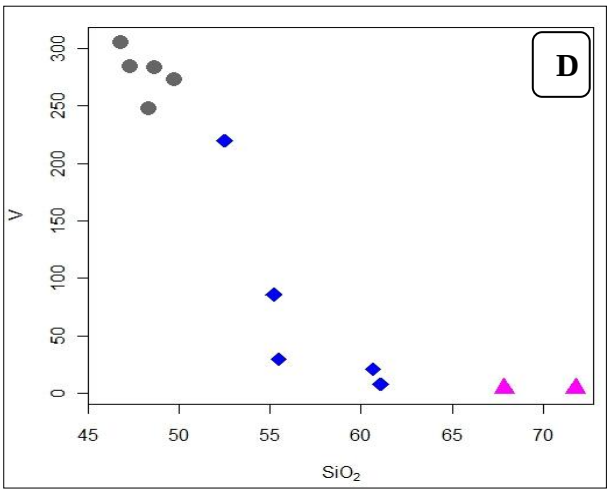
D
V
0
50
100
150
200
250
300
45
50
55
60
65
70
SiO2

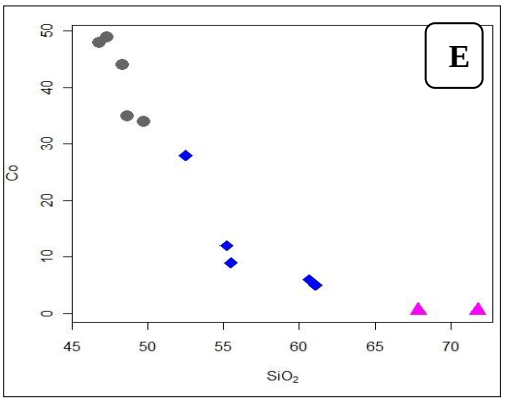
E
Co
0
10
20
30
40
50
45
50
55
60
65
70
SiO2

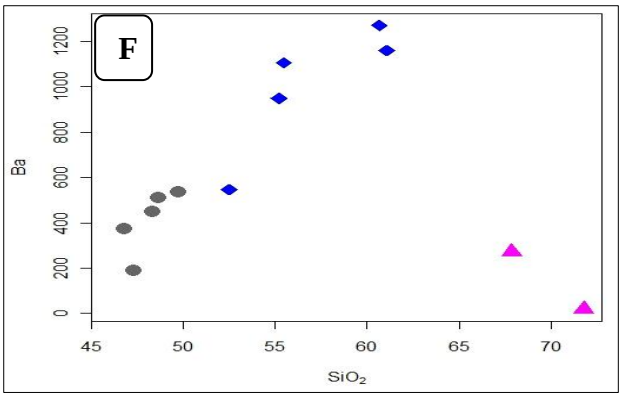
F
Ba
0
200
400
600
800
1000
1200
45
50
55
60
65
70
SiO2

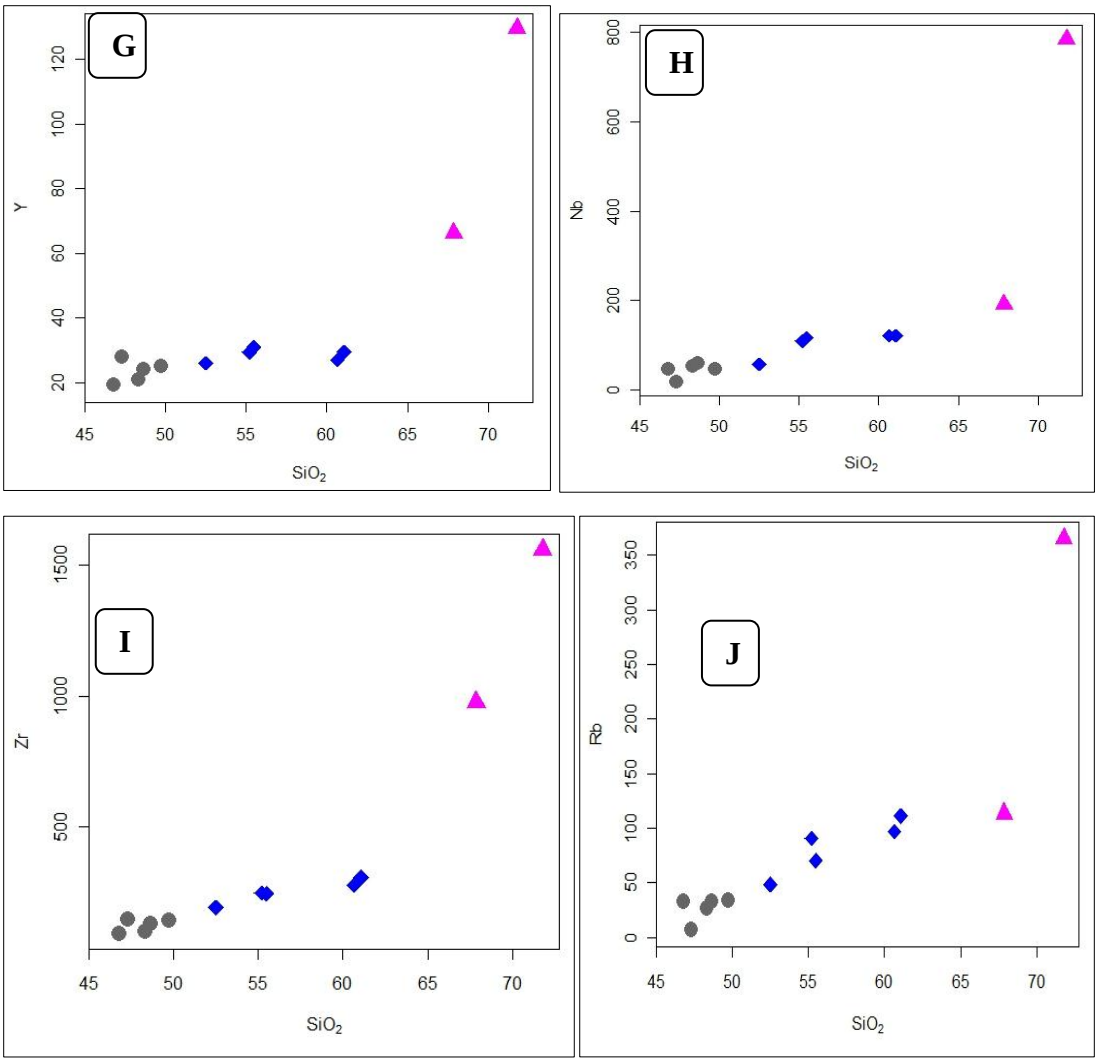

Figure 4. 4: *Variation diagram of trace element versus SiO2.*

On explain of the ionic size of Zr does not enter in to the major crystalline phase. To understand the behavior of element during magma evolution Zr selected as index of X- axis because of Zr prefers the liquid phase and show highly concentration value than from another trace element therefore, it is very important to study the behavior of elements in magmatic evolution by taking Zr as an index. The incompatible trace elements such as Rb/Sr, Y, Nb, Rb

against Zr and Rb against Th show a positive correlation as indicate linear slope in (Fig 4.5)

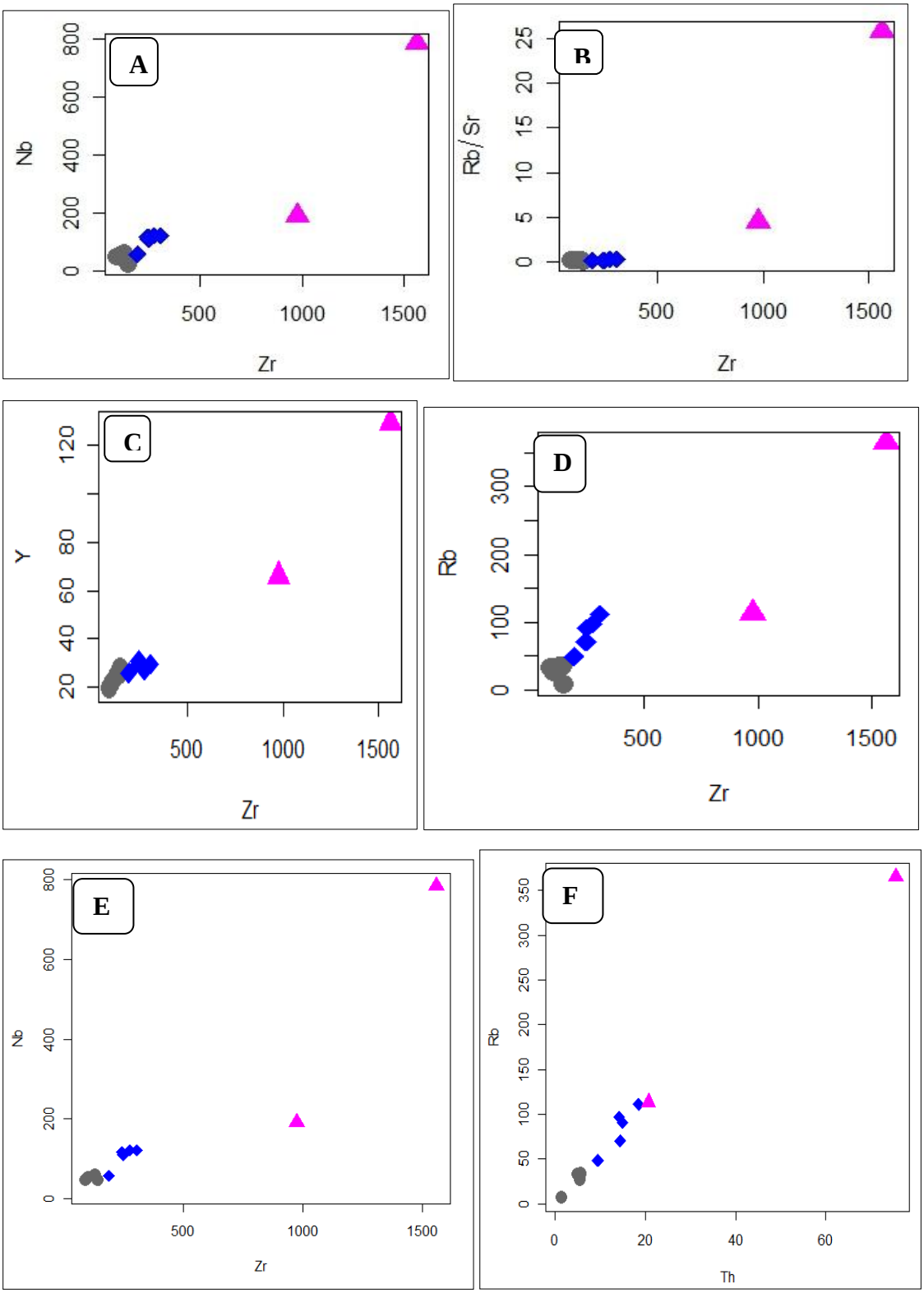

Figure 4. 5: *The plots of selected trace elements against Zr for identification of genetic process.*

From the plots of the following Fig 4.6 give information about evolution of mafic, intermediate and felsic since the Rb/Sr against SiO2 show positive for Acidic rocks that

implies the accommodation of k-feldspar from felsic lava and fractionation of plagioclase (Sr can substitute Ca in the crystal lattice) is related K- feldspar accommodation of k-bearing minerals. The Ba/Y versus Zr show negative trend implies the crystallization of alkali feldspar. The Ti/Zr versus Zr shows general negative trend that steep slope for both Mafic and intermediate rocks; highly differentiated lava indicates significant removal of Fe-Ti oxides and/or pyroxenes in the initial stage of differentiation.

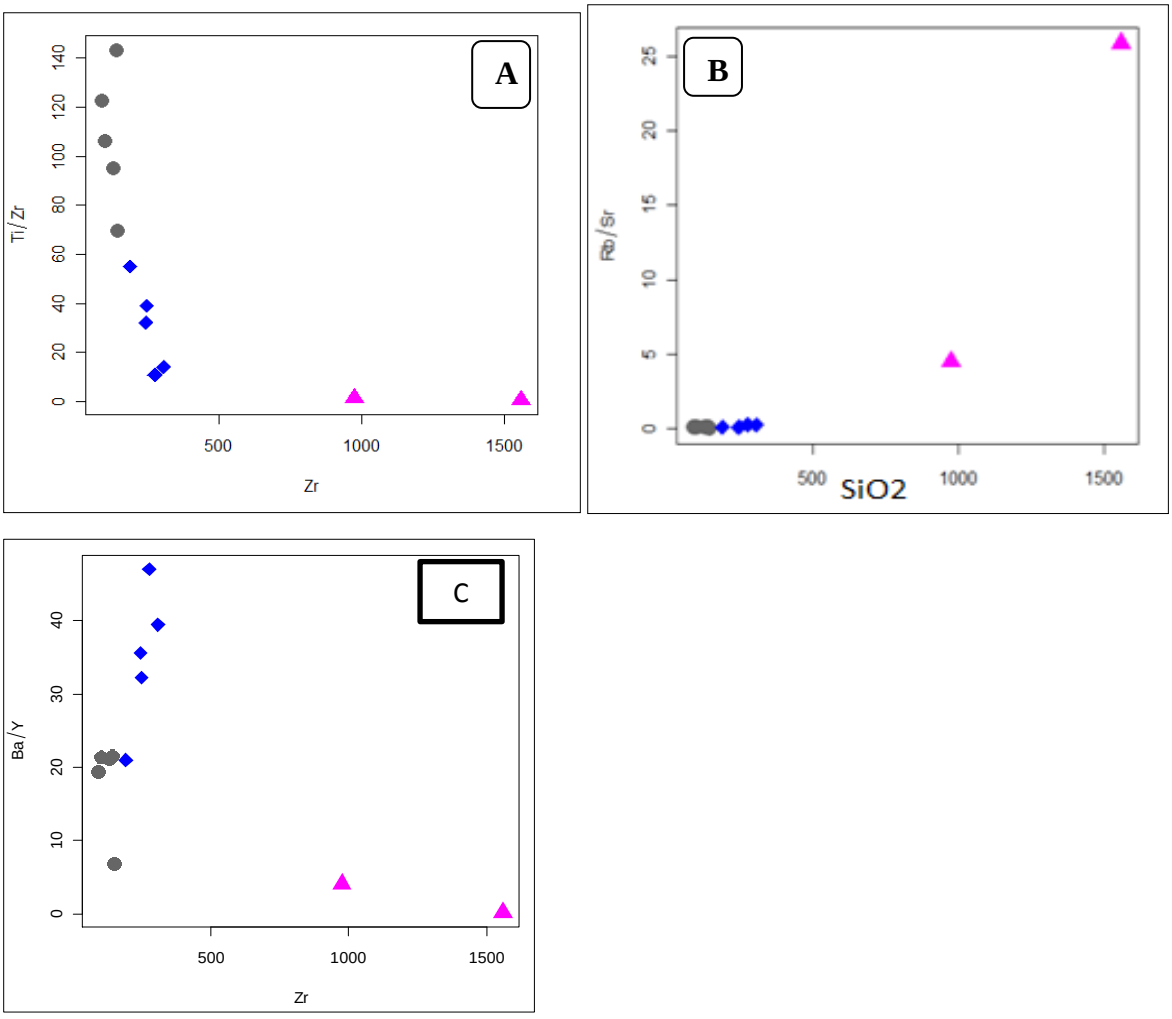

Figure 4. 6: *Trace element ratios against SiO2 and Zr diagram. The unit for the concentration is in ppm (for trace element) and wt. % for major element.*

Rare Earth elements are a group of 15 elements with atomic numbers from (57) lanthanum (La) to (71) lutetium (Lu) and they are particularly useful in petrogenetic studies because they are geochemically very similar. In the following class the REE analyses made for mafic, intermediate and felsic volcanic products in (Fig 4.7). The REE value of concentration is normalized to chondrite according to values of Sun and McDonough (1989) by dividing the concentration of a given element in the rock by the concentration of the same element in

chondritic meteorites because chondrites are primitive solar material which may have been the parental material of Earth. The REE analysis show that highly abundance of LREE for both mafic and intermediate volcanic products and highly abundance for felsic rocks of study area. The mafic rocks show high La/Yb ratio (6.5-19.53). The pattern of REE diagram shows that cross each other's for some mafic samples and slightly parallel to another's. This indicates there is limited residual garnet during melt generation. However, the intermediate and felsic rock evolved from mafic melt. The slightly positive or no anomaly of Eu for both mafic and intermediate rocks suggest the accommodation of plagioclase feldspars (Eu/Eu* = 0.93-1). The REE diagram pattern show for felsic rock show enrichments in the LREE and slightly gentle slope for HREE and similar to mafic and intermediate rocks. There is negative anomaly of Eu for felsic rocks in REE diagram implies that fractionation of plagioclase feldspar, the strong negative anomaly of Eu indicated from rhyolite sample (Eu/Eu* = 0.51-0.072).

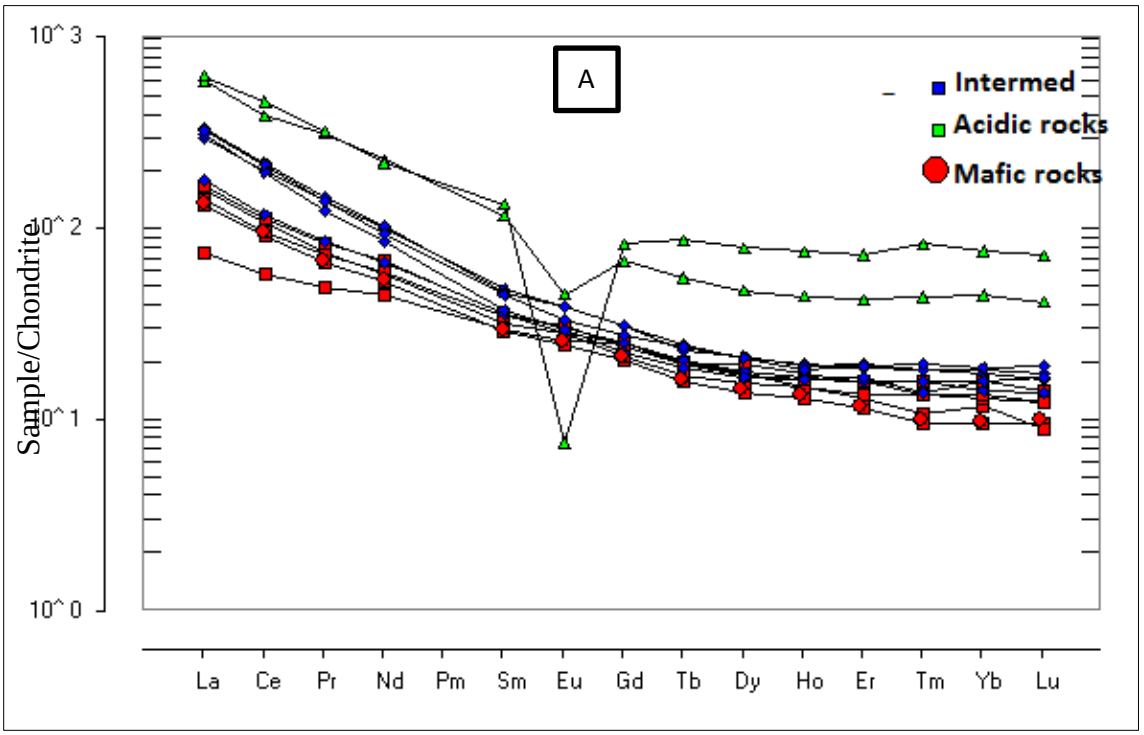

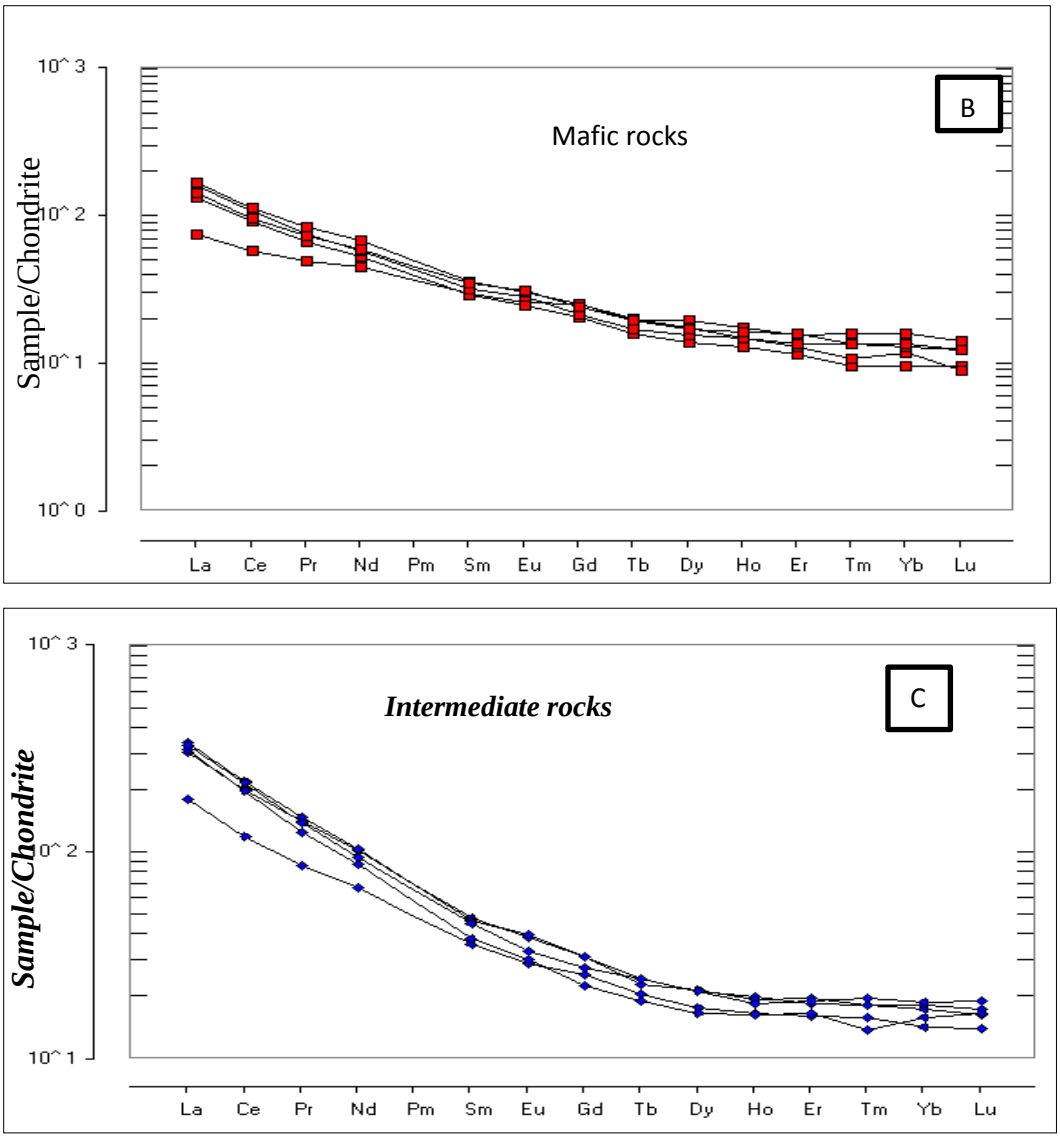

Figure 4. 7: *spider diagram of REE for representative sample from mafic, intermediate and felsic rocks Concentration of the sample normalized by chondrite value determined by Sun and McDonough (1989).*

The multi element variation diagram is plotted in (Fig 4.8) in order to understand generation of NSV volcanic rocks. The concentration of rocks is normalized by primitive mantle plot according to Sun and McDonough (1989). The diagram of mafic materials show positive anomaly at Ba, Nb, Pb, Zr and La whereas negative pick or depletion at K, U and Sr and the negative anomalies of K suggest fractionation of alkali feldspars. The positive anomaly of Nb and Ta indicate absence of crustal contamination. According to Dereje Ayalew et al., 1999 high trace element ratio such as La/Nb and Th/Nb are sensitive to crustal contamination. The Nech Sar mafic rocks have La/Nb and Th/Nb ratio with average value 0.75 and 0.1 respectively. However the peak of Pb indicates the behavior of mobility because Pb is highly mobile incompatible trace element. The intermediate have similar incompatible element

pattern as mafic rocks, showing trough at Ti, and Sr, Th and U and positive anomalies at Ba. The negative anomalies of Ti and Sr for both intermediate and acidic rocks show the removal of Fe-Ti oxide and plagioclase feldspar from the magma respectively.

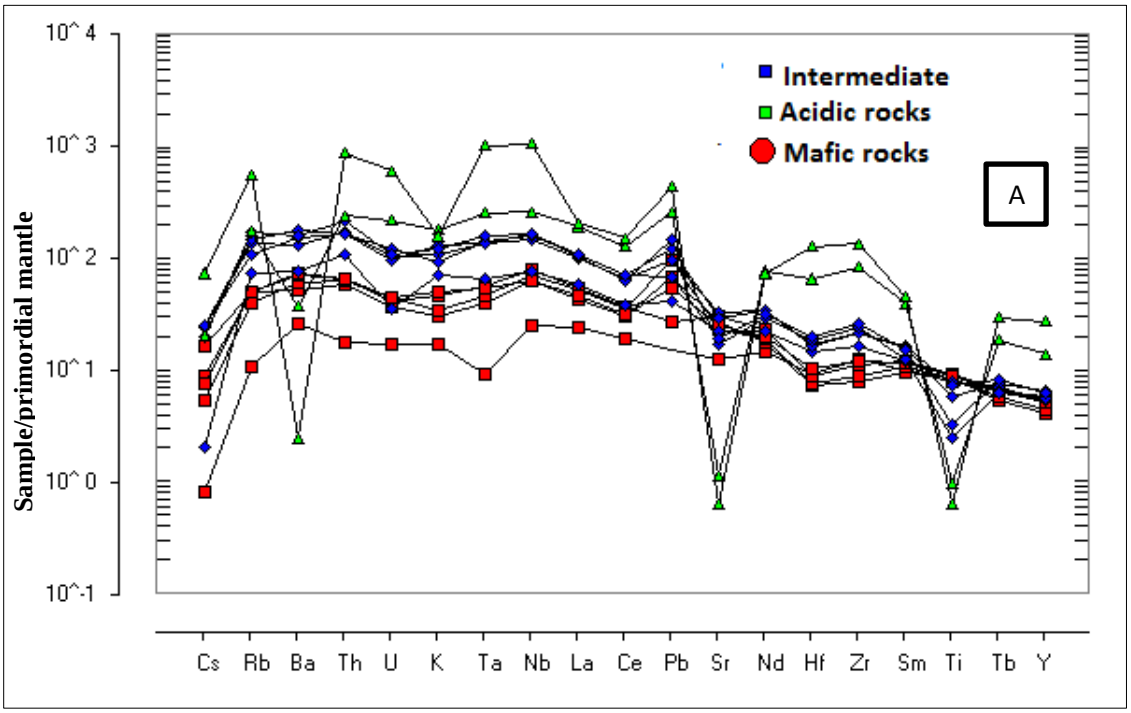

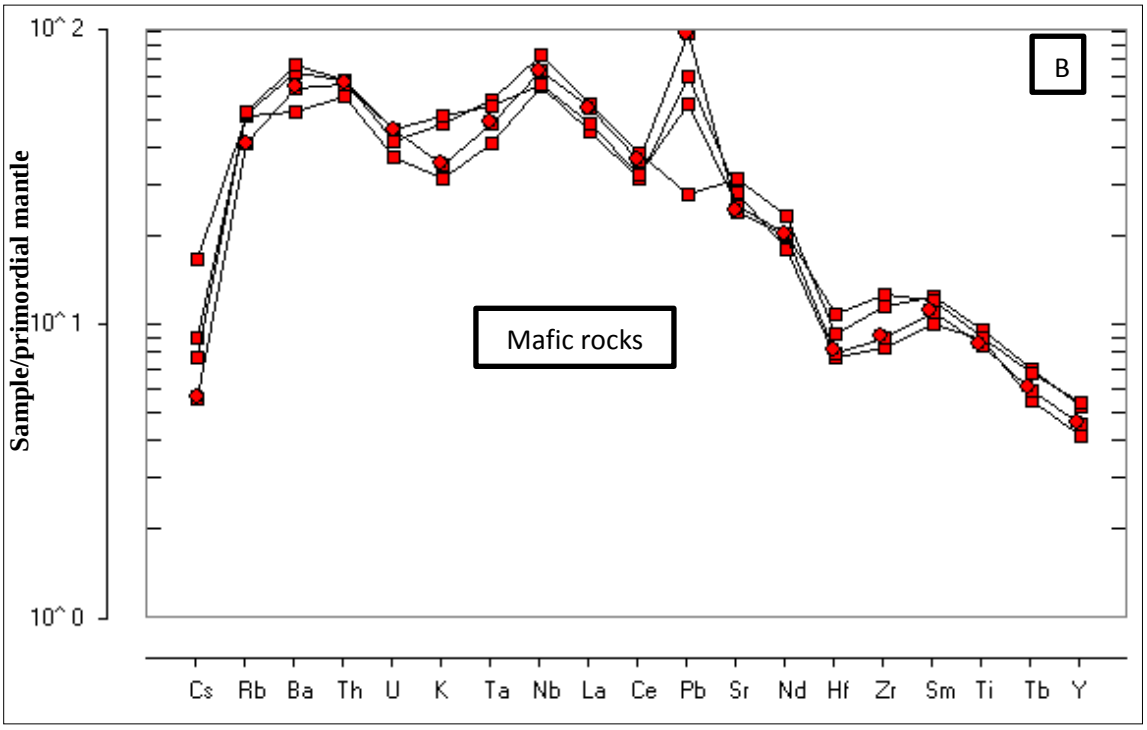

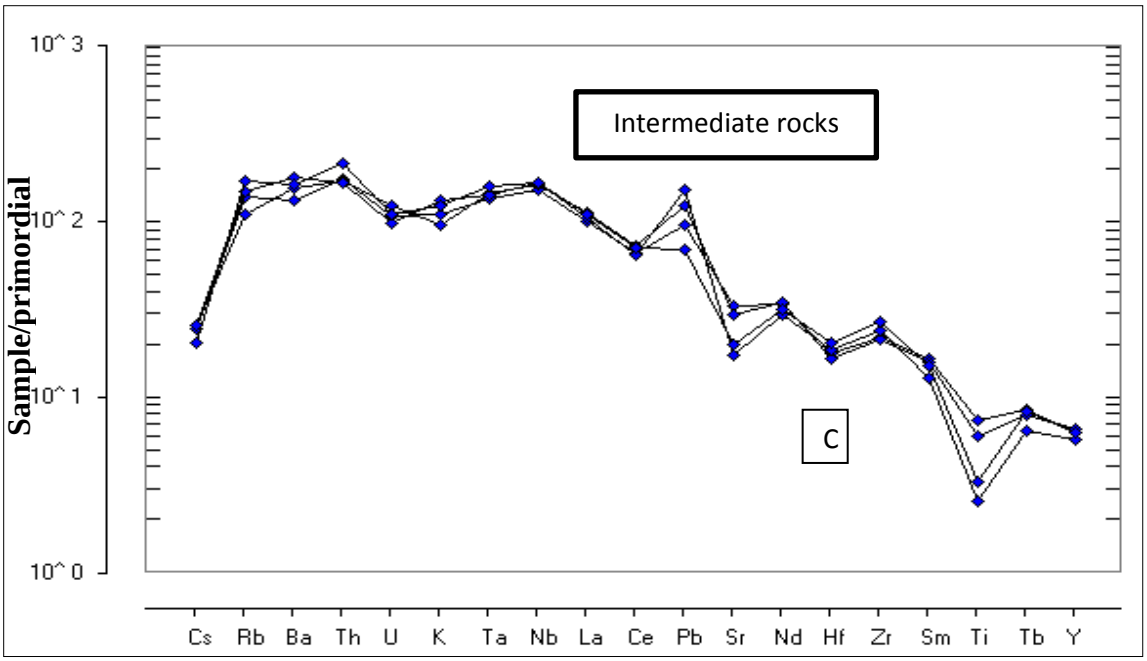

Figure 4. 8: *Multi-element spider diagram of representative mafic (A), inter mediate (B) and Felsic (C) rocks of NVS. The samples are normalized to primordial mantle of value determined by Sun and McDonough (1989)).*

CHAPTER FIVE
5. DISCUSSION

5.1. Introduction

The Quaternary volcanism in the MER is dominated by a bimodal association of mafic and silicic products, with rare intermediate rocks. However, George and Rogers, (1999) reported the Quaternary volcanism along the Tosa Shucha in south main Ethiopian rift is associated mafic to intermediate rocks. The data presented in current study agreed with previous and addition of acidic rocks from volcanic products. Therefore, the Nech sar volcanic rocks belongs of mafic, intermediate to felsic based on field absorption, petrographical investigation and whole rock geochemical data. The mafic lava flow of the study area shows no variation in both petrology and geochemical composition within the restricted province whereas the intermediate and felsic lava show major variation.

5.2. Fractional crystallization

Based on variation diagram of major elements plots from above (Fig 4.3) most samples are show negative and positive trend against SiO_2 and some major oxide are show inflected trend with against SiO_2. According to George and Rogers, (1999) the fractionation increases; MgO, Fe_2O_3, CaO and compatible elements abundance decrease while incompatible element concentration increase with SiO_2. The Nech Sar volcanic rocks major element oxide variation diagram plot show MgO, CaO, TiO_2 and Fe_2O_3 decrease with increasing SiO_2 and incompatible trace element due to fractionation of Mg, Fe, Ti and Ca bearing minerals. The repaid increase of silica and incompatible trace element is the result fractional crystallization of that implies the removal of mineral in composition low in alkaline and silica. For this, the typical example is olivine; pyroxene and plagioclase are dominant phenocryst in the basalts from thin section data. The compatible trace elements make the various elements decrease at different rates during fractional crystallization. For instance, Ni and Cr decrease rapidly during the early stages of fractionation because olivine and pyroxene are crystallizing; in contrast, Sr and V remain initially constant or increase slightly, but decrease during intermediate stages of fractionation when plagioclase and Fe-Ti oxides start to crystallize. However, the both Na_2O and K_2O are incompatible in olivine because increase with SiO_2 and compatible in alkaline feldspars and Na_2O increase from basalt to trachyte and then decrease

in the rhyolite. Therefore, the fractionation order is removal of olivine followed by clino pyroxene, hematite, ilmenite, plagioclase and apatite.

To identify the link between mafic and felsic rocks, the major and trace element geochemistry is very important. Based on major element oxide and selected trace element versus SiO_2 plots show variation diagram the Nech Sar volcanic rocks linked by fractional crystallization of magmatic process.

The two clusters or groups are separated with a wide gap of concentration between mafic and felsic lava called daly gap (Peccerillo et al., 2003) suggest the absence of intermediate rocks but the presence or absence of gap between them is doesn't preclude genetic association of the rocks. There is no gap between mafic and acidic rocks of Nech Sar volcanic products because intermediate rocks are fill the gap that implies there was more or less geochemical concentration similarity between intermediate and basaltic rocks that suggest less significance of fractionation between them but acidic rocks are formed by highly differentiation of magma. In addition to this, the selected samples of multi-elemental spider diagram and REE diagram of mafic, intermediate and acidic rocks show that a parallel pattern with anomalies on different elements indicate the lava have genetically relationship.

The hypothesis of generation of acidic magma by partial melting of basalt is unable to explain the extremely low Sr abundance because basalt rather enriched in Sr and their melt would not produce Sr poor liquid (Peccereillo et al., 1998 and 2003) and the low Sr and incompatible element of acidic can be explained by two stage process of melting of basalt followed by extensive fractional crystallization or AFC of anatectic liquid Barberio et al., (1999). Therefore, analyzed sample of Nech sar volcanic rocks geochemical characters is the mafic intermediates and acidic rocks have high Sr (278-709 ppm) value but the acidic rocks have low Sr (14.4-25pmm) as well as high incompatible abundance of trace element, suggest both acidic and intermediate rocks evolved from mafic magma through fractional crystallization rather than partial melt. Based on this concept in the next section there is the diagrams of incompatible versus compatible element simple plots in (Fig 5.1 A and B) V and Sc against Zr (i.e. compatible versus incompatible plots) show that basalt melting followed by extensive fractional crystallization able to mimic element variation in acidic rocks.

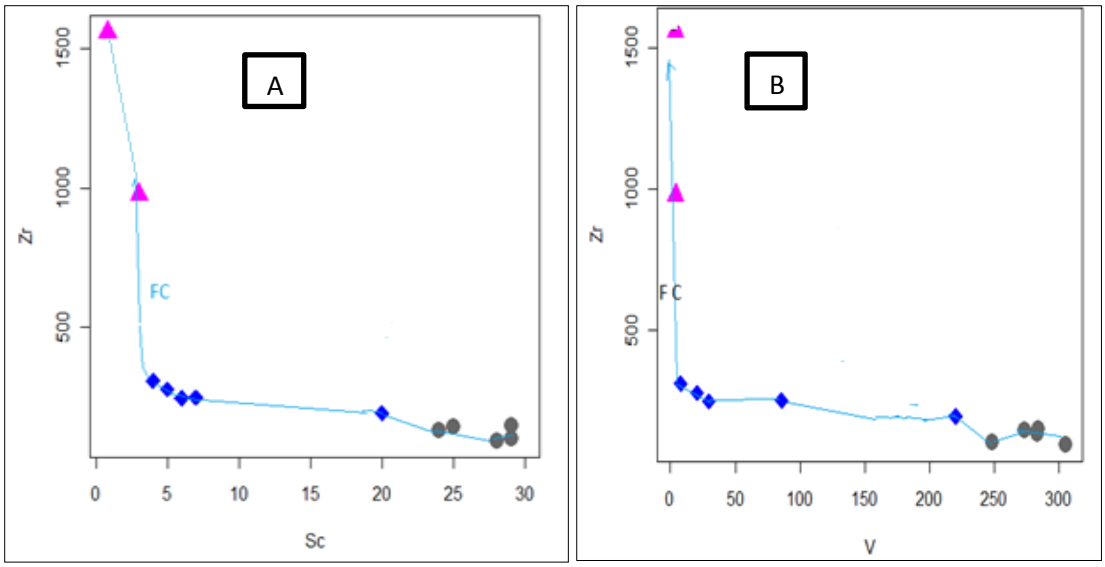

Figure 5. 1: *A and B plots of compatible versus incompatible diagram for Nech Sar volcanic rocks. The diagram indicates the fractional crystallization model starting from melt of basalt anatexis.*

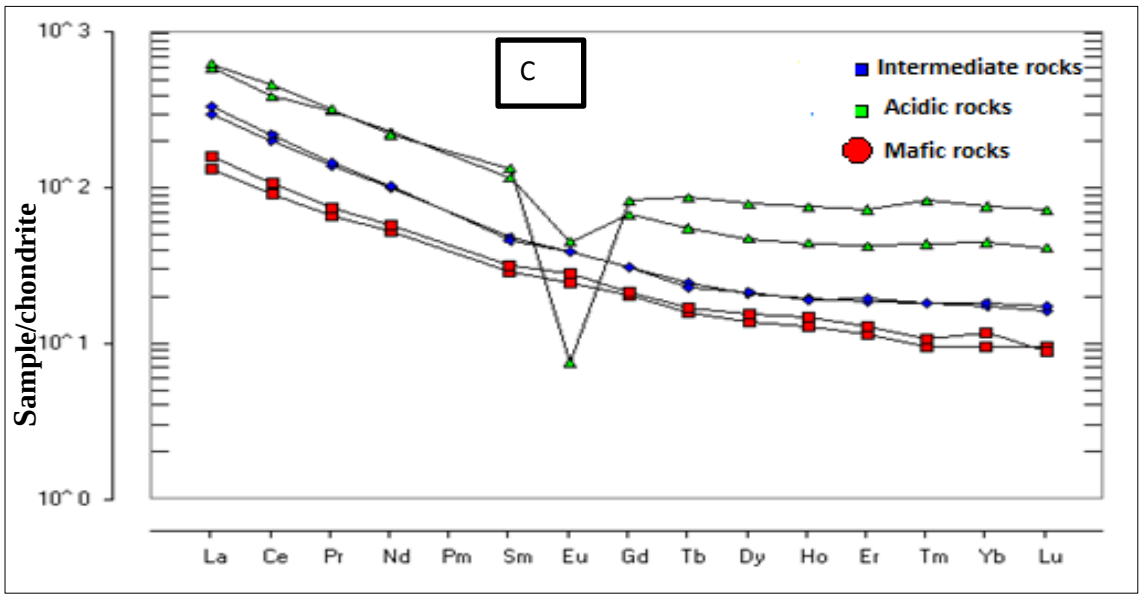

Figure 5. 2: *C plots of REE spider diagram suggesting of both felsic and intermediate lava derived from mafic lava by fraction crystallization*

5.3. Crustal contamination

Crustal contamination is high where crustal thicknesses are considerably large and magma supply rates are low, resulting in greater residence times for individual magma batches within the lithospheric crust (Furman, 2007). The study area samples were characterized by enrichment in LREE and highly incompatible trace element. This enrichment is the result of either consequence of crustal contamination or derivation from enriched mantle source (Thompson, 1984). The ratio of K/Nb and La/Nb versus SiO2 commonly used as indicators

of crustal involvement, if linear relate with SiO_2 increase (George and Rogers, 1999). The study area samples remain broadly constant as SiO_2 increase and all samples show positive anomalies of Nb and Ta in the multi element variation diagram. This suggests that there is absence of any crustal contamination derived from continental crust. However, according to Dereje Ayalew et al.(1999 the result of crustal contamination cannot be entirely neglected since the lavas have traversed the crust and, hence, interaction with crustal rocks was likely and trace element ratio such as La/Nb and Th/Nb are sensitive to crustal contamination. The Nech Sar volcanic rocks especially some intermediate rocks and acidic rocks characterized the ratios of La/Nb (0.2~1) and Th/Nb (0.08-0.16). For instance the sample has slightly high trace element ratio such as La/Nb~1 and Th/Nb~0.16. These features are indicative of limited crustal contamination but it does not significant controlling factor of genetical process for this rocks. Crust has low Ce/Pb values but lithosphere has higher Ce/Pb value (Dereje Ayalew et al., 2006). According to Dereje Ayalew and Gezahign Yirgu, (2003) if the rhyolite have higher Th and Nb concentration and low Rb/Nb and La/N ratio suggest there is limited crustal involvement in their genesis. The rhyolite rocks found in Nech Sar area characterized by high Th (21-76 pmm) and Nb (190-784 pmm) and low Rb/Nb (0.46-0.6) and La/Nb (0.2-0.94) this indicate the rhyolite rocks of study area have limited crustal involvement in their genetic process. In addition the peak in Pb suggests that contribution of mobility of the Pb element rather than crustal contamination as well as there is peak or positive anomaly of Nb and slightly in Ta mafic rocks and have lower La/Nb < 1 (0.19-0.96) indicate absence of crustal contamination. The intermediate rocks multi element spider diagram pattern show through (negative anomalys) in Sr and Ti probably the result of plagioclase and opaque mineral (Fe-Ti oxide) fractionation respectively.

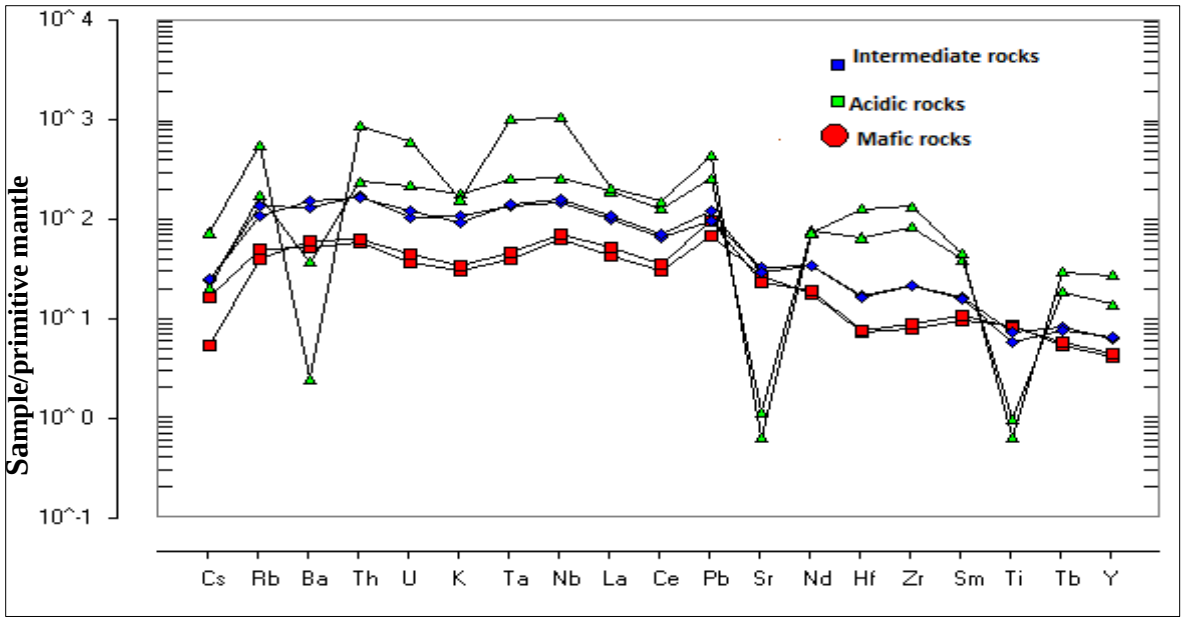

Figure 5. 3: *Multi elements spider diagram of mafic, intermediate and felsic rocks plot of incompatible trace elements, normalized to primordial mantle value determined by Sun and McDonough (1989).*

5.4. Mantle Source

Two compositionally distinct mantle plumes are found beneath East African rift system one beneath the present Ethio-Afar dome and the other beneath the Kenya Plateau Rogers et al., (2006). However, according to Ebinger and Sleep, (1998) there is only a single large plume beneath the Ethiopian plateau which is initiated the oldest basaltic volcanism in southern Ethiopia at ~45 Ma. Ethio-Kenya volcanic province has experienced a complex and long episode of basaltic and felsic volcanism since late Eocene Gezahagne Yirgu et al., 2006). The source, therefore, records the complete sequence of volcano tectonic activities from the plume head to tail and from incipient intra continental rifting to seafloor spreading Miruth Hagos et al., (2010).

In order to get source of mantle for Nech Sar volcanic rocks the trace element geochemical character is used. The analyzed mafic lava of Nech Sar volcanic rocks trace element ratio Ce/Pb (8-35), Ba/La (10-15), La/Nb (0.6-1.2) and Ba/Nb (8-12) which close to substantially the field of OIB like source but not overlap (Sun and McDonough, 1989; Weaver, 1991). According to George and Rogers, (1999, 2002) the basalt melt derived from deplete source have low CaO/Al_2O_3 ratio (< 0.7) and low FeO_T. However, the basalt OIB like source have high CaO/Al_3O_2 ratio (> 0.8). This is not the case for Nech Sar basalts because they have medium to low CaO/Al2O3 ratio (0.57-0.75) and high FeO_T. As stated by Wang et al., (2002) the division between spinel and garnet-dominated melting is de rived from magma

modeling in the Basin and Range from Tb_N/Yb_N which is a useful indicator to distinguish between garnet (Tb_N/Yb_N >1.8) and spinel (Tb_N/ Yb_N<1.8) dominated melting columns. The Nech Sar volcanic rocks Tb_N/Yb_N (0.9-1.6). Therefore, based on this and REE variation diagram the Nech Sar basalts derived from garnet poor source region. However, the enrichment of LREE another incompatible elements of the Nech sar volcanic rocks indicate the mafic lava derived incompatible element enriched mantle source. As Stated by George, (1999) if there is enrichment of LREE and low Rb/Sr in melt this enrichment is due to the presence carbonate enrichment in melt and enrichment of mantle source in south main Ethiopian rift especially in Tosa Shucha volcanic is affected by migrating carbonate rich-melt 500-800Ma during PanAfrican Orogeny. The Nech sar volcanic rocks have enrichment LREE and Rb/Sr (0.025-0.06) ratio. The north Arba Minch Quaternary magmas on the rift floor and Wonji Fault Belt magmas is (Tb_N/Yb_N~1.3–1.7) whereas Silte-Debre Zeyit Fault zone magma has Tb_N/Yb_N (1.3-2.3) Rooney et al., (2010). According to Ayalew and Gibson, (2009) the Ethiopian Rift basalts are the result of variations in the depth of the mantle melting column associated with changes in lithospheric thickness therefore, the source placed the spinel to garnet transition in the mantle beneath the Main Ethiopian rift at 70–90 km and interpreted the top of the mantle melting column as the base of the rigid lithosphere. The low modal abundance of garnet of TSV is characterized at this depth is response to an elevated geothermal produced conductive heating from the underlying Afar plume (George and Rogers, 1999).

The progressive continental rifting thins the lithosphere and allows asthenosphere to rise and melt. The magnitude of this thinning controls depth of the melting column that produces rift basalt. Deeper melting columns produce a greater proportion of melt in the garnet lherzolite field in comparison to the shallower melting columns that are dominated by spinel–lherzolite Wang et al., (2002). There is decreasing of lithosphere thinning from Afar to south main Ethiopian Rift during progressive continental rifting (Ebenjer et al., 1993). The presence of medium to high concentration ratio of Ce/Pb of Nech Sar mafic rocks (12-35) this suggest that the basaltic lava have genetic relation with contribution of mantle.

The chondrite normalized REE pattern of Nech Sar basalts are characterized strong LREE enrichment (La/Yb 6.5-19.5). They have moderately elevated HREE >10 times chondritic value and the ratios of (Tbn/Ybn=1.0-1.7) from the Fig 5.4 A, B and C indicate that the mafic lava derived from spinel peridotite melt. In addition the REE profile (La/Sm versus Sm/Yb)

are typical useful to distinguish melting between garnet and spine pridotite Lassiter and Depaolo, (1996). The Nech Sar basaltic lava have high La/Sm and Sm/Yb ratio (2-2.5), are close to spinel-facies mantle melting curve Fig 5.4 B. The primitive mantle normalized trace element diagram of the both mafic and intermediate rocks are characterized strongly enrichment in HFSE incompatible specially peak at Nb, Ta and Zr, is slightly similar to oceanic island basalt (OIB) like source (Wilson, 1989). However, the NSV based on CaO/Al2O3 ratio of mafic lava range between (0.57 – 0.75 values), suggest that the Nech Sar basalt derived from ganet free incompatible enriched mantle source.

The diagram of Nb-La, Y-Zr, Nb-Zr, Rb-Th and Ta-Th Fig. 5.5: D, E, F, G and H show positive correlation by forming slightly linear slope approximately 1 which indicate there is genetically relationship or co-genetic nature in either mafic, intermediate and falsic rocks and as well as they generated from the same source.

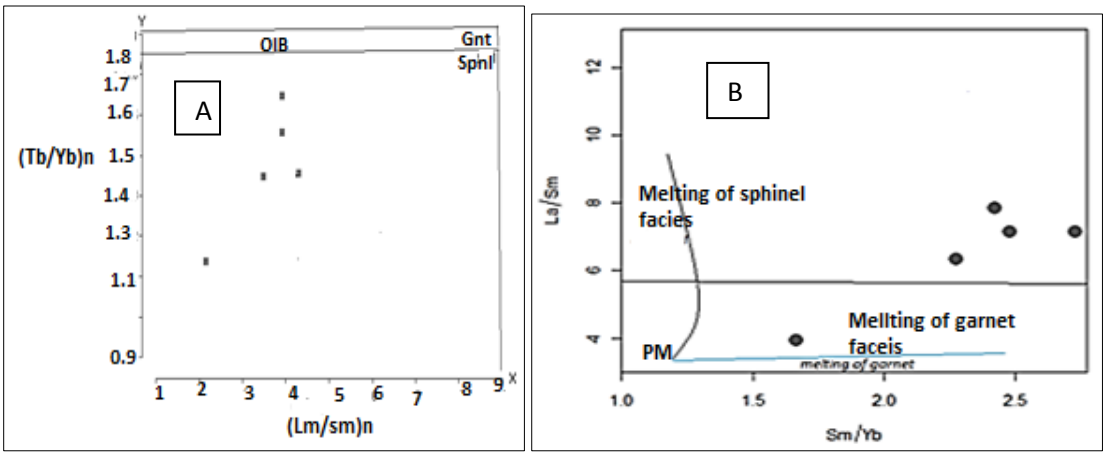

Figure 5. 4: *(A) the plot of Tb/Yb and La/Sm normalized to chondritic values (Sun and McDonough, 1989). There is no obvious correlation between La/Sm and Tb/Yb, indicating that the degree of source enrichment does not control the variation in Tb/Yb. The division between spinel and garnet-dominated melting is derived from magma modeling in the Basin and Range province (Wang et al., 2002). Figure 5.3a (B) plot of La/Sm ratio versus Sm/Yb ratio of Nech Sar volcanic rocks lie close to garnet free melting curve except one sample.)*

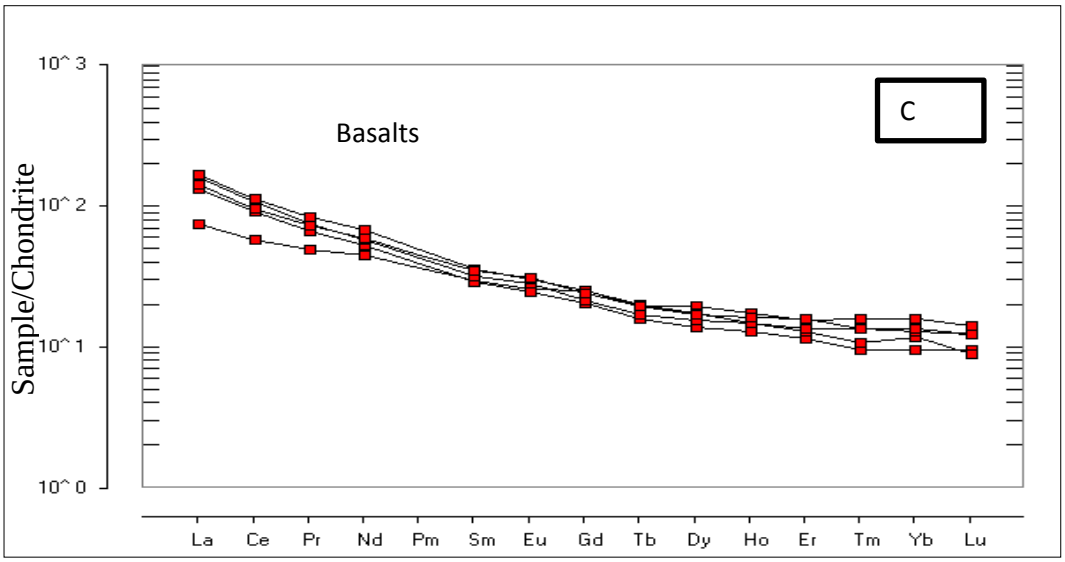
C
Basalts
Sample/Chondrite
10^ 3
10^ 2
10^ 1
10^ 0
La
Ce
Pr
Nd
Pm
Sm
Eu
Gd
Tb
Dy
Ho
Er
Tm
Yb
Lu

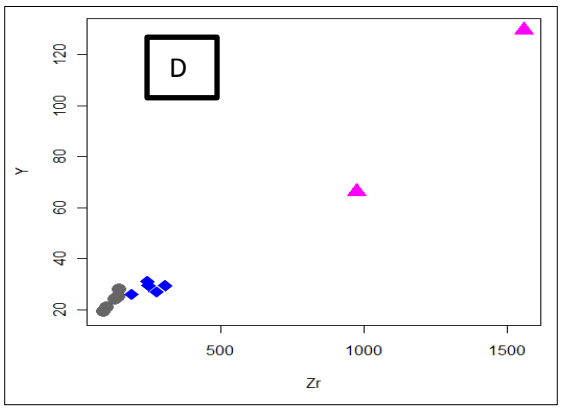
D
Y
Zr
20
40
60
80
100
120
500
1000
1500

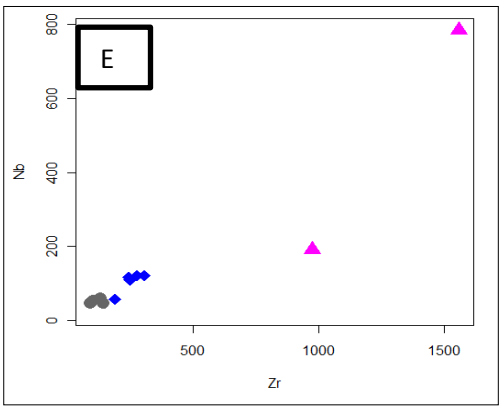
E
Nb
Zr
0
200
400
600
800
500
1000
1500

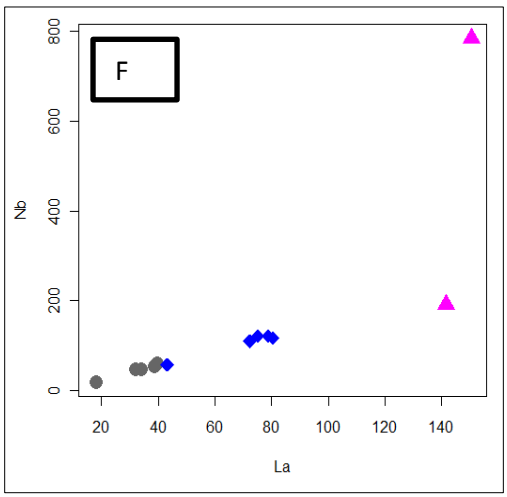
F
Nb
La
0
200
400
600
800
20
40
60
80
100
120
140

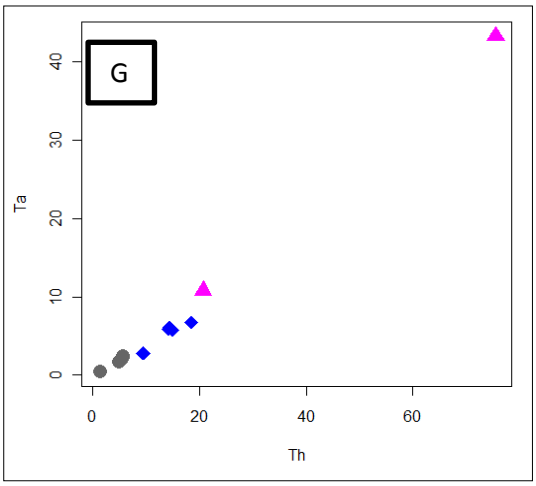
G
Ta
Th
0
10
20
30
40
0
20
40
60

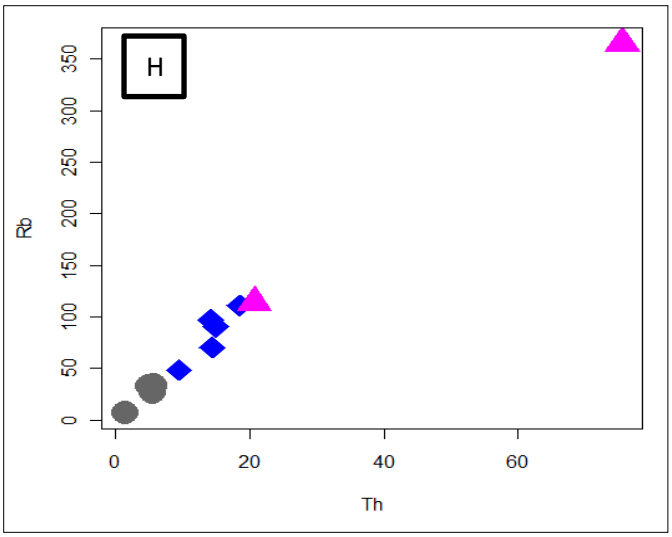

Figure 5. 5: *(D, E, F, G and H) plot of incompatible trace element, Ta-Th, Nb-La, Rb-Th, Nb-Zr and Y versus Zr diagram Shows the Nech sar volcanic rocks generated from the same source.)*

CHAPTER SIX

6. CONCLUSION AND RECOMMENDATION

6.1. Conclusion

Depending on field observation, petrography study and geochemical data distribution of NSV rocks from (south main Ethiopian rift) the general output of this work is explained as following:

The geochemistry, field interpretation and petrographical data suggest that the rocks are typical bimodal distribution of volcanic products with mafic, intermediate and acidic rocks were present in study area; the mafic rocks suite of transition basalt from TAS because it fall in the boundary between Alkaline and sub alkaline. The acidic and intermediates rocks are derived from basalt melt based on their geochemical composition, especially trace element modeling

The geochemical result imply that the three group of rocks; basalt, intermediate and acidic rocks have the same source. The major element Harker diagrm, trace element modeling, REE variation diagram and multi element variation diagram of the three rock groups imply the rocks are genetically related by process of fractional crystallization with the limited involvement of crustal contamination. In addition to that, there is more or less geochemical concentration similarity between mafic and intermediate rocks implies that there was small significance of fractional crystallization between intermediates and basaltic lava that affect the concentration of compatible element rather than that of acidic lava.

The major element oxide and selected trace element variation diagram of the rock groups and typical phenocryst in petrographic data suggest that the fractional crystallization is the main contribution of modification of magma process of the Nech Sar volcanic rocks. Olivine, clinopyroxene, Fe-Ti oxide, plagioclase and apatite minerals are major fractionating phase of melt.

The positive correlation by forming moderately linear slope among highly incompatible trace element and pattern between REE spider diagram of mafic, intermediate and felsic lava indicate that the rocks related by the same source and followed similar genetically process or have co-genetic nature.

The basaltic lava were generated from incompatible element enriched lithospheric mantle which closed to spinel predotite melt based on Tb/Yb versus La/Sm and La/Sm versus Sm/Yb diagram, and REE spider diagram this suggests the Nech Sar basalts were derived from garnet free source mantle.

6.2. Recommendation

This work focused mainly on petrogenesis of Nech Sar volcanic rocks from south main Ethiopia rift. However, there is different regional study over south main Ethiopia rift state that the geological data still spars in this area and that is why less attention given for the south main Ethiopian rift and inaccessibility, especially recent or Quaternary volcanic and their formation as well as rift evolution association with magma source have no information than that of both CMER and NMER.

For better understand of petrogenesis of volcanic rocks, the isotope analysis is very important. Isotope analysis is tool for understand evolution, source region of magma and potential of mantle. Therefore, isotope geochemistry is recommended for further investigations of source region and detail magmatic process of Nech sar volcanic rocks not only for this area but also for all South main Ethiopian rift, especially recent volcanic products.

To date in the south main Ethiopian rift detail petrogenetic study have not been conducted in a well-defined manner so, instead of giving more attention for the northern and central main Ethiopian rift, it is better to give for the unstudied southern Ethiopian rift important to have full and confined data for the whole Main Ethiopian rift.

This studies targeted geological mapping without stratigraphic session in very small area coverage and limited sampling, which has not real representative of volcanic rocks of the area and region as whole, this work recommended that wider area coverage through producing of large scale geological map in addition to stratigraphic session to better understanding of genesis of basalts, intermediate and acidic rocks of the area and to understand general rock correlation with related geological process.

References

Acocella,V and Korme. T. (2002). Holocene extension direction along the Main Ethiopian Rift of East Africa.Terra Nova, v. 14, no. 3, pp. 191-197

Acocella, V., B. Abebe, and T. Korme. (2011). Holocene opening directions along the axes of the Red Sea (Afar) and main Ethiopian rift: An overview, in Volcanism and Evolution of the African Lithosphere, Spec. Pap., vol. 478, edited by L. Beccaluva, G. Bianchini, and M. Wilson, pp. 25–35, Geol. Soc. Am., Boulder.

Acocella, V., Gudmundsson, A and Funiciello, R (2000). Interaction and linkage of extensional fractures: examplesfrom the rift zone of Ice land.J. Structure. Geol., 22, 1233–1246.

Alemayehu Meless., Hong-Fu Z., Patrick Asamoah.S. (2016). Nature and evolution of lithospheric mantle beneath the southern Ethiopian rift zone: evidence from petrology and geochemistry of mantle xenoliths.

Atherton, M.P., Petford, N. (1993).Generation of sodium-rich magmas from newly underplated basaltic crust. Nature 362, 144–146.

Bastow, I.D., Nyblade, A.A., Stuart, G.W., Rooney, T.O., and Benoit,M.H. (2008). Upper mantle seismic structure beneath the Ethiopian hot spot: Rifting at the edge of the African low-velocity anomaly: Geochemistry, Geophysics, Geo systems, v. 9, Q12022, doi: 10.1029 /2008GC002107.

Bastow, I.D., Stuart, G.W., Kendall, J.M., and Ebinger, C.J. (2005).Upper mantle seismic structure in a region of incipient continental breakup: Northern Ethiopian rift: Geophysical Journal International, v. 162, p. 479–493, doi:10.1111/j.1365-246X .2005.02666.x.

Beccaluva, L., Bianchini, G., Natali, C., Siena, F.(2009). Continental flood basalts and mantle plumes: a case study of the Northern Ethiopian Plateau. Journal of Petrology50, 1377–1403.

Bonini, M., Corti, G., Innocenti, F., Manetti, P., Mazzarini, F., Tsegaye Abebe and Pecskay, Z. (2005).Evolution of the Main Ethiopian Rift in the frame of Afar and Kenya rifts propagation.

Boynton, W.V. (1989). Cosmo chemistry of the rare earth elements: condensation and evaporation processes. *In*:.R. Lipin and G.A. McKay (Eds.), Geochemistry and Mineralogy of Rare Earth Elements. Rev. Mineral., v.21, pp.1-24.

Chu,D. and Gordon, R.G (1999).Evidence for motion between Nubia and Somalia along the Southwest Indian Ridge.Nature, 398, 64–67

Corti, G. (2009). The Continental rift evolution: From rift initiation to incipient break-up in the Main Ethiopian Rift, East Africa.

D.H. Feyissa., R. Shinjo., H. Kitagawa., D. Meshesha, E. Nakamura. (2017). Petrologic and geochemical characterization of rift-related magmatism at the northern most Main Ethiopian Rift: Implications for Plume-lithosphere interaction and the evolution of rift mantle sources: Lihos Journal, Lithos 282–283 240–261.

Daniel. Mashesha and Ryuichi shinjo. (2004). Crust contamination and diversity of magma source in north western Ethiopia volcanic province: Journal of mineralogical and petrological science. Volum102.

Davidson.A and Rex, D.C. 1980, Age of volcanism and rifting in South-Western Ethiopia. Nature 283, 654–658.

Dereje Ayalew and Gezahign Yirgu. (2003). Crustal contribution to the genesis of Ethiopian plateau rhyolitic ignimbrites: Basalt and rhyolite geochemical provinciality. *Journal of the Geological Society*, 160: 47-56. Doi: 10.1144/0016-764901-169.

Dereje Ayalew and Sally A. Gibson. (2009). Head-to-tail transition of the Afar mantle plume: Geochemical evidence from a Miocene bimodal basalt–rhyolite succession in the Ethiopian Large Igneous Province.

Dereje Ayalew., Barbey, P.,Marty, B., Reisberg, L., Gezahign Yirgu, and Pik, R.. (2002). Source, genesis and timing of giant ignimbrite deposits associated with Ethiopian continental flood basalts.

Dereje Ayalew., Gezahign Yirgu and Pik, R. (1999). Geochemical and isotopic (Sr, Nd and Pb) characteristics of volcanic rocks from southwestern Ethiopia Journal of African Earth science.

Dereje Ayalew., Jung S., Romer R., Kersten F., Pfander J., Garbe-Schonberg. D .(2016). Petro genesis and origin of modern Ethiopian rift basalts: Constraints from isotope and trace element geochemistry.

Dereje Ayalew., Marty, B., Barbey, P.and Ketefo. E, (2006).Sub-lithospheric source for quaternary alkaline Tepi shield, south west Ethiopia.

Ebinger CJ., TesfayeYemane., Giday Woldegabriel., Aronson J and Walter,R. (1993). Late Eocene-Recent volcanism and rifting in the southern main Ethiopian rift.

Ebinger, C.J.,Bechtel, T., D, Forsyth. D, W and Bowin C, O. (1989). Effective elastic plate thicknesses beneath the East African and Afar domes.

F. Giordano., M. D'Antonio., L. Civetta., S. Tonarini., G. Orsi ., Dereje Ayalew ., Gezahign Yirgu., F. Dell'Erba., M.A. Di Vito. and R. Isaia.(2014).Genesis and evolution of mafic and felsic magmas at Quaternary Volcanoes within the Main Ethiopian Rift: Insights from Gedemsa and Fanta 'Ale complexes: journal homepage:

Ferguson.D.J., Maclennan, J., Bastow, I.D., Pyle, D.M., Keir, D., Blundy, J.D., Plank, T. and Gezahign Yirgu.(2013). Melting during late-stage rifting in Afar is hot and deep: Nature, v. 499,p. 70–73, doi: 10.1038/nature12292.

Furman T., Wendy R. Nelson and Linda T. Elkins-Tanton. (2016). Evolution of the East African rift: Drip magmatism, lithospheric thinning and mafic volcanism.

Furman, T. (2007) Geochemistry of East African Rift basalts from Journal of African Earth Sciences

Furman, T, Kaleta, K M, Bryce J G and Hanan, B. (2006). Tertiary mafic lavas of Turkana, Kenya: constraints on East African plume structure and the occurrence of high-mu volcanism in Africa.

Furman,T., Bryce, J.G., Karson, J.and Iotti. A. (2004).East African Rift System (EARS) plume structure: insights from quaternary mafic lavas of Turkana, Kenya. Journal of Petrology 45, 1069–1088.

Gamo Gofa zone Agriculture department and National meteorological Agency. Annual Report of Department of Agriculture Arbaminch, Ethiopia; 2010

Gamo Gofa Zone. (2017). November 29). In Wikipedia. *The Free Encyclopedia*. Retrieved 14:52, December31,201, fromhttps://en.wikipedia.org/w/index.php?title=Gamo_Gofa_Zone&oldid=812727645

George.R M., Rogers, N.W. (2002). Plume dynamics beneath the African Plate inferred from the geochemistry of the Tertiary basalts of southern Ethiopia.

George, R. and Rogers, N. (1999).The petrogenesis of Plio- Pleistocene alkaline volcanic rocks from the Tosa Shucha region, Arba Minch, southern main Ethiopian rift. *Acta Vulcanol*.**11**, 121–131.

George, R., Rogers, N. and Kelly, S.(1998). Earliest magmatism in Ethiopia: evidence for two mantle plumes in one flood basalt province. *Geology* **26**, 923–926.

Giacomo Corti., Andrea Agostini., Derek Keir., Jolante Van Wijk4., Ian D. Bastow., and Giorgio Ranalli (2015). Magma-induced axial subsidence during final stage rifting: Implications for the development of seaward-dipping reflectors: Geosphere, published online: https://www.researchgate.net/publication/275720465.

Giday Wolde Gabriel., Aronson.J., L Walter and R.C.(1990). Geology, geochronology, and rift basin development in the central sector of the Main Ethiopia Rift.

Hayward, N.J., Ebinger, C.J.(1996). Variations in the along-axis segmentation of the Afar Rift system. Tectonics 15, 244–257.

Kieffer, B., Arndt, N., LaPierre, H., Bastien, F., Bosch, D., Pecher, A., Gezhagn Yirgu, Dereje Ayalew.,Lahitte, P., Gillot, P.-Y., Courtillot, V. (2003). Silicic central volcanoes asprecursors to rift propagation: the Afar case. Earth Planet. Sci. Lett.207, 103–116.

Marty, B., Pik R, Gezahign, Yirgu. (1996). Helium isotopic variations in Ethiopian plume lavas: nature of magmatic sources and limit on lower mantle contribution.

Matthew L., M. Gleeson., Michael J. Stock., David M. Pyle., Tamsin A.Mather., William Hutchison., Gezahegn Yirgu .and Jon. Wade.(2017).Constraining magma storage conditions at a restless

volcano in the Main Ethiopian Rift using phase equilibrium models: Journal of Volcanology and Geothermal Research 337, 44–61

Mohr, P.and Zanettin. B.(1988). The Ethiopian food basalt province. In: Macdougall, J.D. n (Ed.), Continental flood basalts. Kluwer Academic Publishers, pp. 63–110.

Montelli, R., Nolet, G., Dahlen, F.A., Masters, G., Engdahl, E.R., and Hung, S.H.. (2004). Finite-frequency tomography reveals a variety of plumes in the mantle: Science, v. 303,p. 338–343, doi:10.1126/science.1092485.

Mulugeta Alene, William K. Hart., Beverly Z. Saylor., Alan Deino., Stanley Mertzman., Yohannes Haile-Selassie., Luis B. and Gibert.(2017). Geochemistry of Woranso–Mille Pliocene basalts from west-central Afar, Ethiopia: Implications for mantle source characteristics and rift evolution.

Peccerillo, A., Barberio, M., Gezahegn Yirgu, Dereje Ayalew, Barbieri, M. and Wu, T. (2003).Relationships between mafic and peralkaline silicic magmatism in continental rift settings: a petrological, geochemical and isotopic study of the Gedemsa volcano, central Ethiopian rift. *Journal of Petrology 44* (11).

Peccerillo, A., Donati, C., Santo, A., Orlando, A., Gezahegn Yirgu and Dereje Ayalew. (2007). Petrogenesis of silicic peralkaline rocks in the Ethiopian rift: geochemical Petrology 45, 1069–1088.

Philippon M., Corti G., Sani,F., Bonini, M., Balestrieri, M.L., Molin, P., Willing shofer, E.,Sokoutis, D., Cloetingh, S. (2014). Evolution, distribution and characteristics of rifting in southern Ethiopia. Tectonics 33, 485–508.
http://dx.doi.org/10.1002/2013TC00343.

Pik, R., Deniel, C., Coulon, C., Gezhagn Yirgu., Hofmann, C., Dereje Ayalew. (1998). The Northwest Ethiopian plateau flood basalts: classification and spatial distribution of magma types. Journal of Volcanology and Geothermal Research 81, 91–111.

Pik, R., Marty, B.,Carignan, J., Gezhagn Yirgu., T.Ayalew(2008). Timing of East African Riftdevelopment in southern Ethiopia: implication for mantle plume activity andevolution of topography. Geology 36, 167–170.
doi:10.1130/G24233A.1.

Pik, R., Marty, B., Hilton, D.R.(2006). How many mantle plumes in Africa? From geochemical pointofview.ChemicalGeology226, 100– doi:10.1016/j.chemgeo.2005.09.016.

Ray Macdonald. (2002). Magmatism of the Kenya Rift Valley: *Transactions of the Royal Society of Edinburgh: Earth Sciences*, **93,** 239±253, 2003

Rogers, N., Macdonald, R., Fitton, J.G., George, R., Smith, M. and Barreiro, B. (2000). Two mantle plumes beneath the East African Rift System: Sr, Nd and Pb isotope evidence from Kenya Rift basalts. *Earth and Planeta~ Science Letters*, **176**: 387-400.

Rollinson H. (1993).*Using geochemical data: evaluation, presentation, interpretation* Pearson, prentice hall, 380pp.

Rooney.T.(2010). Geochemical evidence of lithospheric thinning in the southern Main Ethiopian Rift. Lithos 117(1–4):33–48.

Rooney, T, Bastow, D and Keir, D.(2011). Insights into extensional processes during magma assisted rifting: Evidence from aligned scoria cones**.** Southwestern Ethiopia.

Rooney, T., Hanan, B., Graham D.W., Furman, T.,Blichert, J. and Schilling J-G. (2012).Upper mantle pollution during afar plume-continental rift interaction.

Rooney, T., K. Hart William. Dereje Ayalew., Ghiorso S., Gezhagn Yirgu. and P. Hidalgo.(2012). Peralkaline magma evolution and the tephra record in the Ethiopian Rift.*Sciences*, **29**: 381-391.

Tadiwos Chernet., Hart WK., Aronson. J., L,Walter .and R.C.(1998). New age constrains on the timing of volcanism and tectonism in the northern Main Ethiopian Rift southern Afar transition zone Ethiopia.

Tesfaye Yemane., Giday WoldeGebriel., Tesfaye, S., Berhe SM., Durary, S., Ebinger, CJ and Kelley, S.(1999).Temporal and geochemical characteristics of Tertiary volcanic rocks and tectonic history in the southern Main Ethiopian Rift and adjacent volcanic fields Acta Vulcano l., 11, 99 – 119.

Thompson, R.N., Morrison, M.A., Hendry, G.L., Parry, S.J.(1984). An assessment of the relative roles of a crustal and mantle in magma genesis: an elemental approach. Phil Trans Royal Society London Wilson, M. (1989). Igneous petrogenesis: a global tectonic approach. Harper Collins Academic, London

Wang, K., Plank, T.,Walker, J.D., Smith, E.I. (2002). A mantle melting profile across the basin and range. SWUSA.Journal of Geophysical Research-Solid Earth 107. Doi:10.1029/2001JB0002092

Weis, D., Jerram, D., Keller, F.and Meugniot, . (2004). Flood and shield basalts from Ethiopia: magmas from the African Supers well. Journal of Petrology 45, 793–834.

Wolde Gabriel, G., Aronson, J.L., Walter, R.C. (1990). Geology,geochronology, and rift basin development in the central sector of the main Ethiopia rift. Geol. Soc. Am. Bull. 102,439–458.

Wolfenden, E., Ebinger, C., Gezhagn Yirgu., Deino. A., Dereje Ayalew (2004). Evolution of the northern Main Ethiopian Rift: birth of a triple junction. Earth Planet Science. Lett. 224, 213–228.

Appendices

Appendix - I

Is about the both Travers and location of study area

Table 3.1 Location details of different rock units of the study area according to the traverse and station they are encountered

Locality name	Travers	Easting	Northing	Elevation	Exposure	Lithology unite
ANRGW	T_1 S_1	0337875	0662490	1322m	Road cut	unwelded tuff/rhyolite
ANBGS	T_1 S_2	0337168	0662568	1357m	hillside	Basalt
ANRCAP	T_1 S_3	0336910	066301	1580	Hill side	Rhyolite/trachyte
ANPBGS	T_1 S_4	0337007	0661910	1420	mountain side	Basalt
ANRCAP	T_1S_5	0336566	0662065	1416	Road cut	Rhyolite
ANBGS	T_2S_1	0337919	0662353	1316m	Hill side	basalt
ANBGS	T_2S_2	0337770	062578	1375m	Quarry site	Basalt
ANRGW	T_2S3	0336342	0660874	1245m	Mountain side	unwolded tuff/rhyolite
-	T_2S_4	0337892	1660479	1189M	insitu	Alluvial deposition
	T_3S_1	0337520	0659901	1209M	insitu	Alluvial
ANRGW	T_3S1	0337210	0657521	1161M	Mountain side	Rhyolite
MT	T_3S_2	033780	0656693	1120m	Road cut	Volcanic Ash
ANSDP	T_3S_3	0338478	0656703	1121m	Quary site	Scoria cone
ANISC	T3S4	0338478	0656703	1123m	Quarry site	Ignimbrite intercalation of scoria
ANSC2	T_4S_1	0338445	0657267	1154m	Mountain top	Aphric basaltt
Mt	T_4S_2	0338987	0659558	1193	Insitu	Alluvial
ANVBKR	T_4S_3	0339505	0660055N	1245m	Mountain side	middleporpyritic basalt
ANVBKR	T_4S_4	0339706	0659672	1162m	Mountain side	Middle porpyriticbasalt
ANSB	T_4S_5	0339938	066024	1273M	River cut	Basaltic Trachy andecite
ANPBAS	T_5S_1	0338102	0662801	1355m	Road cut	Upper porphyritic basalt

ANIAS	T_5S_2	0338204	0662550	1318M	Road cut	Trachyandesite
ANIAS	T_5S_2	0340942	0663452	1111m	Hill side	Trachy andesite basalt
AD	T_5S_4	0341929	0662870 N	1187m	Insitu	Alluvial
ANTB	T_5S_4	0342744E	0661465 N	1194	Road cut	Trachy dacitic basalt
ANTB	T_5S_5	0343674	066204	1568m	Maintai n top	Trachy dacitic
ANSB	T_5S_6	0342334	0660769	1265M	Hill side	Basaltic trachy andecite

Appendix - II

The following tables show orientation of structures from study area.

Table 3.2 Orientation of joints encountered in the study area in different traverses

Travers	Easting	Northing	Elevation	Strike	Apertures	Dip	Name of structure	Lithology unite
T_1S_2	38424	660222	1485m	020 ^{0}	0.1m	67^{0}NW	joint	A. basalt
T_4S_4	340555	659932	1410m	010^0	0.05	89^{0}NW	joint	Mp. basalt
T_1S_5	36453	659628	1360m	050 ^{0}	0.2m	90 ^{0} Ew	joint	Unwelded tuff
T_1S_5	36422	657623	1365m	060 ^{0}	0.04m	79 ^{0} NE	joint	Poryphyritic basalt
T_2s_2	37500	66I509	1200m	020 ^{0}	0.05	80 ^{0} NE	Joint	Unwldded tuff
T_2S_3	37580	662400	1280m	040 ^{0}	0.004m	90 ^{0} Ew	joint	Un welded tuff
T_2S_3	3756	66244	1449m	0 25 ^{0}	0.0002m	75 ^{0} NE	Joint	A.basalt
T_2S_3	38000	662900	1345m	0 30 ^{0}	0.1m	530^{0}NE	joint	A.basalt
T_2S_4	38407	662709	1420m	050 ^{0}	0.01m	50 ^{0}SW	joint	A.basalt
T_5S_4	342500	66290	1425m	010 ^{0}	0.03M	70 ^{0}NE	Joint	Trachytic basalt
T_5S_3	341700	661256	1430m	0 30 ^{0}	0.07m	83^{0}NW	Joint	Trachyandesite
T_5S_4	340710	662905	1238m	009 ^{0}	0.06m	79 ^{0}W	Joint	Trachytic basalt
T_1s_4	38200	662000	1400m	025 ^{0}	0.01m	25^{0}NW	joint	Porphyritic basalt
T_1S_4	37970	660907	1360m	420 ^{0}	0.002m	0^{0}N S	Joint	Porphyritic basalt
T_5S_1	339778	662930	1353M	0 45 ^{0}	0.002m	45^{0}NW	Joint	A.basalt

T_1S_2	38208	662890	1300M	030 ^{0}	0.03m	60 ^{0}NE	Joint	Unweldded tuff
T_5S_3	341000	660700	1280M	0 10 ^{0}	0.1m	77^{0}NW	Joint	Trachytic basalt
T_4S4	340908	660280	1208M	040 ^{0}	0.03m	58 ^{0}NE	Joint	Middle porpyritic
T_4S_3	38930	657608	1206M	0 10 ^{0}	0.1m	81 ^{0} NE	Joint	Scoricias basalt

Table 3.3 Orientation of faults which are found in the study area

Travers	Easting	Northing	Elevation	Strike	Dip	Structure name	Lithological unite
T_5S_2	341944	661558	1187m	020^0	71^{0}SW	Fault	Trachy andesite
T_4 S_4	342754	660775	1225m	079 ^{0}	90 ^{0}SW	Fault	Middle porpyritic basalt
T_2S_3	38230	61907	1335m	008^0	89^0 SE	Fault	A. Basalt
T_1 S_4	337672	662865	1450 m	030^0	91 ^{0}SE	Fault	Rhyolitic lava flow

Appendix - III

Is the modal proportion of mineral from microscope of 8 thin section sample results

Table 3.3.1 Microphoto picture of rhyolite sample

Sample code (WTGR)				
Mineral discrption	Modal proportion%	Phenocryst maximum grain Size (mm)	Phenocryst grain shape	Rock name
Quartz	21%	0.34	Anhedra	Rhyolite
Alkali feldspar	25	0.23	Subanahedral	
Fe- Ti Oxides(Opq	9	0.6	Anhedral	
Plagioclase	2	0.6	Anahedral	
Ground mass	42			

Table 3.3.2 Microphoto picture of scoria cone sample

Sample code WT001				
Mineral discrption	Modal roportion%	Phenocryst maximum grain Size (mm)	Phenocryst grain shape	Rock name
Plagioclase	30	0.1	Subhedral	Cender cone /scoria cone
Opq (Fe-Ti)	8	0.2	Anhedral	
olivine	2	0.2	Anhedral	
Ortho pyroxene	10		Anhedral	
Volcanic glass	20			
Ground mass	25			

Table 3.3 .3 Microphoto picture of Aphyrict asalt sample

Sample code WTG01				
Mineral discrption	Modal proportion%	Phenocryst maximum grain Size (mm)	Phenocryst grain shape	Rock name
Plagioclase	38%	0.1	Anhedral	*Aphyrict Basalt*
pyroxene	20%	0.1	Anhedral	
olivine	8%	0.2	Anhedral	
Fe-Ti Oxide	14%	0.2	Anhedral	
Ground mass	20%			

Table 3.3.4 Microphoto picture of Porphyratic basalt sample

Sample code WT01				
Mineral discrption	Modal proportion%	Phenocryst maximum grain Size (mm)	Phenocryst grain shape	Rock name

Plagioclase	40	0.4mm	Euhedral	Porpyratic basalt
Phyroxene	14	0.2 mm	Euhedral	
Fe-Ti oxide	12	0.3mm	anhedral	
Olivine	9	0.2 mm	subhedral	
Ground mass	24			

Table 3.3.5 A Microphoto picture of middle porphyritic basalt sample

Sample code WT03				
Mineral discrption	Modal proportion%	Phenocryst maximum grain Size (mm)	Phenocryst grain shape	Rock name
Plagioclase	23	0.4	Euhedral	*middle porphyritic basalt*
Pyroxine/opx	14	0.2	Subhedral	
olivine	4	0.1	Sub hedral	
Volcanic glass	3			
Fe-Ti oxide(Opq)	15	0.2	Ahedral	
Gruond mass 41				

Table 3.3.6 Microphoto picture of trachy andesite

Sample code WT02				
Mineral description	Modal proportion%	Phenocryst maximum grain Size (mm)	Phenocryst grain shape	Rock name
plagioclase	26	0.1	Subhedral	Trachy andecite
pyroxine	*11*	*0.01*	anhedral	
Opq (Fe-Ti oxide)	*18*	*0.2*	anhedral	
Alkali feldspar	*2*	-	anhedral	
Groundmass	*40*			

Table 3.3.7 B Microphoto picture of basaltic trachy andesite sample

Sample code WTSB				
Mineral discrption	Modal proportion%	Phenocryst maximum grain Size (mm)	Phenocryst grain shape	Rock name
Plagioclase	31	0.4	Euhedral	Basaltic trachy andesite
Pyroxene	11	0.1	Euhedral	
Alkali	5	0.1	subhedral	

feldspar(ort)				
Fe-Ti oxide	15	0.2	anhedral	
Olivine	13	0.1	anhedral	
Groundmass	20			

Table 3.3.8 Microphoto picture of trachy dasitic basalt sample

Sample code WTLB				
Mineral discrption	Modal proportion%	Phenocryst maximum grain Size (mm)	Phenocryst grain shape	Rock name
Plagioclase	20	0.1	Anhedral	Tracydacite
Alkali feldspar	23	0.5	Euhedral	
Quartz	13	0.01`	Anhedral	
Fe-Ti oxide	13	0.1	Anhedral	
Ground mass	21			

Appendix – IV

Major elements form (wt.%) Calculated by a formula, Conversion Number*Wi; where Wi is the wt. percentages of oxide. Conversion Number = MWi* Ai/MWg; where MWi- molecular weight of cations, Ai-number of cations in the oxide formula and MWg are the molecular weight of oxide.

Samples	Ti	P	K	P/K	Ti/K
ANBGS	1.032	0.170282	0.4222	0.40332	2.444339
ANPBGS	1.152	0.135352	0.753503	0.17963	1.528859
ANSC2	1.08	0.205211	0.836306	0.245378	1.291394
ANPBAS	1.242	0.213943	1.159236	0.184555	1.071396
ANVBKR	1.182	0.200845	1.258598	0.159578	0.93914
ANSB	1.056	0.205211	1.771975	0.115809	0.595945
ANIAS	0.972	0.261971	2.691083	0.097348	0.361193
ANSCP	0.792	0.253239	2.335032	0.108452	0.339182
ANTB	0.3	0.087324	3.121656	0.027974	0.096103
ANISC	0.438	0.113521	3.0305	0.03746	0.144531
ANRCAP	0.132	0.013098	4.496178	0.002913	0.029358
ANRGW	0.084	0.013098	3.825477	0.003424	0.021958

5.2 The selected important trace element ratios

Samples	Rb/Sr	La/Yb	Ce/Pb	La/Nb	K/Nb	Ti/Zr	Th/Nb	Ba/La	La/Sm	Ba/Nb	CaO/Al2O3	Sm/Yb
ANBGS	0.025899	6.534296	0	0.962766	224.5745	69.26174	0.081915	10.49724	3.926247	10.10638	0.579553	1.66426
ANPBGS	0.054409	19.515152	11.54	0.689507	161.3497	122.5532	0.108351	11.61491	7.155556	8.008565	0.704762	2.727273
ANSC2	0.050969	19.019608	9.5	0.743295	160.2118	105.8824	0.106897	11.57216	7.854251	8.601533	0.733108	2.421569
ANPBAS	0.049701	17.733333	35.5	0.677419	196.8142	94.80916	0.097453	12.78195	7.150538	8.658744	0.626866	2.48
ANVBKR	0.062107	14.43038	15.05	0.724576	266.6521	143	0.120339	15.67251	6.345083	11.35593	0.548703	2.274262
ANSB	0.100617	17.489879	24.53333	0.753927	309.2451	55	0.166667	12.63889	7.769784	9.528796	0.488095	2.251012
ANIAS	0.127786	24.133333	17.71429	0.661187	245.761	39.03614	0.136986	13.10773	9.692102	8.666667	0.292308	2.49
ANSCP	0.111374	25.686901	15.11111	0.687179	199.5754	32.19512	0.123504	13.74378	11.12033	9.444444	0.274652	2.309904
ANTB	0.261022	27.509158	11.04545	0.618107	256.9264	10.83032	0.117695	16.91079	12.77211	10.45267	0.172	2.153846
ANISC	0.260563	24.351852	26.6	0.646721	248.4016	14.17476	0.152049	14.70215	11.36888	9.508197	0.178613	2.141975
ANRCAP	4.486166	18.187661	12.73684	0.742782	236.0198	1.352459	0.081915	1.922261	7.839335	1.427822	0.025215	2.320051
ANRGW	25.88652	11.401515	8.9375	0.191964	48.79435	0.538462	0.108351	0.119601	7.235577	0.022959	0.037276	1.575758

Tables 4.2: CIPW normative minerals calculations (in wt. %) were performed using the norm-calculating program based on *(after* Thompson, 1984*)*. In the course of CIPW, norm calculations 10 quartz + hypersthene normative (silica saturated)

Minerals	ANBGS	ANPBGS	ANSC2	ANPBAS	ANVBKR	ANSB	ANIAS	ANSCP	ANTB	ANISC	ANRCAP	ANRGW
Quartz	1.25	0.00	1.28	0.49	2.37	3.53	2.46	2.59	3.62	6.65	21.3	23.97
Plagioclase	52.72	49.59	47.20	53.31	55.10	54.50	59.19	61.94	62.13	59.41	51.57	43.73
Orthoclase	3.07	5.38	6.09	8.27	8.86	12.71	19.38	16.67	22.93	21.51	32.15	28.01
Diopside	6.38	13.25	14.27	10.99	7.16	7.23	0.00	0.36	1.96	1.49	0.00	0.00
Hypersthen	17.82	10.58	14.26	9.75	9.63	6.56	6.15	4.56	1.26	1.60	0.57	0.40
Olivine	0.00	4.46	0.00	0.00	0.00	0.00	0.00	0.00	0.00	0.00	0.00	0.00
Rutile	0.00	0.00	0.00	0.00	0.00	0.00	0.47	0.00	0.00	0.00	0.20	0.05
Ilmenite	0.43	0.34	0.39	0.36	0.36	0.34	0.34	0.47	0.39	0.41	0.04	0.17
Hematite	13.67	11.39	11.42	11.09	11.09	10.14	8.18	9.44	6.34	7.07	2.39	3.31
Apatite	0.93	0.72	1.11	1.14	1.07	1.09	1.41	1.34	0.51	0.60	0.07	0.07
Sphene	3.74	4.29	3.99	4.61	4.34	3.90	2.40	2.63	0.88	1.27	0.00	0.00